STABILITY OF MYOSIN SUBFRAGMENT-2 MODULATES THE FORCE PRODUCED BY ACTO-MYOSIN INTERACTION OF STRIATED MUSCLE

Rohit Rajendraprasad Singh, M.S.

Dissertation Prepared for the Degree of

DOCTOR OF PHILOSOPHY

UNIVERSITY OF NORTH TEXAS

December 2017

APPROVED:

Douglas D. Root, Major Professor
Robert C. Benjamin, Committee Member
Kent D. Chapman, Committee Member
Pamela Padilla, Committee Member
Amanda J. Wright, Committee Member
Arthur Goven, Chair of Department of Biological Sciences
Su Gao, Dean of the College of Sciences
Victor Prybutok, Dean of the Toulouse Graduate School

Singh, Rohit Rajendraprasad. *Stability of Myosin Subfragment-2 Modulates the Force Produced by Acto-Myosin Interaction of Striated Muscle*. Doctor of Philosophy (Biochemistry and Molecular Biology), December 2017, 125 pp., 5 tables, 46 figures, references, 119 titles.

Myosin subfragment-2 (S2) is a coiled coil linker between myosin subfragment-1 and light meromyosin (LMM). This dissertation examines whether the myosin S2 coiled coil could regulate the amount of myosin S1 heads available to bind actin thin filaments by modulating the stability of its coiled coil. A stable myosin S2 coiled coil would have less active myosin S1 heads compared to a more flexible myosin S2 coiled coil, thus causing increased force production through acto-myosin interaction. The stability of the myosin S2 coiled coil was modulated by the binding of a natural myosin S2 binding protein, myosin binding protein C (MyBPC), and synthetic myosin S2 binding proteins, stabilizer and destabilizer peptide, to myosin S2. Competitive enzyme linked immunosorbent assay (cELISA) experiments revealed the cross specificity and high binding affinity of the synthetic peptides to the myosin S2 of human cardiac and rabbit skeletal origins. Gravitational force spectroscopy (GFS) was performed to test the stability of myosin S2 coiled coil in the presence of these myosin S2 binding proteins. GFS experiments demonstrated the stabilization of the myosin S2 coiled coil by the binding of MyBPC and stabilizer peptide to myosin S2, while the binding of destabilizer peptide to the same resulted in a flexible myosin S2 coiled coil. The binding of MyBPC and stabilizer peptide respectively, resulted in 3.35 and 1.5 times increase in force required to uncoil the myosin S2, while the binding of destabilizer peptide resulted in 1.6 times decrease in force required to uncoil the myosin S2. The myofibrillar contractility assay was performed to test the effect of synthetic myosin S2 binding proteins on the sarcomere shortening in myofibrils. The stabilizer peptide resulted in decreased sarcomere shortening of myofibrils as a result of decreased acto-myosin interaction, on the other hand, the binding of destabilizer peptide caused an increase in sarcomere shortening. The in vitro motility

assay was performed to test the effect of altered stability of myosin S2 by binding of these myosin S2 binding proteins on the motility of actin filaments sliding over myosin. The motility of actin filaments was hindered by treating myosin thick filaments with whole length skeletal MyBPC or by treating heavy meromyosin with stabilizer peptide, while the motility of actin filaments was enhanced when heavy meromyosin was treated with destabilizer peptide. This study demonstrates that the myosin S2 coiled coil stability influences the force produced by acto-myosin interaction in striated skeletal muscle. The myosin S2 coiled coil when stabilized by MyBPC and stabilizer peptide resulted in decreased force production by reduced acto-myosin interaction. While the binding of destabilizer resulted in a flexible myosin S2 coiled coil and increased force production by enhanced acto-myosin interaction. The potentially cooperative response of contractility to the instability of the S2 coiled coil promises that this biological mechanism may be the target of drugs to modulate muscle performance.

ACKNOWLEDGEMENT

I would like to extend my deepest gratitude and acknowledge the efforts of the personnel who were involved in the successful completion of my doctoral dissertation. I would like to start with acknowledging the efforts of my major professor, Dr. Douglas D. Root, for all his guidance and careful insights towards the understanding of the scienctific concepts and increment in my scientific acumen. I would also like to thank my committee members, Dr. Robert C. Benjamin, Dr. Kent D. Chapman, Dr. Pamela Padilla, and Dr. Amanda J. Wright for their precious time and all of their prompt correspondence, also the graduate courses offered by them which helped me strengthen my knowledge in the subject of biology. I would like to thank my lab supervisors Dr. Mark Demarest, Geoffrey Brooks and Arland Alberts for giving me the opportunity to teach undergraduate and graduate labs and gain proficiency in explaining the biological concepts to a wide audience. I would also like to thank Kimberly Piccolo and Julie Leary for all their efforts to provide me a smooth transition though my course in obtaining my doctoral degree regarding the administrative paperwork and support. I also want to thank my past and current lab members, James Dunn, Nasrin Taei, Motamed Qadan, Duaa Quedan and especially Negar Aboonasrshiraz for all the support being scientific or friendly. I would also like to extend my gratitude towards my friends here at University of North Texas and back home in Mumbai also to my extended Singh family for their warm wishes and thoughts. Lastly and most importantly, I would like to thank my family, my parents, Dr. Rajendraprasad R. Singh and Mangla R. Singh and my brother, Rajiv R. Singh for constant support throughout my life and I will always be indebted to them.

TABLE OF CONTENTS

Page

ACKNOWLEDGEMENT iii

LIST OF TABLES vii

LIST OF FIGURES viii

ABBREVIATIONS xi

CHAPTER 1. INTRODUCTION 1

1.1 Muscle and Sarcomere 1

1.2 Myosin 2

1.3 Actin 4

1.4 Tropomyosin and Troponin Complex 4

1.5 Myosin Binding Protein C 5

1.6 Muscle Contraction and its Regulation 6

1.7 Familial Hypertrophic Cardiomyopathy 9

1.8 Hypothesis and Testing 12

1.8.1 Myosin Binding Protein C Stabilizes the Myosin S2 Coiled Coil and Decreases the Amount of Force Produced. 15

1.8.2 Stabilizer Peptide is Specific to Myosin S2 Coiled Coil and Stabilizes the Myosin S2 Coiled Coil thus Decreasing the Amount of Force Produced 16

1.8.3 The Destabilizer Peptide is Specific to Myosin S2 Coiled Coil and Destabilizes the Myosin S2 Coiled Coil thus Increasing the Amount of Force Produced 18

CHAPTER 2. MATERIALS AND METHOD 23

2.1 Materials 23

2.1.1 Myofibrils 23

2.1.2 Myosin 23

2.1.3 Myosin Binding Protein C 24

2.1.4 Actin 24

2.1.5 Human β-cardiac Myosin S2 Peptide 26

2.1.6 Monoclonal Antibodies 26

2.1.7 DNA with DTPA tagged dCTP 26

2.1.8 Polyclonal Antibody against Myosin S2 27
2.1.9 Stabilizer Peptide 27
2.1.10 Destabilizer Peptide 28
2.2 Methods 29
2.2.1 Competitive Enzyme Linked Immunosorbent Assay 29
2.2.2 Gravitational Force Spectroscopy 33
2.2.3 Myofibrillar Contractility Assay 43
2.2.4 *In vitro* Motility Assay 45

CHAPTER 3. MYOSIN BINDING PROTEIN C AND MYOSIN SUBFRAGMENT-2 50
3.1 Purification of MyBPC 50
3.2 Gravitational Force Spectroscopy 57
3.2.1 Force versus Distance 57
3.3 *In vitro* Motility Assay 65
3.4 Conclusion 66

CHAPTER 4. STABILIZER PEPTIDE AND MYOSIN SUBFRAGMENT-2 69
4.1 Introduction and Idea behind the Design and Use of Stabilizer Peptide 69
4.2 Competitive ELISA of Stabilizer Peptide to Myosin S2 70
4.2.1 Minimum Dilution of Primary Polyclonal Anti-S2 Antibody to Bind Rabbit Skeletal Myosin 70
4.2.2 Concentration of Human Cardiac Myosin S2 Peptide Required to Bind Primary Polyclonal Anti-S2 Antibody 71
4.2.3 Stabilizer Peptide versus Polyclonal Anti-S2 Antibody 73
4.3 Gravitational Force Spectroscopy with the Stabilizer Peptide 75
4.4 Myofibrillar Contractility Assay with Stabilizer Peptide 79
4.5 *In vitro* Motility Assay of Actin Filaments over Myosin HMM Incubated with Stabilizer Peptide 81
4.6 Conclusion 84

CHAPTER 5. DESTABILIZER PEPTIDE AND MYOSIN SUBFRAGMENT-2 87
5.1 Introduction and Idea behind the Design and Use of Destabilizer Peptide 87
5.2 Competitive ELISA of Destabilizer Peptide to Myosin S2 90
5.3 Gravitational Force Spectroscopy with Destabilizer Peptide 92
5.4 Myofibrillar Contractility Assay with Destabilizer Peptide. 95

5.5 The *In vitro* Motility Assay of Actin Filaments over Myosin HMM Incubated with Destabilizer Peptide 97
5.6 Conclusion 100

CHAPTER 6. DISCUSSION 102
6.1 Binding to Myosin S2 102
6.2 Stability of the Myosin S2 Coiled Coil 103
6.3 Sarcomere Shortening of Myofibril 105
6.4 The *In vitro* Motility of Actin Filaments 106
6.5 Conclusions 107

REFERENCES 117

LIST OF TABLES

Page

Table 1. Length of uncoiled myosin S2 molecule in absence and presence of MyBPC measured with GFS. 64

Table 2. Length of uncoiled myosin S2 molecule in absence and presence of stabilizer peptide measured with GFS. 78

Table 3. Table for student's t-test to signify the effect of stabilizer peptide over the velocity of actin filaments. 84

Table 4. Length of uncoiled myosin S2 molecule in absence and presence of MyBPC measured with GFS. 95

Table 5. Table for student's t-test to signify the effect of destabilizer peptide over the velocity of actin filaments. 99

LIST OF FIGURES

Page

Figure 1. Schematic of a sarcomeric unit of muscle with all the parts labelled. 2

Figure 2. Cartoon representation of myosin II coiled coil structure with different parts labelled from the C-terminal region to the N-terminal region (from left to right). 3

Figure 3. Diagram of myosin binding protein C and its different domains. 6

Figure 4. Stages of acto-myosin interaction during muscle contraction. 7

Figure 5. Smooth muscle myosin activation by phosphorylation of myosin light chain. 9

Figure 6. Anatomy of cardiomyopathic hearts. 10

Figure 7. Familial hypertrophic cardiomyopathy point mutations. 11

Figure 8. Acto-myosin switch of MyBPC by phosphorylation. 14

Figure 9. Simulated image of stabilizer peptide. 28

Figure 10. Simulated image of destabilizer peptide. 29

Figure 11. Sketch of cELISA setup. 31

Figure 12. Schematic of a gravitational force spectroscope. 34

Figure 13. Rotational mode of gravitational force spectroscopy. 36

Figure 14. Free-fall mode of Gravitational force spectroscopy. 38

Figure 15. Schematic for preparation of slide for measuring absolute molecular length using Gravitational force spectroscopy. 41

Figure 16. Schematic of a myosin molecule suspended between edge of the coverslip and a silica bead with the help of antibody raised against myosin. 42

Figure 17. Schematic of myofibrillar contractility assay. 44

Figure 18. Schematic of a typical *in vitro* motility assay. 45

Figure 19. Perfusion chamber for *in vitro* motility assay. 48

Figure 20. Hydroxyapatite column chromatography of crude MyBPC extract. 51

Figure 21. Size exclusion chromatogram of MyBPC fractions. 52

Figure 22. Ion exchange chromatography purification and determination of molecular weight of MyBPC. 54

Figure 23. Chromatogram for verification of MyBPC by chromatofocusing. 56

Figure 24. Parallel stretching of myosin and DNA molecule by GFS..... 59

Figure 25. Force vectors acting on a molecule in GFS..... 60

Figure 26. Free-fall mode data of Myosin S2 without and with MyBPC..... 62

Figure 27. Data fit for average of force versus distance of myosin S2 in absenc e and presence of MyBPC. 63

Figure 28. Effect of MyBPC on Myosin S2 flexibility..... 64

Figure 29. Histogram of *in vitro* motility assay with MyBPC..... 66

Figure 30. Optical density versus dilutions of primary anti-S2 antibody. 71

Figure 31. cELISA for competitive binding of polyclonal anti-S2 antibody to human β-cardiac myosin S2 and rabbit skeletal myosin S2. 72

Figure 32. cELISA of stabilizer peptide versus polyclonal anti-S2 antibody..... 74

Figure 33. GFS curve fit for average forces to distance for the effect of stabilizer peptide on the myosin S2 coiled coil..... 77

Figure 34. Comparison of force-distance curves of myosin molecule without stabilizer peptide (blue) and myosin molecule with stabilizer peptide added (red). 78

Figure 35. Dose response of stabilizer peptide on myofibril contraction. 80

Figure 36. Histogram for the velocity of actin filaments in the presence of stabilizer peptide. ... 83

Figure 37. Force-distance trace for myosin treated with polyclonal anti-S2 antibody. 89

Figure 38. Percentage contraction in myofibrils without (blue) and with polyclonal anti-S2 antibody (red)..... 89

Figure 39. The cELISA of destabilizer peptide versus polyclonal anti-S2 antibody..... 91

Figure 40. The force-distance curve for the GFS experiment with rabbit skeletal myosin treated with destabilizer peptide.. 94

Figure 41. Comparison of force-distance curve for control (blue) and test (red) assay for myosin molecule treated with destabilizer peptide..... 95

Figure 42. Percentage contraction in sarcomeres versus destabilizer peptide concentration. 96

Figure 43. Histogram for the velocity of actin filaments in presence of destabilizer peptide. 99

Figure 44. Effect of myosin S2 binding proteins on myosin S2 coiled coil. 111

Figure 45. Cooperative effect of MyBPC, stabilizer and destabilizer peptide over the orientation of myosin S1 heads on myosin thick filament. 112

Figure 46. Representation of MyBPC binding to myosin in single molecule and thick filament form. 113

ABBREVIATIONS

µm	Micrometer
µM	Micromolar
A band	Anisotropic band
A	Concentration of primary antibody
a	Proportionality constant
ADP	Adensoine diphosphate
ATP	Adenosine triphosphate
b	Length of linker
B_A	Concentration of bound primary antibody
BCIP	5-bromo-4-chloro-3-indolyl phosphate
B_P	Concentration of bound peptide
c	Change in enthalpy
cELISA	Competitive enzyme linked immunosorbent assay
Da	Dalton
DCM	Dilated cardiomyopathy
d_{max}	Maximum length of molecule
d_{min}	Minimum length of molecule
f	Intrinsic force of myosin head
F_e	Ensemble force
FHC	Familial hypertrophic cardiomyopathy
G	Free energy
GFS	Gravitational force spectroscopy
H	Enthalpy
HMM	Heavy meromyosin
I band	Isotropic band
IC50	Half maximal inhibitory concentration
ICCD	Intensified charged couple device
IgG	Immunoglobulin G
k	Boltzman’s constant
K_A	Dissociation constant of primary antibody

K_d	Dissociation constant
kDa	Kilodalton
K_P	Dissociation constant of peptide
LMM	Light meromyosin
M	Molar
mM	Millimolar
MyBPC	Myosin binding protein C
MyBPH	Myosin binding protein H
nm	Nanometer
nM	Nanomolar
N_t	Total number of myosin heads available to bind to actin
OD	Optical density
P	Concentration of peptide
PBS	Phosphate buffer saline
Pi	Inorganic phosphate
pI	Isoelectric point
pi	Probability for existence of microstate
pN	Piconewton
rpm	Rotation per minute
S	Entropy
S1	Myosin subfragment-1
S2	Myosin subfragment-2
SDS-PAGE	Sodium dodecyl sulfate polyacrylamide gel electrophoresis
t	Myosin head in strongly bound state
T	Temperature
t_c	Total cycle time of myosin from bound to unbound state
v	Proportionality constant between extension and existing microstate
x	Extension of a molecule
Ω	Number of microstates

CHAPTER 1

INTRODUCTION

1.1 Muscle and Sarcomere

Muscle is a soft tissue present in nearly all the metazoans. Contraction of the muscle imparts several important physiological functions such as locomotion, circulation and peristalsis of the digestive tract. Muscle is present in three forms namely skeletal, smooth and cardiac muscle. Contraction of these muscle types is achieved by the acto-myosin interaction between the myosin thick filament and actin thin filament upon enzymatic cleavage of the adenosine triphosphate (ATP) by ATPase activity of myosin subfragment-1 (S1) heads to provide energy (Huxley, A.F. 1964; Lymn, R.W. and Taylor, E.W. 1971; Huxley, A.F. and Niedergerke, R. 1954). The sarcomere is a functional unit of muscle present in skeletal and cardiac muscle types but absent in smooth muscle type (Wang, K. 1985). The sarcomere is a precise arrangement of all the contractile proteins of a muscle in a repetitive manner. A schematic of the muscle sarcomere is detailed in figure (Figure 1). The length of the sarcomere is measured between two I bands of a muscle myofibril. An I band is followed by an A band followed by another I band and so on in a repetitive manner. The I band contains Cap Z which is the anchor point of actin thin filaments, where the new actin monomers are added to form the filamentous thin actin filament.

The A band contains the central H zone, and this H zone consists of an M line which is the anchor point of myosin thick filament. At M line the myosin filaments are anchored by the interaction of light meromyosin (LMM) of several myosin thick filaments. Spanning both the directions away from H zone in A band there is the overlap of myosin thick filament and actin thin filaments. Hence, when the myofibril is viewed under a microscope, there is a lighter I band followed by a dense A band (Price, H.M. 1963).

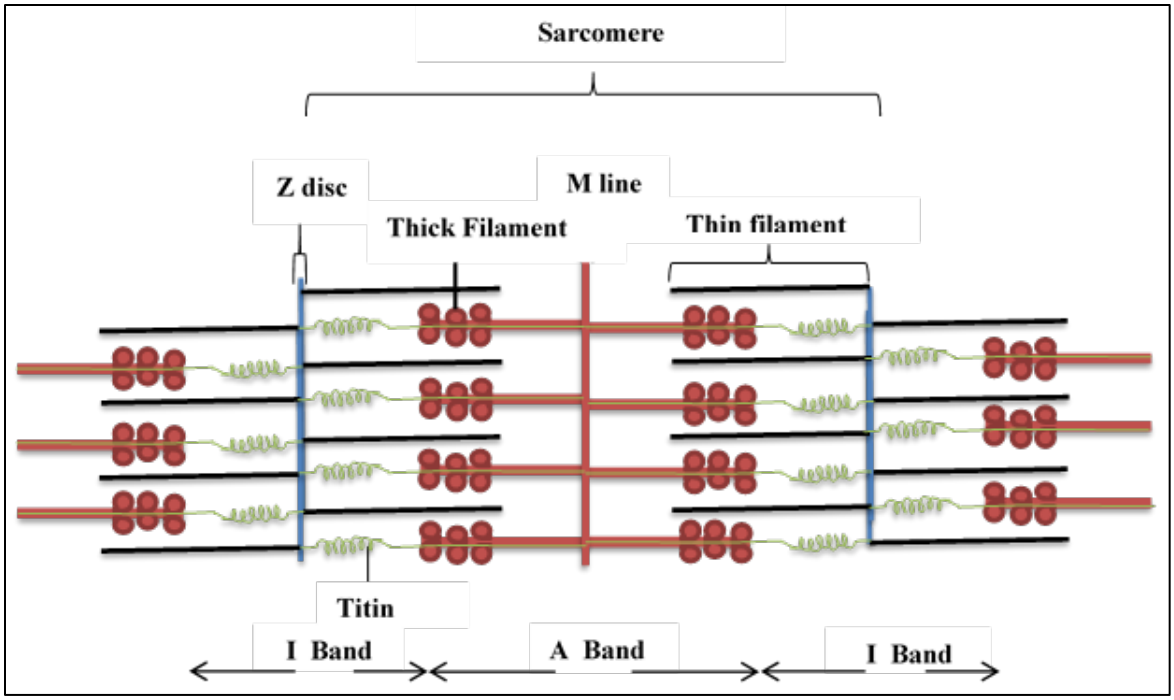

Figure 1. Schematic of a sarcomeric unit of muscle with all the parts labelled.

In skeletal muscles, the myofibrils are present in tight bundles, thus these sarcomeres appear in a more regular manner giving the skeletal muscles a much more striated appearance (Price, H.M. 1963). Even though sarcomeres are present in the cardiac muscle, the myofibrillar bundles are more branched rather than a neat stack compared to skeletal muscles, thus cardiac muscles do not have as regular striations (Challice, C.E. and Viragh, S. 1973; Muir, A.R. 1965). Smooth muscle has a spindle shaped association of actin and myosin, but they have a related contractile apparatus to skeletal and cardiac muscle (Cooke, P. 1976). The striated muscle contractile apparatus comprises of actin thin filaments, myosin thick filament, tropomyosin, troponin complex and myosin binding protein C.

1.2 Myosin

Myosin is a superfamily of ATP dependent motor protein, where hydrolysis of ATP drives

the movement of the myosin on actin (Ruppel, K.M., and Spudich, J.A. 1996). Myosin is a large protein with a molecular weight of 220 kDa and comprises approximately 1936 amino acids in the heavy chain with variations due to different genes and alternative splicing. The myosin protein has an N-terminal globular head and a long α-helical tail towards the C-terminal end.

The myosin thick filament comprises the majority of the contractile apparatus. Two heavy chains and four light chains form a dimeric subunit of the myosin filament. The dimers of myosin in thick filaments are formed by the coiled coil formation of long □-helical tail at the C-terminal end of the myosin thick filament, which results in two free and independent myosin globular heads at the N-terminal end (Warrick, H.M., and Spudich, J.A. 1987; Al-Khayat, HA. 2013). The myosin heavy chain is structurally classified into two parts heavy meromyosin and light meromyosin. A schematic of myosin II coiled coil structure is detailed in the figure (Figure 2). Heavy meromyosin is further divided into two subfragments, namely myosin subfragment-1 (S1) and myosin subfragment-2 (S2) connected by the myosin S1-S2 hinge (Rayment, I., and Holden, H.M. 1994).

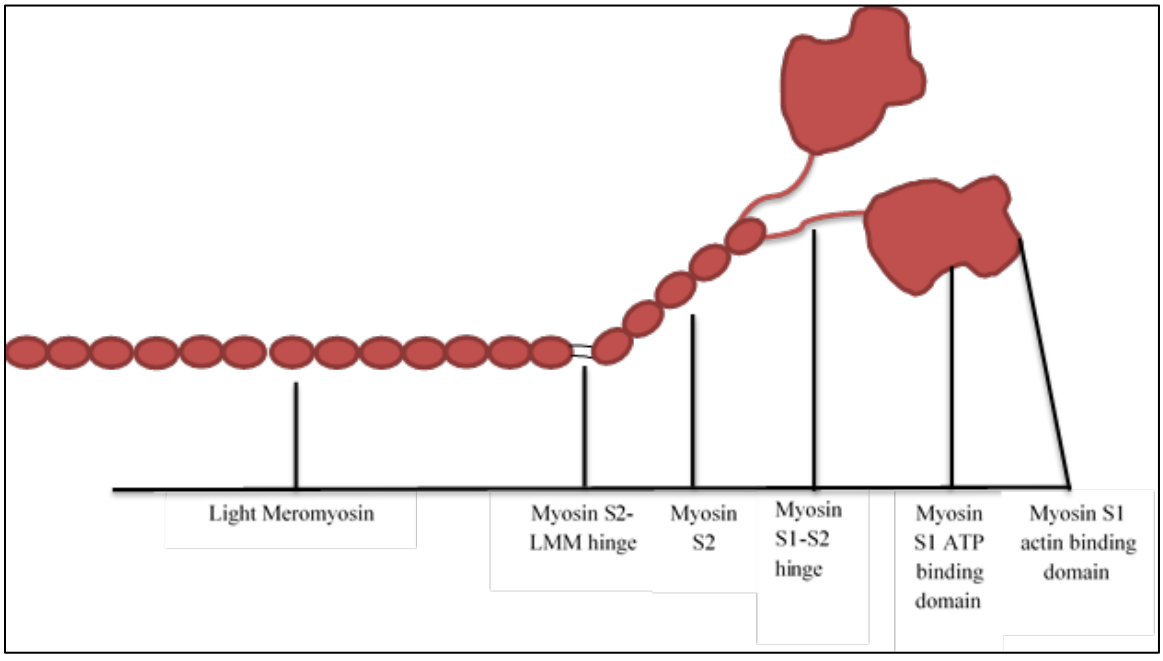

Figure 2. Cartoon representation of myosin II coiled coil structure with different parts labelled from the C-terminal region to the N-terminal region (from left to right).

Myosin S1 forms the two free globular heads of the myosin at its N-terminal end, each comprised of the ATP binding domain and actin binding site. Myosin S1 heads have the essential role of binding and hydrolysis of ATP at the ATP binding site and actin association at the actin binding site. The myosin S1 has two myosin light chains bound to them namely, myosin essential light chain and myosin regulatory light chain. Following the myosin S1-S2 hinge is the myosin S2 which is a coiled-coil linker between myosin subfragment-1 and light meromyosin. The light meromyosin is an extensive coiled coil which polymerizes with the light meromyosin of other myosin to form the thick filament backbone (Goodson, H.V. and Spudich, J.A. 1993)

1.3 Actin

Globular G-actin with bound ATP can polymerize to form the filamentous F-actin (Rees, M.K., and Young, M. 1967). Cap Z on I band of sarcomere marks the actin filament assembly center where new ATP bound G-actin monomers are added to maintain the F-actin assembly. G-actin has a molecular weight of 42 kDa. Every seventh actin on actin thin filament binds troponin and associated tropomyosin (Ebashi *et al*., 1969). The thin filament spans from the Cap Z of I band to the perimeter of H zone of A band of sarcomere.

1.4 Tropomyosin and Troponin Complex

Tropomyosin and the troponin complex are regulatory proteins associated with the thin filament. They have a regulatory role in allowing the myosin heads to bind productively to actin upon calcium signaling for active contraction of the muscle. Tropomyosin, a coiled coil filament made up of two different helical peptides is wound around the actin thin filament occupying or inhibiting the myosin binding region on the thin filament (Holmes *et al*., 1990). The troponin

complex has three different α-helical proteins namely troponin T, troponin C and troponin I (Greaser, M.L. and Gergely, J. 1971). Troponin C binds to calcium ions upon signal for muscle contraction, troponin T binds to tropomyosin to form a conjugate between tropomyosin and troponin complex and troponin I form a connection between actin thin filament and troponin-tropomyosin complex. Upon calcium binding to troponin C, the troponin complex undergoes a conformational change which results in displacement of tropomyosin on actin thin filament. Displacement of tropomyosin upon calcium binding to the troponin complex results in unblocking the myosin head binding domain on the actin thin filament which was blocked prior to calcium activation by tropomyosin (Vibert *et al*., 1997; Gordon *et al*., 2000; de Tombe *et al*., 2010).

1.5 Myosin Binding Protein C

Myosin binding protein C (MyBPC) is an accessory protein found in the sarcomere of cardiac and skeletal muscles (Starr, R., and Offer, G. 1971; Offer *et al*., 1973). MyBPC is 1270 amino acids long with molecular weight of around 140 kDa. It is located near the C zone of the sarcomere. The MyBPC comprises only 2% of the entire sarcomeric protein with myosin being nearly ten times more abundant. Typical structure of MyBPC and its association in contractile apparatus is detailed in the diagram (Figure 3). MyBPC comprises 11 protein domains labelled as C0-C10 from N-terminal to C-terminal. C0 at the N-terminal domain is specific to cardiac muscles and binds the regulatory light chain (Ratti *et al*., 2011), while it is absent in the skeletal muscles (Jeffries *et al*., 2011). There is a proline-alanine linker (P/A linker) between the C0 and C1 domains. There is also an m-domain between the C1 and C2 domains. The M-domain has three serine residues, which can undergo phosphorylation under β-adrenergic simulation (Lim, M.S., and Walsh, M.P. 1986; Mohamed *et al*., 1998; Schlender, K.K., and Bean, L.J. 1991; Kooij *et al*., 2013). Evidence suggests that the N-terminal region of MyBPC can bind to both actin and myosin

S2 weakly while the C-terminal domain binds LMM strongly (Moos *et al*., 1975).

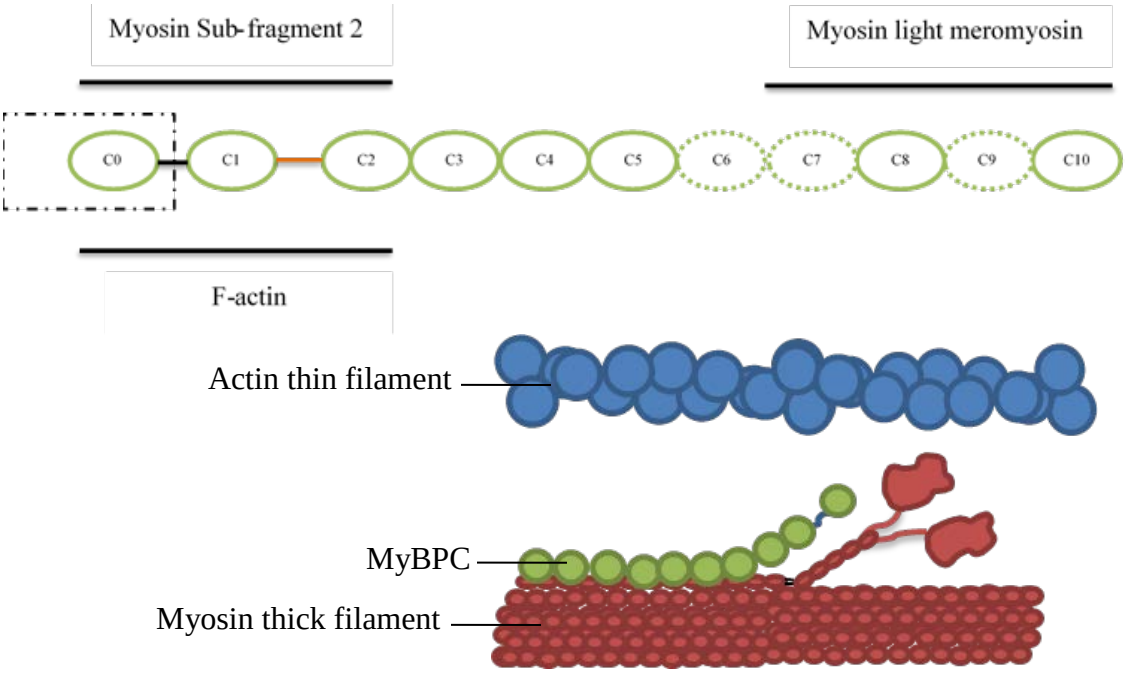

Figure 3. (Top) Diagram of myosin binding protein C and its different domains, with seven immunoglobulin domains (green circle), 3 fibronectin domains (dotted green circle), m-domain (orange line) between C1 and C2 domain and cardiac muscle specific C0 domain with proline alanine linker marked with dotted square. Labelled are the parts of the contractile apparatus binding to MyBPC. (Below) MyBPC binds to a thick filament at its C-terminal end.

When serine residues at the m-domain are dephosphorylated, MyBPC binds to myosin at the S2 region with increased affinity (Nag *et al*., 2017; Levine *et al*., 2001; Starr, R., and Offer, G., 1978; Weisberg, A., and Winegrad. S., 1996). When serine residues at the M-domain are phosphorylated, MyBPC binds to actin thin filaments (Munn *et al*., 2011; Whitten *et al*., 2008; Rybakova *et al*., 2011). This myosin-actin switch upon phosphorylation seems to play an important role in regulating acto-myosin interaction in cardiac and skeletal sarcomere (Previs *et al*., 2012, 2016; Gautel *et al*., 1995).

1.6 Muscle Contraction and its Regulation

The contraction of muscle occurs in four stages. Four stages of muscle contraction are

represented in Figure 4. This mode allows the docking of myosin S1 heads on to actin thin filaments and sliding actin thin filaments towards the M line of the sarcomere through binding and hydrolysis of ATP on myosin S1 heads (Lymn, R.W. and Taylor, E.W. 1971; Taylor, E.W. 1977).

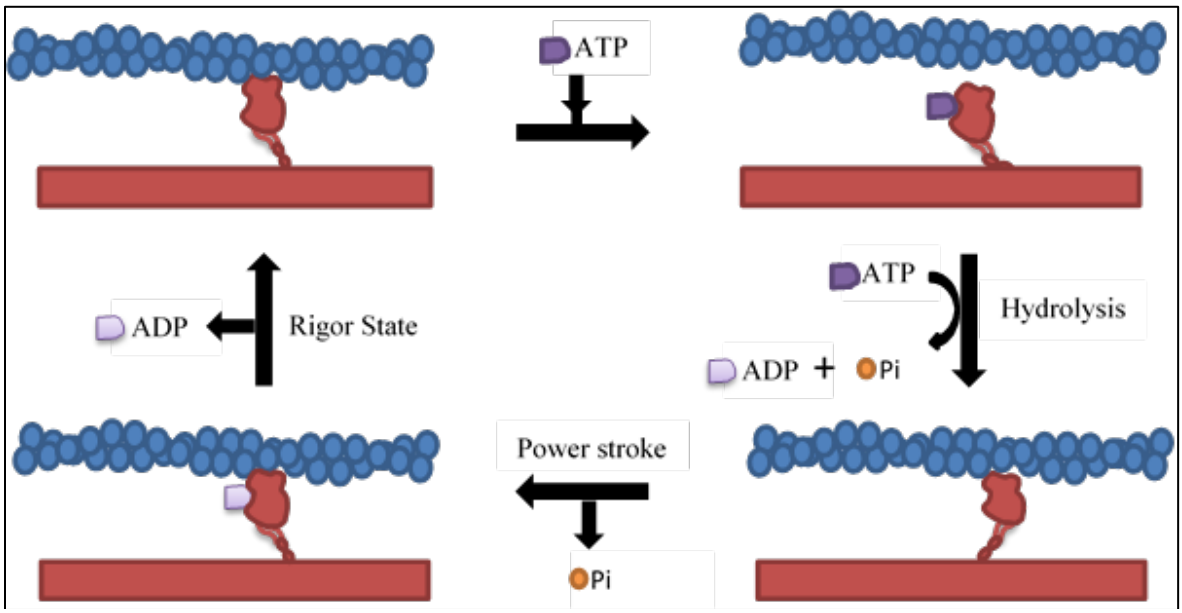

Figure 4. Stages of acto-myosin interaction during muscle contraction. (1) Myosin S1 head (red) bound to actin thin filament after power stroke (blue). (2) Release of myosin S1 heads upon binding of ATP. (3) After hydrolysis of ATP to ADP and Pi, myosin S1 has a cocked conformation followed by weak binding to actin thin filament (4) After weak binding of myosin S1 head to the actin thin filament, the release of Pi results in the power stroke step allowing the actin thin filament to be pulled in the direction of M-line of sarcomere. Release of ADP brings the myosin to rigor state where it is ready to accept another molecule of ATP for another cycle of force generation.

There are four stages to this mode; the first stage is the release of already bound myosin S1 heads to actin thin filament upon binding of ATP molecule on myosin S1 heads. The binding of ATP molecule on nucleotide binding site of myosin S1 heads changes the conformation of the actin binding region on myosin S1 heads thus reducing the affinity of myosin S1 heads to the actin thin filament. This conformational change results in the release of myosin S1 heads from actin thin filaments.

Second stage is the hydrolysis of ATP in to adenosine diphosphate (ADP) and inorganic

1 2

phosphate (Pi) on myosin S1 heads. Myosin S1 heads achieves the cocked position after hydrolysis of ATP; the change in position of myosin S1 head is along the thick filament in the direction of Z line. At this stage, ADP and Pi remains tightly bound to myosin S1 head (Rayment *et al*., 1996).

The third stage is the force generating step in which myosin S1 heads first bind weakly to actin thin filament which results in the release of Pi from myosin S1 head. Pi release from myosin S1 heads elicits the power stroke, in which the myosin S1 heads bind tightly in a new conformation on actin thin filament and pull the actin thin filament in the direction of M line of a sarcomere. In the course of power stroke, ADP is also released from myosin S1 heads returning them to their original conformation (White and Taylor, 1976; Siemankowski *et al*., 1985; Goldman, 1987).

The fourth stage is where the myosin S1 heads remain attached to actin filament where it is ready to bind another ATP molecule and undergo the same cycle of power stroke.

Muscle contraction has two modes working synchronously to actively contract the muscle through acto-myosin interaction. The two modes are the influx of calcium ions in the cytosol of muscle fiber and the hydrolysis of ATP by the myosin S1 heads. The signal for muscle contraction passed on by nerve results in the opening of calcium release channels on sarcoplasmic reticulum of the muscle fiber. Opening of the channels releases the calcium ions in to the cytosol of fiber (Walker, S.M., and Schrodt, G.R. 1967). These calcium ions are taken up by the troponin complex, which consequently undergoes a conformational change. This change induced to the troponin complex displaces the tropomyosin position on the actin thin filament. Prior to this displacement, tropomyosin blocks the myosin S1 head binding domains on actin thin filament. Upon displacement, the tropomyosin unblocks the myosin S1 head binding domains on actin thin filament thus allowing myosin S1 heads to dock on actin thin filament (Vibert *et al*., 1997).

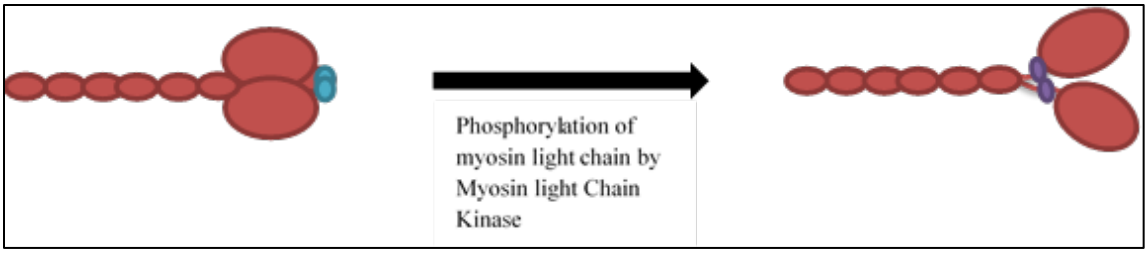

Figure 5. Smooth muscle myosin activation by phosphorylation of myosin light chain by myosin light chain kinase from dephosphorylated (cyan) to phosphorylated (purple) stage.

These modes of regulation are found in cardiac and skeletal muscles, however smooth muscle has a different regulatory mechanism. In smooth muscle, the calcium signaling is triggered by binding of calcium to calmodulin which then binds to caldesmon, this calmodulin-caldesmon complex then dissociates from actin thin filament thus clears off the myosin binding site on actin thin filament. However, the primary mode of regulation is the phosphorylation of light chains in smooth muscle myosin by myosin light chain kinase (Ochsnaer, M. 1997). This phosphorylation allows myosin S1 heads to be free from each other and the myosin S2 and bind to the actin thin filament through the previously explained hydrolysis of ATP and generation of the power stroke (Figure 5).

1.7 Familial Hypertrophic Cardiomyopathy

Familial hypertrophic cardiomyopathy (FHC) is an autosomal dominant genetic disorder of the heart muscles. FHC results in the enlargement of heart and potentially sudden death of the person (Semsarian *et al.*, 2015). Mutations for FHC are mostly point mutations and missense mutations in proteins of the contractile apparatus of cardiac muscle. Most mutations are found to be in the myosin heavy chain followed by cardiac myosin binding protein C and fewer mutations reported in myosin light chains, titin, actin, tropomyosin and troponin complex (Erdmann *et al.*, 2003; Richard *et al.*, 2003; McNally *et al.*, 2015). Haploinsufficiency of mutant MyBPC is a reason

for this disorder when a single allelic product is not enough to rescue the phenotype. A single mutation in a protein of the contractile apparatus of heart muscle could cause a detrimental effect, since the heart muscle undergoes constant cycles of contraction and relaxation to circulate the blood throughout the body of an organism. Any slight change in heart's contractile apparatus could throw off this tight regulation which would result in this severe disorder. There are two types of cardiomyopathies caused by mutations to contractile proteins, namely familial hypertrophic cardiomyopathy (FHC) and dilated cardiomyopathy (DCM). Anatomy of FHC and DCM hearts compared to normal human heart are illustrated in Figure 6.

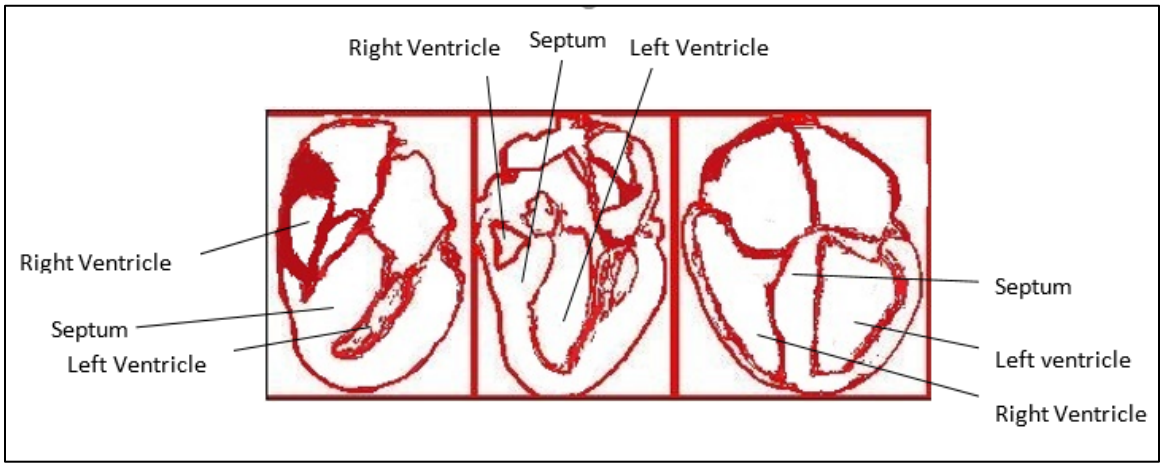

Figure 6. Anatomy of cardiomyopathic hearts. From left to right, FHC human heart with asymmetrical thickening of ventricles leaves less blood volume for pumping. Healthy heart with plenty of negative space in the left ventricle. Heart with dilated cardiomyopathy phenotype.

FHC results in the hypertrophy of the ventricles of the heart. Ventricles of FHC heart are thickened due to hypertrophy of ventricular muscles. Thickening of the ventricles of heart significantly reduces the negative space present in the ventricles of heart thus decreasing the amount of blood pumped through a FHC heart resulting in the sudden death of the person suffering from FHC. In DCM the ventricles of heart are loosened and thin, even though the negative space in ventricles of DCM heart is increased but the ventricular muscles of DCM are weak to pump the

blood causing the death of the person by heart failure (Cho *et al*., 2016; Semsarian *et al*., 2015; Jean, M. 2003).

FHC point mutations have been reported all along the cardiac muscle myosin protein (Richard *et al*., 2003). Mutation in the myosin S1 head would affect the binding of myosin S1 heads to actin thin filament upon muscle contraction, thus having a strong implication on the force output of the cardiac muscle. Mutations in the LMM region could be argued that it would interfere with bundling of LMM to each other at M line thus affecting the overall assembly of myosin thick filament on the M line of sarcomere. But there is a cluster of mutations in the proximal myosin S2 region reported for cardiomyopathy highlighted in Figure 7. The families suffering from these myosin S2 cardiomyopathic mutations had 50% of their family dead by sudden cardiac arrests (Tesson *et al*., 1998; Waldmüller *et al*., 2003).

The myosin S2 has not been assigned any functional role yet apart from being a coiled coil linker between myosin S1 heads and extensive coiled coil LMM. This begs the question if there is more functional role to myosin S2 rather than just being a coiled coil linker. Myosin S2 coiled coil might have a role in regulating the acto-myosin interaction and overall force produced.

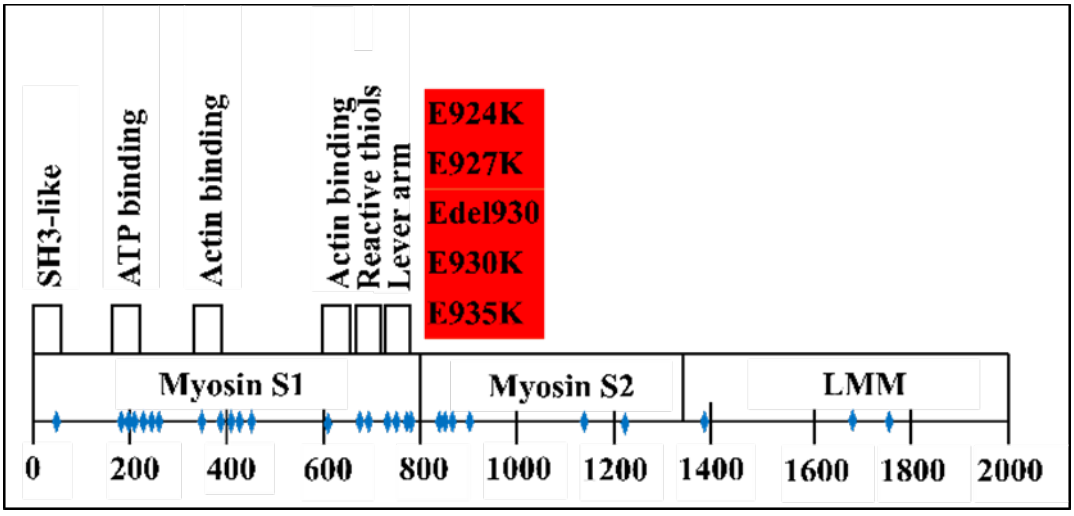

Figure 7. Familial hypertrophic cardiomyopathy point mutations (blue diamonds) across MYH7 gene with point mutations highlighted at the proximal myosin S2 region.

1.8 Hypothesis and Testing

Mutations in myosin S2 coiled coil structure are responsible for a deadly cardiac disorder, indicates that myosin S2 region might have an effect on the acto-myosin interaction thus having an overall effect on the force produced through this interaction. Ensemble force produced by the sarcomere in muscle is summarized by the formula (Spudich, J.A. 2014);

$$F_e = f\,[(t_s/t_c)*N_t]$$

where; F_e = Ensemble force

f = intrinsic force of myosin head

t_s = myosin head in strongly bound state

t_c = total cycle time of myosin from bound to unbound state

N_t = total number of myosin heads available to bind to actin

In cardiomyopathies and skeletal myopathy the Fe is either higher or lower than normal which results in the disease due to hypo contraction or hypercontraction. Fe can be changed by the variation in either f, t_s, t_c or N_t. Mutations in myosin S1 heads would affect the f, t_s, t_c or N_t. For example a mutation which would increase the intrinsic force of myosin S1 head as well as the time it spends in the strongly bound state and decrease the amount of time it spends to go from bound to unbound state would increase the ensemble force and vice versa.

If the N_t is increased or decreased as well then it would increase or decrease the ensemble force. But what about the myosin S2 mutations, myosin S2 which is just a linker could not have a direct effect on f, t_s or t_c but it could regulate the amount myosin heads available to bind actin. The myosin S2 region might modulate the amount of total number of myosin heads available to bind to actin (N_t) thus having an effect over the force produced during an active acto-myosin interaction.

Earlier work has shown that both smooth and skeletal myosin S1 heads are dynamic and they can achieve a bent conformation. Electron micrographs have suggested that these myosin S1 heads can fold back on its long tail domain (Elliott, A., and Offer, G. 1978). Sedimentation velocity of smooth muscle myosin gave two structures which were interchangeable depending on ionic concentration. The 6S and 10S monomeric structures were identified where the 10S monomeric myosin had its head folding back on to its tail while 6S myosin monomer had its heads free and unbound to its tail (Trybus *et al*., 1982; Reisler *et al*., 1986). Electron micrographs of a chimera created by skeletal myosin HMM with smooth muscle myosin light chain also show the folding of myosin S1 heads on to the available myosin S2 region (Sata *et al*., 1997). Potentially related anisotropy experiments with rabbit skeletal myosin gave two regions of dynamic wobbling one being the myosin S1 head and other being a 14 nm long region following the myosin S1-S2 hinge or the proximal myosin S2 region which corresponds with the attachment site of myosin heads to S2 (Kinosita *et al*., 1984).

Cryo-electron micrograph and atomic modelling studies of tarantula thick filaments has shown that myosin S1 heads have a much more switched off state where they bind to each other and then fold back and bind to proximal myosin S2 region (Woodhead *et al*., 2005). The transition of this myosin heads from switched off to switched on state is achieved by calcium mediated phosphorylation of myosin light chain in these invertebrate thick filaments. Currently a mechano-sensing model for the transition of myosin heads from switched off to switched on state has been proposed where the stress on the thick filament axis regulates the amount of myosin heads available with no mediation by phosphorylated myosin light chains (Fusi *et al*., 2016).

In addition to these studies showing that myosin heads can fold back and bind myosin S2 and that myosin S2 is dynamic, namely in the 14 nm of proximal myosin S2 region, it is

hypothesized that in vertebrate striated skeletal muscles and cardiac muscles, the phosphorylation of myosin light chain by myosin light chain kinase could release the myosin heads from their folded back switched off state to a freely available switched on stage. All these data together raise the next plausible thought that a stable myosin S2 with the binding of myosin binding protein C could keep the myosin S1 heads in the blocked or switched off stage. When MyBPC is phosphorylated the myosin S1 heads transition from the switched off to the switched on state to produce active contraction (Figure 8) (Jeffries *et al*., 2011). This regulation could be affected by cardiomyopathy mutations in either MyBPC or myosin.

When there is a myosin S2 mutation, the myosin S2 coiled coil could become either highly stable or highly unstable. The highly stable myosin S2 would cause the myosin S1 to remain bound to myosin S2 and in a prolonged switched off state in spite of MyBPC phosphorylation, thus there will be shortage in the amount of active myosin S1 heads available to bind actin leading to hypo-contraction which is a characteristic of DCM.

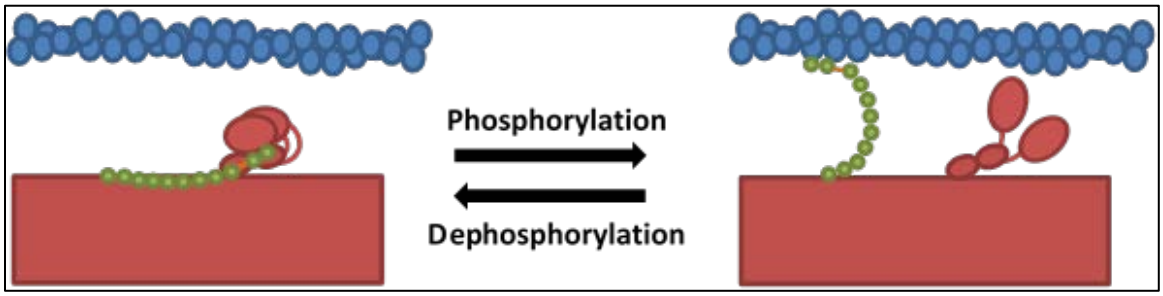

Figure 8. Acto-myosin switch of MyBPC by phosphorylation. The serine residues at m-domain (orange line) of MyBPC (green) when desphosphorylated, MyBPC remains bound to myosin S2 at its N-terminal end and allowing myosin S1 heads to fold back and bind myosin S2, when phosphorylated MyBPC binds to actin thin filaments (blue) allowing myosin S1 heads to be free from myosin S2 and able to bind actin filaments (Jeffries et al., 2011).

On the other hand, highly unstable myosin S2 would lose the binding of myosin S1 heads, thus making them readily available to bind actin leading to hypercontraction a characteristic of FHC. Mutations in myosin binding protein C have been documented to cause the truncation of N-

terminal region in MyBPC. This would result in the hindering of the stability of myosin S2 caused by the binding of MyBPC to it and unstable myosin S2 would result in more myosin S1 heads available to bind actin thus leading to hypercontraction and sudden death in case of FHC. Thus availability of myosin S1 heads (N_t) and its effect over the ensemble force (F_e) could be correlated with the flexibility or stability of myosin S2.

The effect of stable or unstable myosin S2 region over the myosin filament and the force produced can be studied using gravitational force spectroscopy, *in vitro* motility assay and myofibril contractility assay. Several myosin S2 binding proteins like its natural binding partner myosin binding protein C (MyBPC), and synthetically produced myosin S2 site specific stabilizer peptide and destabilizer peptide are utilized to modulate the flexibility of myosin S2 region. The effect of this modulated myosin S2 over the stability of the myosin S2 coiled coil and the force produced could be studied and answer whether unstable or stable myosin S2 coiled coil would increase or decrease the amount of contraction in myofibrils and net force produced through acto-myosin interaction through several force, contractility and motility assays.

1.8.1 Myosin Binding Protein C Stabilizes the Myosin S2 Coiled Coil and Decreases the Amount of Force Produced.

Myosin binding protein C isolated and purified from rabbit skeletal myofibrils is used to test the flexibility and stability of the myosin S2 region in rabbit skeletal myosin molecules. The gravitational force spectroscopy (GFS) assay is set up by using polyclonal antibody raised against single α-helix of myosin S2 coiled coil to anchor the single skeletal myosin between immobile edge and mobile bead. Force required to pull the myosin molecule at this S2 region would be measured and attested as a control. The next assay is similar but with the myosin molecule treated with purified MyBPC. The force-distance curve at myosin S2 in the absence and presence of

MyBPC confirms the effect of MyBPC over the stability of myosin S2 coiled coil. The initial hypothesis is that the force required to pull apart the myosin S2 coiled coil in the presence of MyBPC would be more compared to the force required to pull apart the myosin S2 coiled coil in absence of MyBPC.

The next question is if the stabilization of myosin S2 coiled coil by MyBPC has an effect over acto-myosin interaction. This effect is tested by performing the actin filament sliding over myosin thick filament in presence and absence of MyBPC through the classic *in vitro* motility assay. Here the use of myosin thick filaments rather than myosin HMM facilitates measurements with full length MyBPC, since MyBPC binds to LMM and myosin S2. The myosin thick filament is ideal to represent the natural binding scenario for MyBPC and its effect over the sliding velocity of actin filaments. The initial hypothesis is that MyBPC slows down actin filament sliding over myosin thick filaments. GFS and *in vitro* motility data together verify the stabilizing effect over myosin S2 coiled coil, and this stable myosin S2 coiled coil reduces actin sliding over the myosin thick filament.

1.8.2 Stabilizer Peptide is Specific to Myosin S2 Coiled Coil and Stabilizes the Myosin S2 Coiled Coil thus Decreasing the Amount of Force Produced

The stabilizer peptide designed earlier through computer simulations binds and wraps around the proximal myosin S2 coiled coil at amino acids 924-942. This peptide was designed to stabilize the myosin S2 coiled coil in the context of reducing the amount of myosin S1 heads available to bind actin.

The first test is to check the binding specificity and affinity of stabilizer peptide to myosin S2 coiled coil. Competitive Enzyme Linked Immunosorbent Assay (cELISA) is performed to confirm the binding specificity and affinity of the stabilizer peptide to myosin S2 coiled coil. A

site-specific polyclonal antibody raised against a single α-helix of myosin S2 is used to compete with the stabilizer peptide to bind myosin S2 in rabbit skeletal myosin molecule as well as human cardiac myosin S2 peptide. The wells are coated with rabbit skeletal myosin and to the well is added an appropriate amount of human cardiac myosin S2 peptide that binds the polyclonal antibody and when washed away there won't be enough polyclonal antibody to bind myosin S2 of rabbit skeletal myosin. This leads to low or no color development leading to lower OD. Expected result is to see the change in OD from lower OD with no stabilizer to higher OD with increasing amounts of stabilizer peptide and then again back to lower OD with higher amounts of stabilizer peptide would be able to confirm the dissociation constant of stabilizer peptide binding to myosin S2 as well convey the cross-specificity of stabilizer of myosin S2 of human cardiac and rabbit skeletal myosin.

After confirming the specificity and binding affinity of the stabilizer peptide to myosin S2, next is to check whether the stabilizer peptide has an effect over myosin S2 coiled coil stability. The GFS assay is performed to confirm the stabilization of myosin S2 coiled coil by binding of stabilizer peptide. In this assay, the actin and myosin S1 rigor binding is used to suspend the myosin molecule between the immobile edge and a mobile bead. The initial hypothesis is that to uncoil the myosin S2 in presence of stabilizer peptide requires more force than to uncoil the myosin S2 in absence of stabilizer peptide.

The next test is to check whether this stabilization of myosin S2 coiled coil has an effect over contraction of the myofibril. The myofibril contractility assay is performed to confirm the effect of the stabilizer peptide. In this assay, the lengths of the sarcomere are measured before and after adding ATP to simulate contraction in myofibrils. Control is to measure the shortening of sarcomeres without any stabilizer peptide and test the shortening of sarcomeres in the presence of

stabilizer peptide. The expected result is to observe less contraction in the sarcomeres of myofibrils treated with stabilizer peptide compared to the myofibrils sans stabilizer peptide. This reduction in amount of contraction in sarcomeres of stabilizer-treated myofibrils would confirm that stabilized myosin S2 coiled coil would reduce the amount of myosin S1 heads available to bind actin thus reducing the amount of force produced through acto-myosin interaction.

The *in vitro* motility assay of actin filaments over myosin HMM treated with stabilizer peptide confirms the effect of stabilizer peptide over amount of force produced through acto-myosin interaction. The control for this assay is purified rabbit skeletal myosin HMM immobilized on dichloromethylsilane-treated coverslip and actin filaments allowed to slide over these immobilized myosin HMM. Test would be to allow the actin filament to slide over the same immobilized myosin HMM by adding stabilizer peptide to the same setup. Thus calculating sliding filament velocity of actin thin filaments over myosin HMM in absence and presence of stabilizer peptide confirms the effect of stabilizer peptide over the total force produced through acto-myosin interaction. The initial hypothesis is to observe a reduction in sliding filament velocity of actin filaments over myosin in presence of stabilizer peptide.

All of these experiments performed together validate the binding specificity and affinity of the stabilizer peptide to the myosin S2 region. These experiments also confirm the stabilizing effect by binding of stabilizer peptide to myosin S2 coiled coil. Its stabilization results in reduction of contractility in myofibrils along with the amount of force produced through acto-myosin interaction.

1.8.3 The Destabilizer Peptide is Specific to Myosin S2 Coiled Coil and Destabilizes the Myosin S2 Coiled Coil thus Increasing the Amount of Force Produced

The destabilizer peptide was designed through computer simulations to interfere with the

formation of the myosin S2 coiled coil. The destabilizer peptide binds to one α-helix of the myosin S2 coiled coil and disrupts the natural coiled coil formation of two individual α-helices of myosin S2 molecule. The destabilizer peptide was designed against the same proximal myosin S2 region amino acid residues from 924-942 as the site-specific polyclonal antibody with the intention of producing a similar effect. This peptide was designed to destabilize the myosin S2 coiled coil in the anticipation of increasing the amount of contraction and force produced through acto-myosin interaction.

The first assay is to check the binding specificity and affinity of destabilizer peptide to myosin S2 coiled coil. cELISA is performed as previously with the polyclonal antibody raised against myosin S2 competing with the destabilizer peptide to bind the myosin S2 region of rabbit skeletal myosin coated on the wells and human cardiac myosin S2 suspended in the wells. Similar effects are observed as explained earlier for the stabilizer peptide. The lower-higher-lower OD trend depending on increasing concentration of destabilizer peptide confirms the binding specificity and affinity of destabilizer peptide to myosin S2.

After confirming the binding specificity and affinity of the destabilizer peptide to myosin S2, the next assay is to test whether the destabilizer peptide destabilizes the myosin S2 coiled coil. GFS confirms the effect of destabilizer peptide over the flexibility and stability of myosin S2 coiled coil. Again the actin myosin S1 binding property is used to suspend the myosin molecule between immobile edge and mobile bead. The GFS assay is performed with the myosin molecule in presence and absence of destabilizer peptide. Force-distance curves of myosin molecule in the presence and absence of destabilizer peptide establish the effect of the destabilizer peptide. The initial hypothesis is that the force required to pull apart the myosin coiled coil in the presence of the destabilizer peptide is less than when compared with the myosin molecule in absence of

destabilizer peptide thus confirming the destabilizing effect of destabilizer on myosin S2 coiled coil.

After confirming the destabilization of myosin S2 coiled coil by destabilizer peptide, the next experiment is to see the effect of this destabilization on myofibril contraction. The myofibril contractility assay establishes the effect of the destabilizer. The length of the sarcomeres are measured in myofibrils before and after adding ATP to establish the control and next assay would be to measure the length of sarcomeres in myofibrils treated with destabilizer. The initial hypothesis is that the percent contraction observed in myofibrils treated with destabilizer is more than compared to that of sarcomeres in myofibrils without the destabilizer treatment. This assay confirms that destabilization of myosin S2 coiled coil increases contraction in myofibrils and thus causes a net increase in force production through acto-myosin interaction.

Increase in motility due to destabilization of myosin S2 coiled coil with destabilizer peptide is tested by measuring the actin sliding velocity of myosin HMM treated with destabilizer peptide. The *in vitro* motility of actin filaments sliding over HMM in the presence and absence of destabilizer peptide is performed. The initial hypothesis is to observe a higher sliding velocity of actin over myosin HMM treated with destabilizer peptide compared to HMM without destabilizer peptide. This increase in actin sliding velocity confirms that destabilization of myosin S2 coiled coil increases the amount of force produced through acto-myosin interaction.

All these experiments performed together confirm the binding specificity and affinity of the destabilizer peptide to the myosin S2 region. Destabilization of the myosin S2 coiled coil by destabilizer peptide would result in an increase in amount of myofibril contraction and the amount of force produced through acto-myosin interaction.

Competitive ELISA confirms the binding specificity and affinity of the stabilizer and the

destabilizer peptide to the myosin S2 coiled coil. MyBPC has been already proven to bind myosin at LMM and myosin S2. Gravitational force spectroscopy verifies the stabilization of the myosin S2 coiled coil by binding of MyBPC and the stabilizer peptide by higher amount of force required to pull myosin S2 coiled coil apart in presence of these molecules. On the other hand GFS establishes the destabilization of myosin S2 coiled coil by destabilizer peptide by observing a lower amount of force required to pull myosin S2 coiled coil in presence of destabilizer peptide.

The myofibril contractility assay confirms the effect of stability of myosin S2 over the myofibril contraction. Stabilizer peptide stabilizes the myosin S2 coiled coil and reduction in the percentage of sarcomere shortening in presence of stabilizer peptide compared to sarcomere shortening in absence of it and confirms that the stable myosin S2 reduces the amount of contraction in myofibrils. The destabilizer peptide makes the myosin S2 coiled coil unstable and increases sarcomere shortening in myofibrils treated with destabilizer peptide compared to myofibrils without the destabilizer peptide, thus confirming that unstable myosin S2 coiled coil increases the amount of contraction in the myofibril.

The *in vitro* motility assay confirms the effect of stability of myosin S2 coiled coil over amount of force produced through acto-myosin interaction. The MyBPC and the stabilizer peptide stabilize the myosin S2 coiled coil and the destabilizer destabilizes the myosin S2 coiled coil. Decreased sliding velocity of actin over myosin in presence of stabilizer peptide and MyBPC and increased sliding velocity of actin in presence of destabilizer peptide confirm that stable myosin S2 decreases the amount of force produced and unstable myosin S2 increase the amount of force produced through acto-myosin interaction.

All these experiments performed confirm that when the myosin S2 coiled coil is stabilized by MyBPC and the stabilizer peptide, the contraction in myofibrils and the amount of force

produced by acto-myosin interaction decreases. When the myosin S2 coiled coil is destabilized by destabilizer peptide the contraction in myofibrils and the amount of force produced by acto-myosin interaction increases. Stable myosin S2 coiled coil decreases and unstable myosin S2 coiled coil increases the amount of contraction and net force produced which indirectly gives substantial support to the idea that myosin S2 stability regulates the amount of myosin S1 heads available to bind actin. Stable myosin S2 coiled coil reduces the amount of myosin S1 heads available thus reducing myofibril contraction and net force production and vice versa in case of unstable myosin S2 coiled coil.

CHAPTER 2

MATERIALS AND METHOD

2.1 Materials

2.1.1 Myofibrils

Rabbit psoas and back muscle, approximately 20 grams was suspended in 200 ml of buffer (20 millimolar (mM) potassium chloride, 10 mM bis-tris and 4 mM ethylenediaminetetraacetic acid with pH 6.8) at 4 ^{0}C. The suspension was homogenized in a blender for five seconds at high speed. The homogenate was centrifuged in a Sorval RC-5 centrifuge at 5000 rotations per minute (rpm) for five minutes. The pellet obtained was washed three times in ten times the volume of the buffer used above. For each wash, the pellet was suspended in buffer and centrifuged and supernatant was discarded for each wash. The pellet obtained after last wash was suspended in the same buffer containing 50% glycerol and stored in -20 ^{0}C for future use (Root, D.D., and Reisler, E. 1992).

2.1.2 Myosin

Myosin is extracted by placing ground rabbit skeletal back muscles in cold extraction buffer (0.3 molar (M) potassium chloride, 0.072 M sodium phosphate monobasic, 0.063 M potassium phosphate dibasic, and 0.001 M ethylene diamine tetraacetic acid with pH 6.5) with volume of buffer being three times the volume of ground rabbit back muscles. The mixture was stirred gently for 15 minutes. Followed by addition of distilled water at 4 ^{0}C, with volume ten times the volume of ground rabbit muscles. Again the mixture was stirred gently for 20 minutes. The mixture was filtered using the cheese cloth covered funnel in to a flask, to the filtrate obtained, ditilled water was added at around fifteen times the volume of filtrate and allowed to precipitate over night at 4 ^{0}C. The clear supernatant was decanted and the remaining precipitate was

centrifuged at 7000 rpm for 10 minutes in the GSA rotor. The precipitate obtained was suspended in approximately 5 ml of 2 M potassium chloride. The volume was measured and the concentration was adjusted to 0.3 M with cold distillled water. The mixture was centrifuged at 9000 rpm for 45 minutes to precipitate the contaminants. The concentration of the supernatant obtained was adjusted to 0.033 M potassium chloride with cold distilled water. Myosin concentration was determined by extinction coefficient of 0.55 $(mg/ml)^{-1}$ cm^{-1} at 280 nm. These rabbit skeletal myosin is then flash freezed in liquid nitrogen and stored at -70 ^{0}C in small aliquots. (Xu, J., and Root, D.D. 2000; Godfrey, J.E., and Harrington, W.F. 1970; Frederiksen, D.W., and Cunningham, L.W. 1982; Gundapaneni *et al*., 2005).

2.1.3 Myosin Binding Protein C

MyBPC was purified from frozen rabbit back skeletal myofibrils with the method described (Furst *et al*., 2011). Multiple chromatography techniques were employed to purify MyBPC from crude extract of MyBPC. MyBPC isolated had a pI around 5.6 and molecular weight of 150 kDa and concentration was determined at extinction coefficient of 1.09 $(mg/ml)^{-1}$ cm^{-1} at 280 nm (Offer *et al*., 1973; Yamamoto, K. 1984). The concentration of MyBPC obtained was 0.84 µM, and approximately 75% was the major isoform of MyBPC isolated from rabbit skeletal myofibrils and stored in small aliquots at -70 ^{0}C in the freezer.

2.1.4 Actin

Actin was isolated from the acetone powder of the rabbit back muscles as described (Xu, J., and Root, D.D. 2000; Spudich, J.A. and Watt, S. 1971; Kron *et al*., 1991; Gundapaneni *et al*., 2005)). The filtered material obtained on to the cheese cloth of myosin extraction was extracted

and added to the two times the volume of buffer (0.6 M potassium chloride, 0.4 M sodium bicarbonate and 0.01 M sodium carbonate). The extract was further diluted in equal volume of distilled water and filtered through the cheese cloth. The residue obtained was washed with five volumes of 0.4% sodium bicarbonate solution for 30 minutes at room temperature and again filtered through cheese cloth. The residue was washed with ten volumes of distilled water for 5 minutes and filtered again through cheese cloth. The residue obtained was washed with three voulmes of acetone for 10 minutes and filtered through cheese cloth. Acetone wash step was repeated twice, and the residue obtained was allowed to dry at room temperature overnight. Acetone powder obtained was scraped off and stored dessicated at -20 ^{0}C.

Acetone powder of muscle about 5 grams was suspended in 30 ml of G-buffer (2 mM Tris hydrochloric acid, 0.2 mM adenosine triphosphate, 0.5 mM 2-mercaptoethanol, and 0.2 mM calcium chloride with pH 7.6) for 120 minutes at 4 ^{0}C. This mixture was centrifuged at 15,000 rpm for 15 minutes and supernatant was collected. The supernatant was filtered through 0.45 µm millipore filter. To the filtered supernatant a final concentration of 50 mM potassium chloride and 1 mM magnesium chloride was added to polymerize actin for 120 minutes at room temperature. Later to that 0.6 M potassium chloride was added and stirred continuously for 30 minutes followed by centrifuging at 40,000 rpm for 30 minutes at 4 ^{0}C. Pellet obtained was suspended in G-buffer and dialyzed against G-buffer with continuous stirring for 72 hours. G-buffer was refreshed every 24 hours. The dialyzed product was centrifuged at 40,000 rpm for 60 minutes at 4 ^{0}C and supernatant containing G-actin was extracted. The concentration of actin was determined at extinction coefficient of 0.63 $(mg/ml)^{-1}$ cm^{-1} at 290 nm (Xu, J., and Root, D.D. 2000). This G-actin was polymerized in 50 mM potassium chloride, later flash frozen and stored at -70 ^{0}C in small aliquots for experimental use.

2.1.5 Human β-Cardiac Myosin S2 Peptide

Identification of FHC mutation hotspots in the myosin S2 region especially in the proximal end of myosin S2 gave the thought of that region being important for the function of muscle regulation in heart (Richard *et al*., 2003). Several point mutations such as glutamate substitution to lysine at 924^{th}, 927^{th}, 930^{th} and 935^{th} residues (Figure 7) and glutamate deletion at 930^{th} residue, gave the idea to chemically synthesize the peptide from amino acid range 924 to 942 from human β-cardiac myosin gene MYH7. The sequence was obtained from the PDB structure of the human β-cardiac myosin S2 (2FXM) (Blankenfeldt *et al*., 2006).The 19 amino acid long peptide sequence is as follows from NH_2-EMNERLEDEEEMNAELTAK-COOH where E = glutamate, M = methionine, N = asparagine, R = arginine, L = leucine, D = aspartate, A = alanine, T = threonine, K = lysine amino acids. This human cardiac myosin S2 peptide was synthesized chemically by Bio-synthesis Inc., Lewisville, Texas, United States.

2.1.6 Monoclonal Antibodies

Monoclonal antibody, MF30 to myosin subfragment-2 and MF20 to light meromyosin were obtained from the Developmental Studies Hybridoma Bank. The antibodies were purified by gel filtration chromatography Sephadex G-75. MF30 samples were later flash frozen and stored at -70 ^{0}C and MF20 samples were stored in 4 ^{0}C for experimental use.

2.1.7 DNA with DTPA Tagged dCTP

Lambda Phage DNA (N3110S, New England Biolabs, Inc.) was extended at its overhanging ends for an hour at 30 ^{0}C in presence of *Taq* DNA polymerase (D1806, Millipore Sigma) and deoxyadenosine triphosphate (dATP), deoxyguanosine triphosphate (dGTP),

deoxythymidine triphosphate (dTTP) (Thermo Fisher Scientific) with diethylenetriamine pentaacetate (DTPA) tagged deoxycytosine triphosphate (dCTP). dCTP was tagged with DTPA in the presence dimethylsulfoxide at equimolar concentrations. DTPA tagged dCTP was further purified by ion exchange chromatography and stored in small aliquots in -70 ^{0}C for experimental use.

2.1.8 Polyclonal Antibody against Myosin S2

Polyclonal antibody was raised against the same small peptide sequence of α helix human cardiac myosin S2. This peptide was chemically synthesized and conjugated to albumin. The peptide size was not large enough to illicit an immune response hence was conjugated to albumin to invoke an immune response. This albumin conjugated to human cardiac myosin S2 peptide was injected in to a guinea pig and the polyclonal antibodies were harvested from the serum. Chemical synthesis of peptide and antibody production was performed by Bio-synthesis Inc., Lewisville, Texas, United States.

2.1.9 Stabilizer Peptide

Stabilizer peptide was designed against the same glutamate rich human cardiac myosin S2 peptide. Computer simulations were performed with several lengths of levo (l) form of positively charged poly lysine residues (Singh, R.R., Qadan, M.M *et al*., 2017). The idea behind using positively charged poly lysine was to allow them to bind negatively charged glutamate rich human cardiac myosin S2 peptide, also use of ‘l or levo’ form was to allow them to easily incorporate in an organism without eliciting an immune response.

Through several computer simulations, stabilizer peptide was designed. The stabilizer peptide designed was able to wrap around the coiled coil formed by human β-cardiac myosin S2 peptide shown here through computer simulation (Figure 9). This stabilizer peptide was chemically synthesized and provided by Bio-synthesis Inc., Lewisville, Texas, United States.

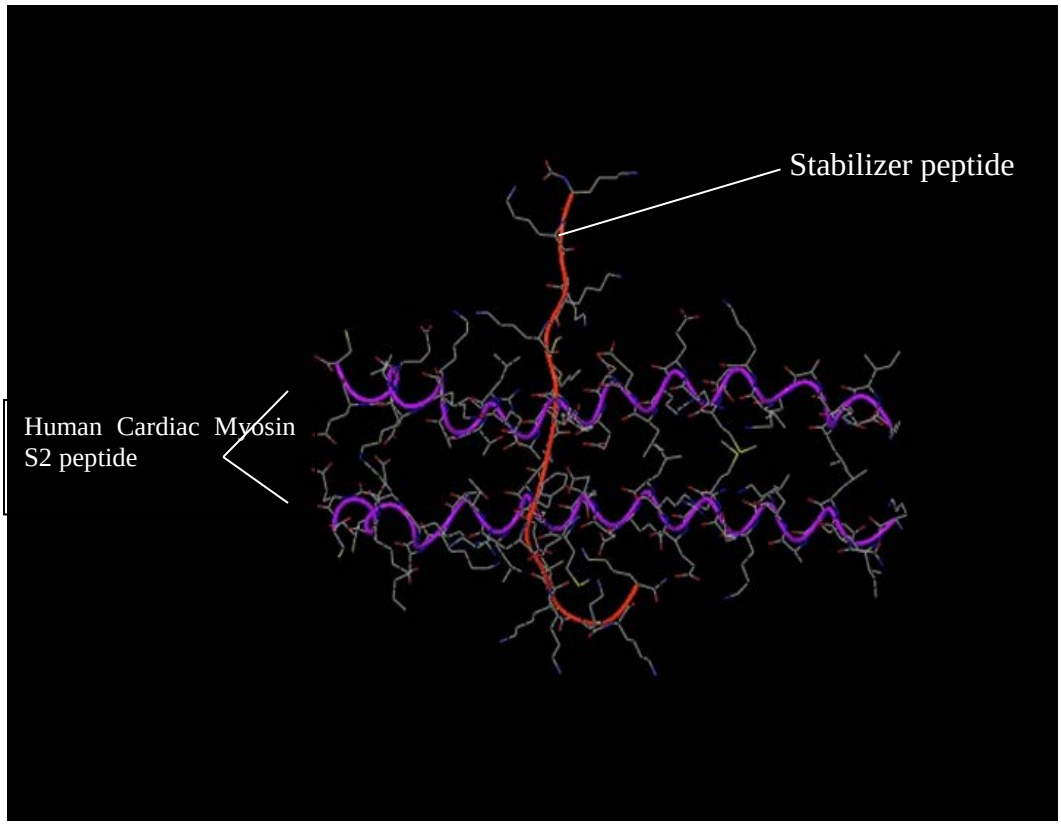

Figure 9. Simulated image of stabilizer peptide (red) wrapping around human cardiac myosin S2 peptide (purple). (Image courtesy of Motamed Qadan).

2.1.10 Destabilizer Peptide

The idea behind destabilizer peptide was to disrupt the natural coiled coil formation of human cardiac myosin S2 peptide. Thus peptide sequence of single α helix of human cardiac myosin S2 was modified so that the modified peptide would have higher binding affinity to a single α-helix of myosin S2 coiled coil (Singh, R.R., Qadan, M.M *et al*., 2017). Consequently natural formation of myosin S2 coiled would be interrupted due to binding of single helix of coiled coil to

the modified peptide as seen in the computer simulations (Figure 10). This modified peptide thus named destabilizer due to its action on myosin S2 coiled coil. Destabilizer peptide was chemically synthesized and provided by Bio-synthesis Inc., Lewisville, Texas, United States.

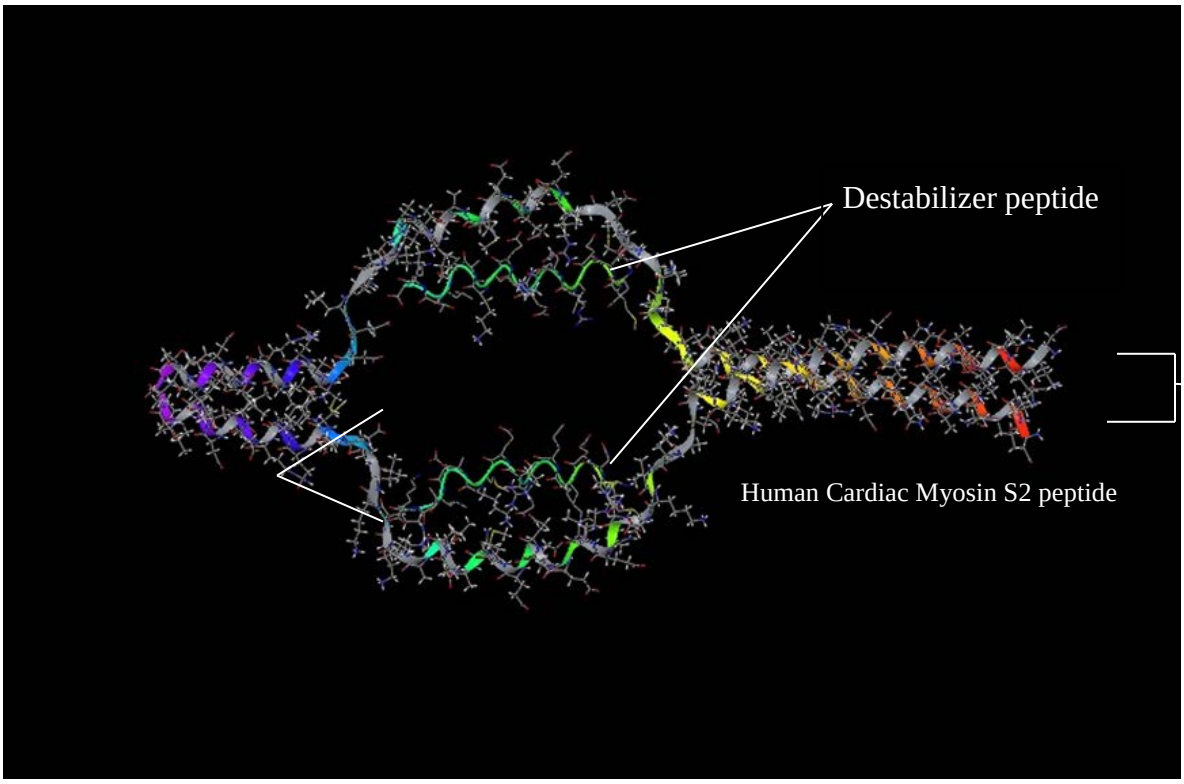

Figure 10. Simulated image of destabilizer peptide (green) binding to each helix of human cardiac myosin S2 coiled coil peptide. (Image courtesy of Motamed Qadan).

2.2 Methods

2.2.1 Competitive Enzyme Linked Immunosorbent Assay

2.2.1.1 Materials

Phosphate buffer saline (PBS) contained 0.14 M sodium chloride, 2.7 mM potassium chloride, 1.5 mM potassium phosphate monobasic, and 8.1 mM sodium phosphate dibasic and adjusted to pH 7.4. Detergent buffer was made with 0.05% triton X-100 in PBS, blocking buffer was made with 3% powdered milk in detergent buffer. Assay buffer contained 100 mM potassium

phosphate dibasic, 100 mM potassium phosphate monobasic, 1 M potassium chloride and 10 mM magnesium chloride with pH 7.0. Stocks of primary antibody (polyclonal antibody anti-S2), rabbit skeletal myosin, human cardiac myosin S2 peptide, stabilizer and destabilizer peptide. Secondary antibody conjugated with alkaline phosphatase was anti-guinea pig immunoglobulin G (IgG)-alkaline phosphatase (Sigma-Aldrich, catalog number A5062) produced in goat and isolated by affinity chromatography. Substrate was 5-bromo-4-chloro-3-indolyl phosphate (BCIP) tablets dissolved in 10 ml of distilled water per tablet and 96 well microtiter plate.

2.2.1.2 Methodology

Competitive Enzyme Linked Immunosorbent Assay (cELISA) is a classical immunochemical test to validate the binding affinity and specificity in lower molar concentrations (Yorde *et al*., 1976; Voller *et al*., 1978; Walker, J.M. 1996). In this assay the polyclonal antibody anti-S2 raised against single alpha helix of myosin S2 would be used to compete with stabilizer or destabilizer peptide to bind myosin S2 in rabbit skeletal myosin molecule as well as small human cardiac myosin S2 peptide (Figure 11). This cELISA, thus have two molecules polyclonal anti-S2 and stabilizer peptide which have two binding sites one on rabbit skeletal myosin and the other one being on small human cardiac myosin S2. Since both polyclonal anti-S2 and stabilizer peptide were designed against human β-cardiac myosin S2 they both would have a stronger affinity towards the smaller human β-cardiac myosin S2 peptide against the myosin S2 on rabbit skeletal myosin.

To test the binding specificity and affinity of stabilizer or destabilizer peptide the following setup was used. Start of the setup would be to coat the wells with rabbit skeletal myosin molecule and add appropriate amount human cardiac myosin S2 peptide that would bind the primary

polyclonal anti-S2 antibody and when washed there won't be enough primary polyclonal anti-S2 antibody to bind myosin S2 of rabbit skeletal myosin adsorbed on the wells. When alkaline phosphatase conjugated secondary antibody is added on to the wells, it won't have enough or none primary polyclonal anti-S2 antibody to bind. After addition of color developing BCIP substrate to the wells it would lead to low or no color development leading to lower optical density (OD).

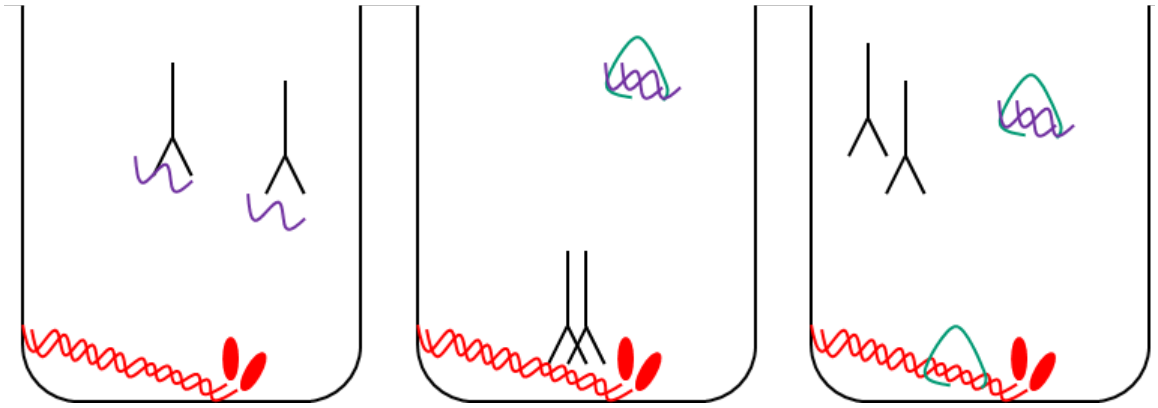

Figure 11. Sketch of cELISA setup. (Left) Rabbit whole skeletal myosin (red) coated on to the wells with human β-cardiac myosin S2 peptide (purple) with primary polyclonal anti-S2 antibody (black). (Middle) Lower amounts of stabilizer or destabilizer peptide (green) added will bind human cardiac myosin S2 peptide (purple) and primary polyclonal anti-S2 antibody (black) will bind rabbit skeletal myosin (red). (Right) Higher amounts of stabilizer or destabilizer peptide (green) added will bind both human cardiac myosin S2 peptide (purple) and rabbit skeletal myosin (red) allowing the dissociation of primary polyclonal anti-S2 antibody (black) from the assay.

Next would be to add increasing amounts of stabilizer or destabilizer peptide to the above setup, if stabilizer or destabilizer peptide is specific and has higher binding affinity to myosin S2, observed results would be that at lower concentration of stabilizer peptide, the stabilizer or destabilizer peptide would bind to human cardiac myosin S2 and block the binding of primary polyclonal anti-S2 antibody to human cardiac myosin S2 peptide. Thus polyclonal anti-S2 antibody would bind to myosin S2 in rabbit skeletal myosin coated on wells, this in turn would

allow enzyme conjugated secondary antibody to bind this polyclonal antibody on wells leading to color development and increase in OD after addition of BCIP substrate.

As the concentration of stabilizer or destabilizer peptide increases, it saturates all the human cardiac S2 peptide available. The next available myosin S2 would be on rabbit skeletal myosin and this stabilizer or destabilizer peptide then binds to this myosin S2 on the wells. Thus, polyclonal anti-S2 antibody won't have any other myosin S2 sites to bind, leading to no sites available to bind enzyme linked secondary antibody consequently causing low color development or lower OD upon addition of BCIP substrate. This change in OD from lower OD with no stabilizer or destabilizer to higher OD with increasing amounts of stabilizer or destabilizer peptide and then again back to lower OD with higher amounts of stabilizer or destabilizer peptide would be able to confirm the binding affinity of stabilizer peptide to myosin S2 as well as convey the relative cross-specificity of stabilizer or destabilizer peptide to myosin S2 of human cardiac and rabbit skeletal myosin.

To perform this specific set up of cELISA, two values had to be determined: the first being the minimal amount of primary polyclonal anti-S2 antibody required to bind myosin S2 on rabbit skeletal myosin coated on to the wells of microtiter plates thus giving a response by color development upon addition of enzyme linked secondary antibody following BCIP substrate; the second being the minimal concentration of human cardiac myosin S2 that would bind all of the primary polyclonal anti-S2 antibody leading to no color development or low OD upon addition of enzyme linked secondary antibody following BCIP substrate. These two values confirm that no or low OD at the beginning when there is no stabilizer or destabilizer added is because human cardiac myosin S2 peptide is bound to all available primary antibody, thus no sites for enzyme linked secondary antibody to bind. After addition of increasing amounts of stabilizer and destabilizer

peptides, these peptides bind human cardiac myosin S2 peptide first allowing primary polyclonal anti-S2 to bind myosin S2 of rabbit skeletal myosin causing a rise in OD. With increasing amounts of stabilizer and destabilizer peptides added comes a stage when they saturate all the available human cardiac myosin S2 peptide available thus progressing towards to bind next available myosin S2 which is on rabbit skeletal myosin. As a result, the primary polyclonal anti-S2 antibody won't have any myosin S2 region available to bind leading to low OD or decline in OD when enzyme linked secondary antibody with BCIP are added.

2.2.2 Gravitational Force Spectroscopy

2.2.2.1 Materials

A light microscope was equipped with 10X and 40X objectives mounted on an alt-azimuthal mount with the eyepiece replaced with a digital video camera (Sony, XCD-V60). This alt-azimuthal mount is suspended with the help of compression and extension springs on steel bracket. The reagents are 3-aminopropyltriethoxysilane, acetone, coupling buffer (0.01 M pyridine in water with pH 6.0), glutaraldehyde, quenching solution (1 M glycine in water with pH 7.0), wash buffer (0.01 M Tris, 0.1% sodium azide, 0.1% bovine serum albumin, 0.15 M sodium chloride, and 0.001 M ethylenediaminetetraacetic acid with pH 7.0), low salt buffer (0.1 M potassium chloride, 0.02 M imidazole, 5 mM magnesium chloride, with pH 7.0), sodium hydroxide, 1-ethyl-3-(3-dimethyaminopropyl) carbodiimide, N-hydroxysuccinamide, monodisperse silica beads, glass slides, glass coverslips, vacuum grease, rabbit skeletal myosin, purified actin, polyclonal anti-S2 antibody, purified MyBPC, stabilizer peptide, and destabilizer peptide.

2.2.2.2 Methodology

Gravitational force spectroscopy (GFS); a single molecule force spectroscopy method developed in Root lab to measure absolute molecular length with the help of gravitational force. GFS can also impart graded force to a single molecule to study the unwinding or uncoiling of the same molecule. It can also estimate the actual amount of amino acids involved in the uncoiling of the molecule. GFS imparts forces in femtonewton to nanonewton range, which might be the range of force exhibited by a single molecule. Another advantage of GFS would be that it does not require a prior force calibration step unlike other force spectroscopy methods (Dunn, J.W., and Root, D.D. 2011). All these properties combined GFS was the ideal choice to test the flexibility of single myosin S2 in the presence of myosin S2 binding proteins. Myosin S2 flexibility measured on a single myosin molecule has the same force-distance curve for a myosin S2 on myosin present in a thick filament organization (Singh, R.R., Dunn, J.W *et al*., 2017). Thus myosin S2 flexibility is independent of myosin thick filament. Hence any changes reflected on myosin S2 flexibility in presence of myosin S2 binding proteins can pertain to myosin S2 present on myosin in thick filament assembly. The schematic of GFS is illustrated in diagram (Figure 12).

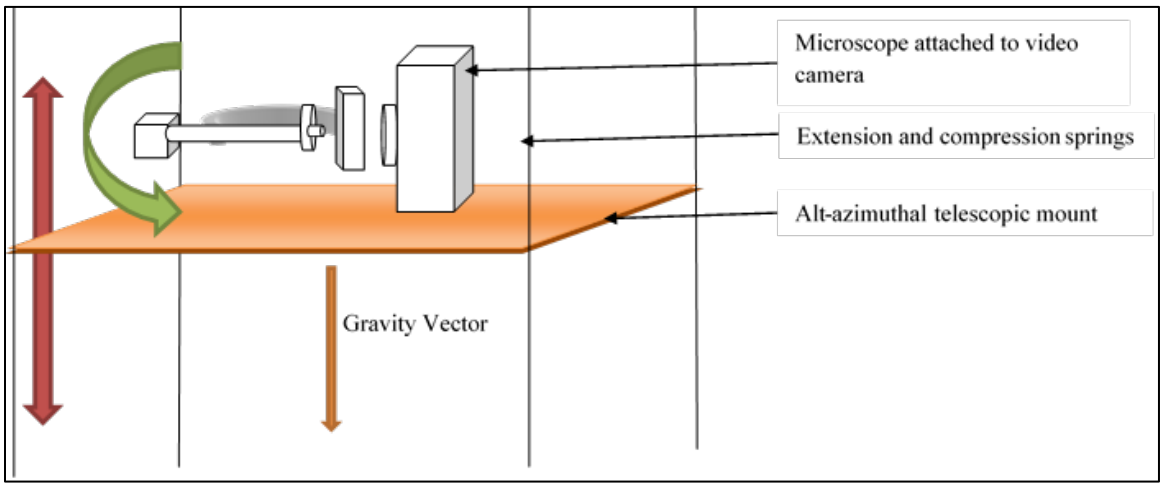

Figure 12. Schematic of a gravitational force spectroscope. GFS can operate in two modes; one being rotational mode (green arrow) and other being free-fall mode (red arrow).

GFS utilizes a light microscope mounted horizontally on an alt-azimuthal mount suspended on springs attached to a steel bracket. On the light microscope the ocular lens or the eyepiece is replaced by a digital video camera to capture the image or video of the single molecule tethered between an immobile bead or edge and mobile bead. A flow cell containing the tethered molecule of interest created on a glass slide is mounted on the light microscope of GFS and oriented in the direction of gravity vector so the gravitational force can be exerted on to the tethered molecule. There are two modes of measurements namely rotational mode to calculate the absolute molecular length of single molecule and free fall mode to calculate the force required to uncoil the attached single molecule.

2.2.2.2.1 Rotational Mode

The rotational mode of GFS measures the absolute molecular length of single molecule (Figure 13). In this mode the molecule of interest tethered between an immobile edge and mobile bead are enclosed in a flow cell on a glass slide and mounted on the light microscope of GFS. The mobile bead tether through the single molecule to immobile edge in the direction of gravity vector is identified; later the light microscope is oriented in a direction either clockwise or anticlockwise about 45 degrees or less to the gravity vector. This marks the start of the measurement for absolute molecular length. After achieving this orientation the microscope is rotated in a direction opposite to the orientation of bead at the start of measurement, i.e. if the bead at the start of measurement was at clockwise direction it is rotated in anticlockwise direction and vice versa.

The measurement is stopped, when microscope is rotated till 45 degrees or less against the gravity vector in opposite direction to the start of measurement. For example; start of measurement with bead in a direction 45 degrees or less anticlockwise to the gravity vector and stop of the

measurement in a direction 45 degrees or less clockwise to the gravity vector. The rotational speed of the microscope during the course of measurement is half a degree per second. Video from the start and stop of the measurement is recorded and then analyzed through Image J; an image processing software. Each frame of the video is processed to yield x and y coordinates of the centroid of the bead and the immobile edge. These x and y coordinates are utilized to determine the length of molecule based on the collected data through entire course of measurement.

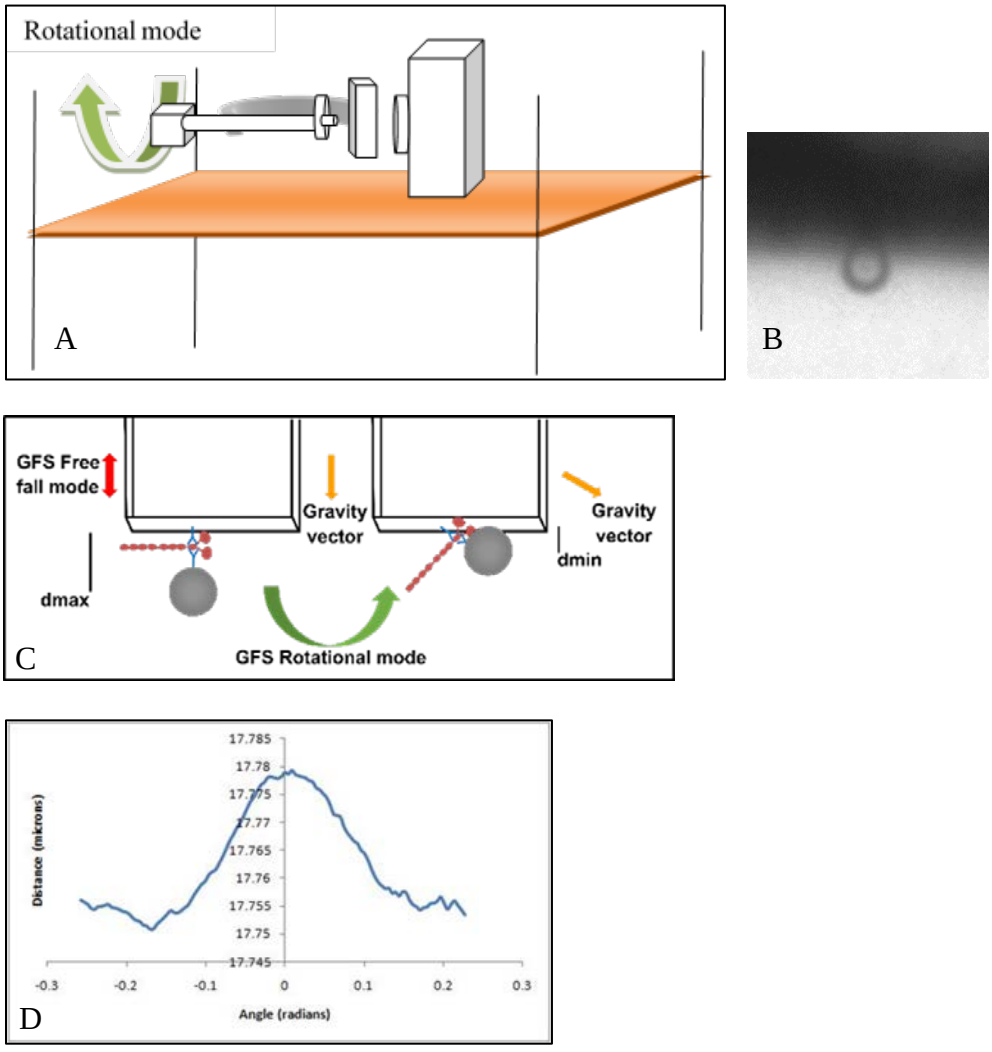

Figure 13. Rotational mode of gravitational force spectroscopy. (A) Setup of GFS with rotation of microscope (green arrow). (B) Image of mobile bead observed bound to immobile edge. (C) Different length of molecule suspended between mobile bead and immobile edge with different angles of rotation. (D) A typical bell shaped curve observed with minimum length of the molecule at the base of the curve and maximum length of the molecule at the peak of the curve.

Length of the molecule tethered between immobile edge and mobile bead is extracted from measurements between a line equation parallel to the immobile edge and the centroid of the mobile bead at every frame of the video. The distance between the mobile bead and the line plotted versus rotation angle yields a bell shaped curve, where at the start of measurement, the molecule will have a conformation where its length will be the minimum (d_{min}), and during the course of measurement when the mobile bead being rotated is in line with or completely parallel to gravity vector the molecule will assume a conformation where the length of the molecule is the maximum (d_{max}) and at the end of measurement the molecule will again be in the d_{min} position. Subtracting d_{max} from d_{min} will yield the absolute length of the molecule. The force acting on the molecule at the d_{max} position is obtained by multiplying the mass of the bead adjusted for its buoyancy and the gravitational acceleration. The mass of the bead is obtained by calculating the volume of the bead first from the radius of bead and then multiplying the volume of bead with the known density of bead.

2.2.2.2.2 Free-Fall Mode

The free fall force mode of GFS allows a graded force to be implemented on a single molecule. The entire GFS or the alt-azimuthal mount with light microscope and camera mounted on a spring supported platform can be dropped. At the initial free-fall, the force acting on the bead is close to zero. The movement of the platform acted upon by gravitational acceleration yields an acceleration trace that is a function of the spring constant. This acceleration trace decays as the platform approaches the equilibrium position. During the experiment, the GFS now has a single molecule tethered to an immobile edge and mobile bead, and when dropped the mass of the bead

along with the acceleration of GFS under differential tension of spring will impart different force loads on the molecule (Figure 14).

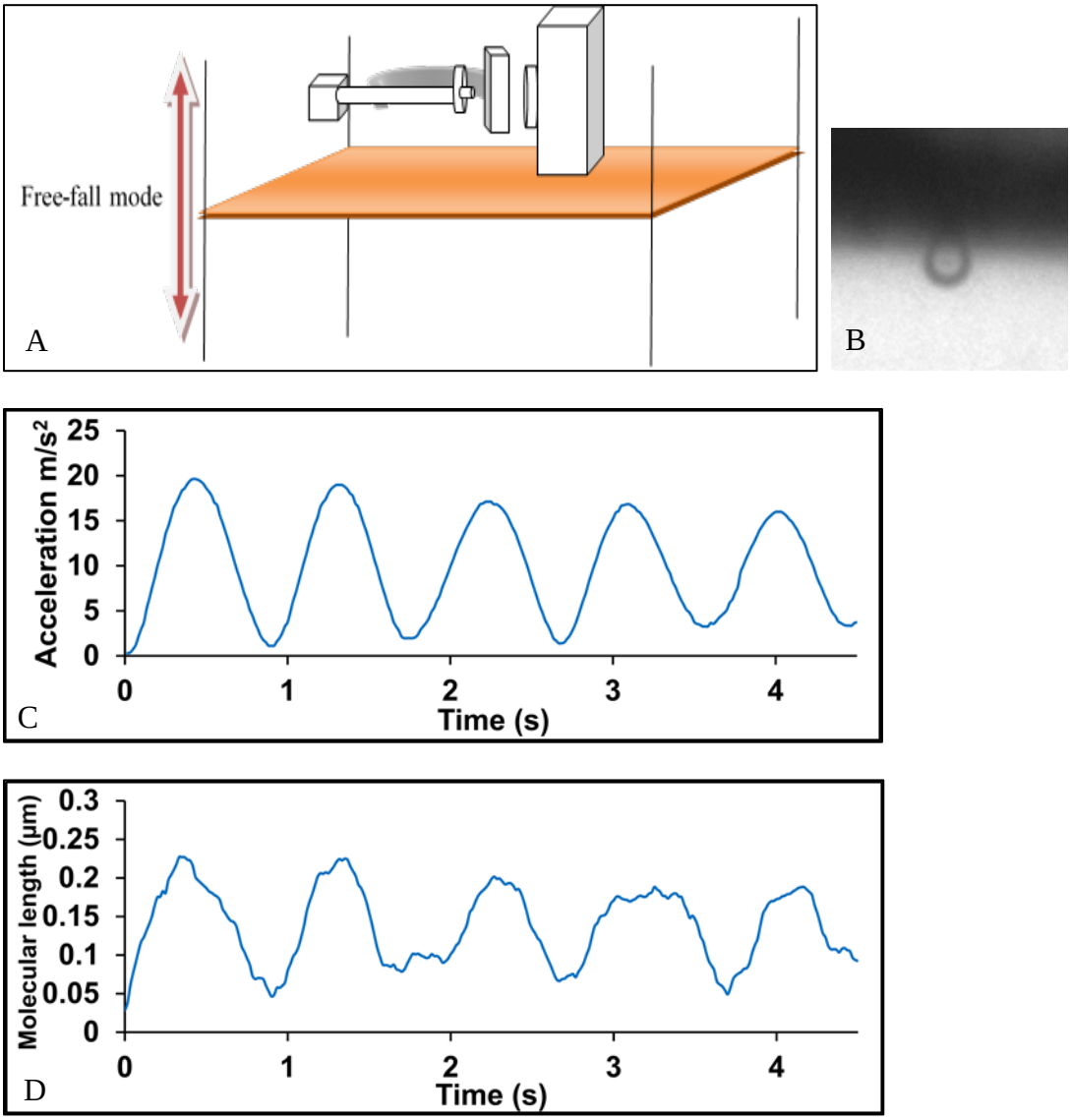

Figure 14. Free-fall mode of Gravitational force spectroscopy. (A) Set up of GFS for free-fall mode (Red arrow) where GFS can be dropped in the direction of gravity vector. (B) Image of mobile bead observed bound to immobile edge. (C) Acceleration trace of the GFS. (D) A trace of the length of molecule represented by the relative distances between the centroids of the mobile and anchored edge.

The assay begins with orienting the bead molecule in the direction of gravity vector and then simultaneously dropping the platform while starting the video recording of bead under

investigation. The video recording is stopped as the GFS achieves equilibrium with the spring tension. All the video frames are processed through Image J to get the x and y coordinates of the centroid of the mobile bead and a fixed spot on the immobile edge. Using these coordinates and the known molecular length from the rotational assay at constant force, the length of the molecule is calculated for all the frames of video captured, and this in turn yields a force-distance trace in which the distance is the length of the molecule.

The GFS acceleration under spring tension when multiplied with the mass of the mobile bead will yield a force trace for the bead when dropped in the free fall mode of the GFS. This force trace when aligned with the distance trace for the length of the molecule will yield the length of the molecule under different force loads. Thus a coiled coil molecule like myosin, when tethered with one helix to an immobile edge and another helix to the mobile bead undergoing the free fall mode of GFS would give the information about the force required to unwind the coiled coil. The stability of the coiled coil can be identified with the amount of force required to unwind the coiled coil. The greater the force required to unwind the coiled coil the more stable the molecule, and vice versa when less force is required.

For the purpose of testing the myosin S2 flexibility there are two points of attachment used to tether the rabbit skeletal myosin between the immobile edge and mobile edge. One point of attachment is by using the polyclonal anti-S2 antibody to tether the rabbit skeletal myosin at myosin S2 region with anti-S2 treated immobile edge and mobile edge. A different point of attachment is utilizing the binding property of actin to myosin S1 and tether the skeletal myosin molecule at myosin S1 position with G-actin treated immobile edge and mobile bead.

2.2.2.2.3 Conjugation of Polyclonal Anti-S2 Antibody to Immobile Edge and Mobile Beads

To tether the myosin molecule at myosin S2 position between immobile edge and mobile bead, both this edge and the mobile bead have to be treated with polyclonal anti-S2 antibody. For the immobile edge, the edge of the glass coverslips and for mobile bead, silica beads are used. The glass coverslips and silica beads are treated with 0.04% 3-aminopropyltriethoxylsilane in acetone to add aminosilane groups to hydroxyl groups on the surface of glass coverslips and silica beads. To the aminosilane groups, the antibody is coupled in the presence of 2% glutaraldehyde in coupling buffer. The antibody is conjugated via its free amino groups to the free aldehyde group on glutaraldehyde coupled to aminosilane on glass coverslip and silica bead. Unbound antibody is washed by mixing it with glycine quenching buffer and later washed several times with wash buffer. Finally, the antibody coated glass coverslips and silica beads are washed with low salt buffer and stored in low salt buffer for force spectroscopy purposes.

2.2.2.2.4 Conjugation of G-Actin on the Immobile Edge and Mobile Beads

The process of conjugating G-actin on glass coverslips and silica beads begins with adding the aminosilane groups to both glass coverslips and silica beads by treating them both with 0.04% 3-aminopropyltriethoxylsilane in acetone. G-actin is then cross linked to the aminosilanated glass coverslips and silica beads with the help of 740 mM 1-ethyl-3-(3-dimethyaminopropyl) carbodiimide. 60 µM N-hydroxysuccinamide is added to help the cross linking of G-actin on glass coverslips and silica beads. The unreacted groups are blocked by adding the glycine quenching solution to the mix. After quenching the actin cross linked glass coverslips and silica beads undergo several washes with low salt buffer and are later stored in this low salt buffer for force spectroscopy purposes.

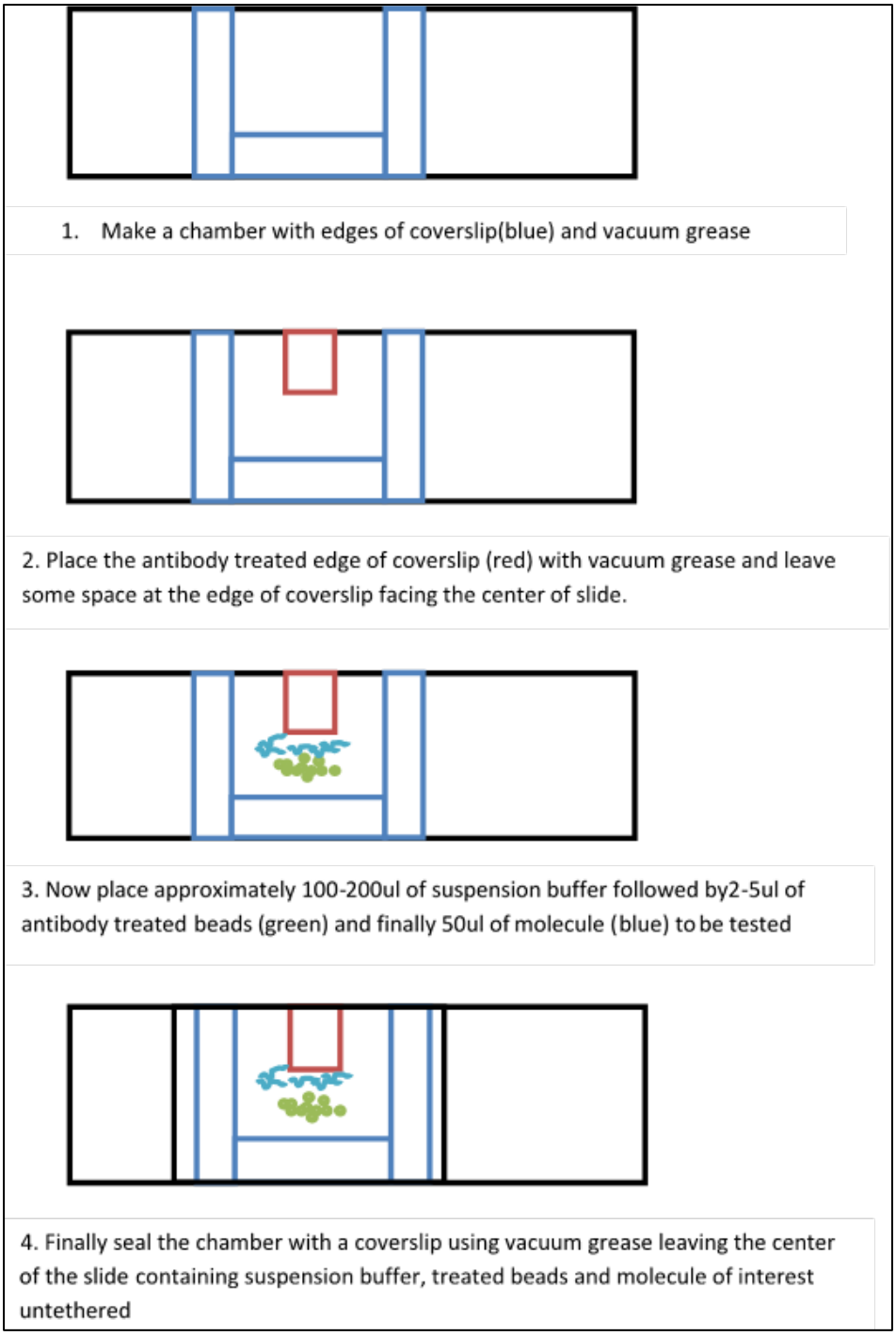

Figure 15. Schematic for preparation of slide for measuring absolute molecular length using Gravitational force spectroscopy.

Preparation of the slide for the GFS is illustrated in the figure (Figure 15). A clean glass slide selected. A four walled chamber is created with small rectangular pieces of glass coverslips and vacuum grease. Of the four walls, one of the wall (north wall) is the glass coverslip coated

with either antibody or G-actin. With this setup there will be one edge of the treated coverslip facing the inside of the chamber. In the chamber, few microliters of antibody or actin coated silica beads are added followed by molecule of interest diluted in assay buffer around 100 µl to fill the chamber. Next step is to seal the chamber with another clean glass coverslip with help of vacuum grease. This slide is rotated for a few hours to allow the molecule of interest to be tethered between edge of the coverslip and mobile bead. The slide is now ready for GFS measurements. The slide is placed in such a way that the wall of the chamber with treated coverslip is in the north direction when viewed through microscope (Figure 16).

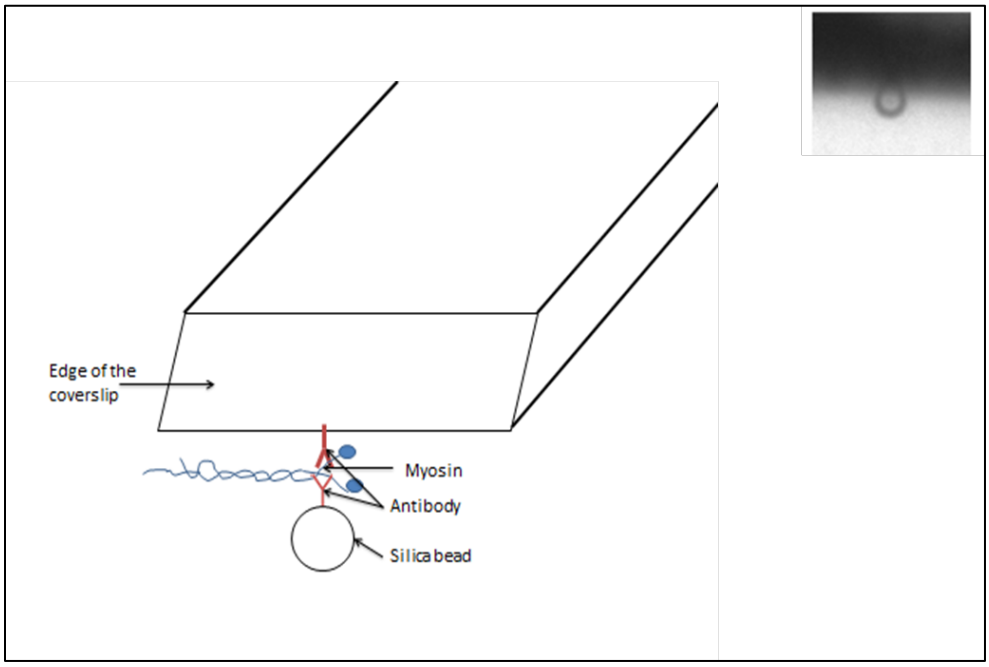

Figure 16. Schematic of a myosin molecule suspended between edge of the coverslip and a silica bead with the help of antibody raised against myosin. (Inset) Image of mobile bead observed bound to immobile edge.

Myosin S2 stability and flexibility is measured with GFS by unwinding the myosin molecule in free fall mode. GFS also establishes the effect of myosin S2 binding proteins on the myosin S2 region of myosin molecule by unwinding the same in presence of these proteins.

2.2.3 Myofibrillar Contractility Assay

2.2.3.1 Materials

Rabbit skeletal myofibrils, stabilizer peptide, destabilizer peptide, adenosine triphosphate, light microscope with 32X objective lens, micrometer slide, wide glass coverslips and assay buffer (0.1 M potassium chloride, 1 mM magnesium chloride, 0.5 mM calcium chloride and 50 mM imidazole with pH 7.0)

2.2.3.2 Method

The myofibrillar contractility assay is a simple method to measure the shortening of sarcomeres in a striated skeletal myofibril that is based on observation that the extent of myofibril shortening is related to the amount of force generated (Root and Reisler, 1992; Sugi et al., 1992; Figure 17). The assay involves the measurement of sarcomere lengths in a myofibril suspended in relaxing solution without ATP, followed by measurement of sarcomere length after adding ATP to the same myofibril in assay buffer. Upon addition of ATP the myofibril undergoes contraction, by hydrolysis of ATP by myosin S1 heads. Shortening of the sarcomere upon addition of ATP can be measured through the images. Difference in the length of sarcomere before and after adding ATP is calculated and percentage contraction is calculated by the following formula;

$$= \left(\frac{\text{Difference in sarcomere length before and after ATP}}{\text{Length of sarcomere before ATP}}\right) \times 100$$

Performing the myofibrillar contractility assay with the myofibrils treated with myosin S2 binding proteins yields the percentage contraction in the sarcomeres of myofibrils treated with myosin S2 proteins thus explaining the effect of these proteins on the contractility of the myofibrils.

Before performing the myofibrillar contractility assay, the myofibrils are washed multiple times with the assay buffer to allow the relaxation of sarcomeres in myofibrils. Small amount of these myofibrils in approximately 100 µl of assay buffer are placed on coverslip and imaged through microscope. ATP is added to the myofibril to a total concentration of 1 mM and imaged after 30 minutes to allow the contraction of myofibrils. Images are then processed through Image J to measure the sarcomere lengths. Similar procedure is performed with myofibrils treated with myosin S2 binding proteins to procure the effect of these proteins over the contractility of myofibrils.

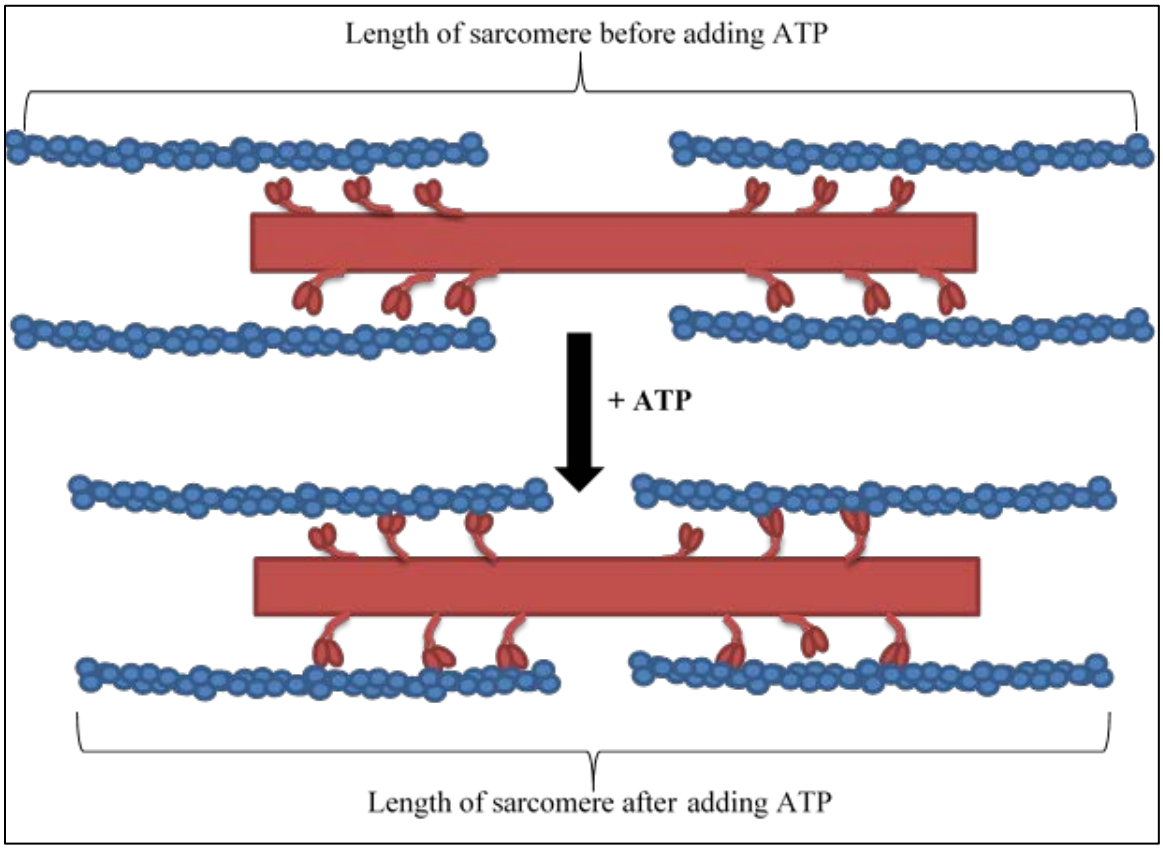

Figure 17. Schematic of myofibrillar contractility assay. Actin thin filament (blue) binding to myosin thick filament (red) upon addition of ATP results in reduction of sarcomeric length.

2.2.4 *In vitro* Motility Assay

2.2.4.1 Materials

Fluorescent microscope with 100X glycerol immersion lens and temperature regulated stage, Intensified charged couple device (ICCD), Rabbit skeletal myosin, purified G-actin, purified MyBPC, stabilizer peptide, destabilizer peptide, potassium chloride, imidazole, magnesium chloride, dithioerythritol, bovine serum albumin,α chymotrypsin, catalase, glucose oxidase, glucose, methyl cellulose, phenylmethylsulfonylfluoride, methanol, adenosine triphosphate, dichlorodimethylsilane, chloroform, rhodamine phalloidin, glass slides, glass coverslips and vacuum grease.

2.2.4.2 Method

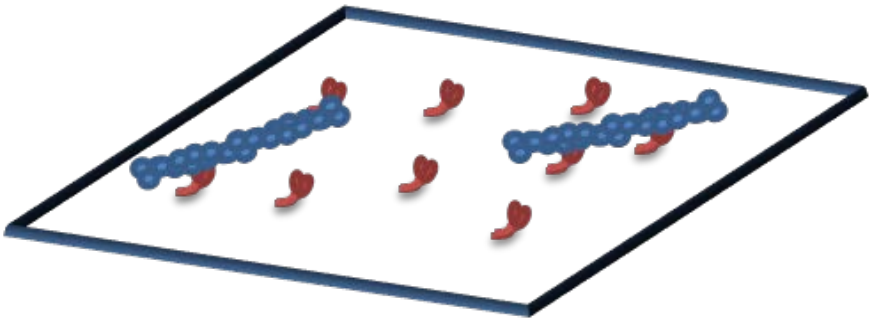

Figure 18. Schematic of a typical *in vitro* motility assay. Fluorescently labelled actin filaments (blue) sliding over coverslip coated with myosin molecules (red).

In vitro motility assay a classic method to determine the sliding velocity of actin filaments over immobilized myosin in the presence of ATP (Kron *et al*., 1991). The assay involves the immobilization of myosin either in thick filament assembly or through individual myosin molecules on a nitrocellulose or dichlorodimethylsilane treated coverslip. Fluorescently labelled actin filaments are induced to slide across the bound myosin filaments upon addition of ATP. Sliding of actin over myosin treated with myosin S2 binding proteins establishs their effect over

acto-myosin interaction. The use of heavy meromyosin which contains S2 but no LMM would be enough to test the effect of stabilizer and destabilizer over the acto-myosin interaction; however to test the effect of MyBPC, myosin reconstituted in its thick filament form would be required since MyBPC binds to both light meromyosin and myosin S2. Myosin in its thick filament form will improve the binding of MyBPC to a myosin molecule rather than a single myosin molecule immobilized on a glass surface.

2.2.4.2.1 Purification of Heavy Meromyosin with ATP Sensitive Heads

Rabbit skeletal myosin is dialyzed against buffer containing 0.5 M potassium chloride and 10 mM imidazole with pH 7.0 overnight to remove the impurities. Dialyzed myosin undergoes trypsin digestion with 1 mM magnesium chloride and α-chymotrypsin, digestion was stopped after addition of phenylmethylsulfonylfluoride in methanol at room temperature. Tryptic digest of myosin is dialyzed overnight at 4 ^{0}C against buffer containing 0.04 M potassium chloride and 10 mM imidazole with pH 7.0. Dialyzed tryptic digest of myosin is centrifuged at 21000g for 60 minutes at 4 ^{0}C to yield myosin heavy meromyosin in the supernatant. This myosin heavy meromyosin achieved has a mixture of ATP sensitive and ATP insensitive heads. To purify myosin heavy meromyosin with ATP sensitive myosin S1 heads, F-actin is added at an equimolar concentration to the unpurified myosin heavy meromyosin extract along with 1 mM ATP and magnesium chloride. Low salt assay buffer (25 mM potassium chloride, 10 mM imidazole, 2 mM magnesium chloride and 10 mM dithioerythritol with pH 7.0) was used as mixing solvent for the myosin heavy meromyosin purification step. Purified myosin heavy meromyosin with ATP sensitive heads are suspended in the supernatant when unpurified myosin heavy meromyosin with F-actin, ATP and magnesium chloride is centrifuged with the speed of 21,000g at 4 ^{0}C. ATP

insensitive heads will bind F-actin irreversibly thus forming the precipitate in the centrifugation step. Purified myosin heavy meromyosin with ATP sensitive heads are ready for the *in vitro* motility assay.

2.2.4.2.2 Purification of Myosin Thick Filament with ATP Sensitive Heads

Rabbit skeletal myosin is diluted in high salt buffer (0.3 M potassium chloride, 2 mM magnesium chloride, 10 mM imidazole and 10 mM dithioerythritol with pH 7.0) to around 10 µM. Equimolar concentration of F-actin along with 1 mM ATP and magnesium chloride is added to the diluted skeletal myosin. Myosin molecule with ATP insensitive heads will bind to F-actin and gets precipitated out upon centrifugation with speed of 21000g at 4 ^{0}C, while myosin molecules with ATP sensitive heads will form the supernatant. High salt will help to maintain the skeletal myosin in its nonfilamentous form thus allowing purification of myosin molecules with ATP sensitive heads from insensitive heads. Exchanging this purified myosin molecule with ATP sensitive heads from high salt buffer to low salt assay buffer allows the myosin thick filament formation with ATP sensitive myosin S1 heads. Myosin thick filaments thus formed are ready for *in vitro* motility assay.

2.2.4.2.3 Rhodamine Phalloidin Labelling of F-Actin

F-actin and rhodamine phalloidin are mixed in 1:5 micro molar concentration ratio with low salt assay buffer. Rhodamine phalloidin binds in between the grooves of actin subunits of F-actin. The mixture of F-actin and rhodamine phalloidin is allowed to incubate overnight at 4 ^{0}C to allow maximal labelling of F-actin.

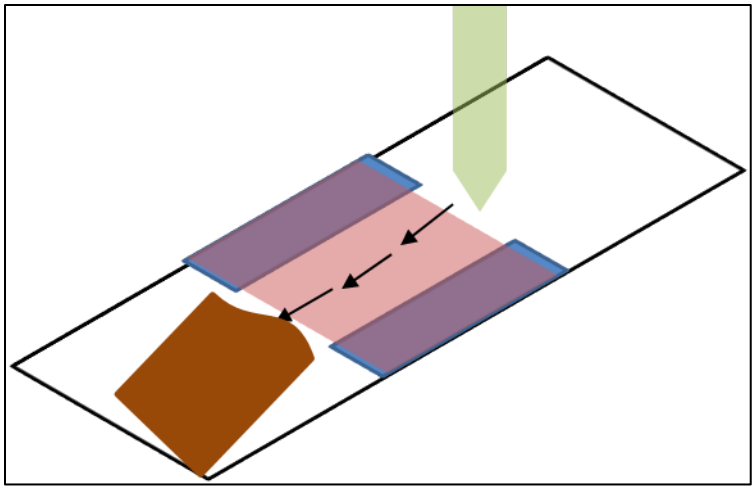

Figure 19. Perfusion chamber for *in vitro* motility assay. Pieces of glass coverslips (blue) attached on to a glass slide (black) and coverslip treated with myosin (red) added to create a chamber. Buffer and solution added from one side (green arrow point) and wicked through other end with tissue paper (brown).

Glass coverslips are coated with freshly prepared 2% dichlorodimethylsilane in chloroform. Perfusion chamber is created by two halves of glass coverslips on a clean glass slide with help of vacuum grease. The perfusion chamber is then sealed with a dichlorodimethylsilane-treated coverslip with two sides open to allow perfusion of buffer from one end and wicking on the opposite end. First step in preparation of slide is to immobilize either purified myosin heavy meromyosin or myosin thick filaments. These purified products are diluted with low salt assay buffer to achieve a final concentration of 0.1 µM before adding them in to perfusion chamber. The heavy meromyosin or myosin thick filaments are allowed to immobilize on the dichlorodimethylsilane-treated coverslip for a minute. Unbound myosin is washed away by low salt assay buffer once and multiple washes with assay buffer mixed with 0.5 mg/ml bovine serum albumin (AB-BSA) blocks the unbound protein. The next step is to add 10 µM of F-actin diluted in AB-BSA to the chamber to bind F-actin to myosin S1 heads. After this step, ATP diluted in AB-BSA is added to allow F-actin to dissociate it from active myosin S1 heads while F-actin would stay bound to inactive myosin S1 heads. This is an additional step to select the ATP sensitive

myosin S1 heads. The next step is to give multiple washes with AB-BSA to block the unbound proteins. Following this washing step is addition of rhodamine phalloidin labelled F-actin freshly diluted one thousand times with AB-BSA to 10 nM. Fluorescently labelled F-actin is allowed to bind myosin S1 heads for a few minutes. Later is the addition of ATP diluted to 1 mM in low salt buffer containing 0.5 mg/ml bovine serum albumin, 25 µg/ml glucose oxidase, 45 µg/ml catalase, 10 mg/ml glucose and 0.5% methyl cellulose (AB-BSA-GOC).

After this step, slide is placed on to the stage of fluorescent microscope maintained at 37 ^{0}C to allow efficient movement of fluorescently labelled actin filaments over myosin S1 of myosin heavy meromyosin and myosin thick filament. Slide is viewed through ICCD to image fluorescently labelled actin filaments and video is recorded for few minutes to record the sliding of actin filaments. Final step is to add ATP diluted to 1 mM in AB-BSA-GOC along with myosin S2 binding proteins to check their effect over acto-myosin interaction. Again the video is recorded to measure the actin sliding over myosin bound to myosin S2 binding proteins. The video recorded is analyzed by Image J software and manual tracking plugin of the software allows to track the movement of actin filament and yield the velocity of actin filaments in microns per second.

Thus measuring the actin sliding velocity over myosin S1 heads of myosin heavy meromyosin in presence of destabilizer and stabilizer peptide, as well as sliding velocity of actin over myosin S1 heads of myosin thick filament in presence of MyBPC would reveal the effect of these myosin S2 binding proteins over acto-myosin interaction and overall force produced.

CHAPTER 3

MYOSIN BINDING PROTEIN C AND MYOSIN SUBFRAGMENT-2

Myosin binding protein C, as the name suggests, binds to the myosin molecule with the C-terminal end of MyBPC binding to the LMM region of myosin and N-terminal binding to the myosin S2. When MyBPC is dephosphorylated at its m domain, it binds to myosin S2, and phosphorylated MyBPC binds to the actin thin filament (Levine *et al*., 2001; Starr, R., and Offer, G. 1978; Weisberg, A., and Winegrad. S. 1996; Munn *et al*., 2011; Whitten *et al*., 2008; Rybakova *et al*., 2011; Previs *et al*., 2012, 2016; Gautel *et al*., 1995). Thus MyBPC, a natural binding partner to myosin S2, is an ideal choice to test the stability of myosin S2 coiled coil and its effect over the overall force produced due to acto-myosin interaction.

3.1 Purification of MyBPC

Crude extract of MyBPC was extracted from the stored rabbit skeletal myofibrils by the method described (Furst *et al*., 2011). Crude MyBPC was extracted in a two-step process first by suspending myofibrils in extraction buffer (0.6 M potassium chloride, 2 mM magnesium chloride, 2 mM ethylene glycol-bis(β-aminoethyl ether)-N,N,N',N'-tetraacetic acid, 1 mM 2-mercaptoethanol, 1 mM sodium azide, 10 mM imidazole, pH 7.0) and centrifuging it to collect supernatant. For the second step, the supernatant was dialyzed against the dialysis buffer (2 mM ethylene glycol-bis(β-aminoethyl ether)-N,N,N',N'-tetraacetic acid, 1 mM 2-mercaptoethanol, 1 mM sodium azide, 50 mM Tris-hydrochloric acid, pH 7.9). After dialysis, the supernatant collected through centrifugation gave the crude extract of MyBPC. Purification of MyBPC from the crude extract was performed through a series of chromatography techniques.

Hydroxyapatite column chromatography was performed with the crude extract of MyBPC. Hydroxyapatite column has both positively charged calcium (Ca^{+2}) ions and negatively charged

phosphate (PO_4^{-2}) ions, thus both acidic and basic proteins are adsorbed on to the column in presence of low phosphate buffer (0.3 M potassium chloride, 4.8 mM potassium phosphate dibasic, 5.2 mM potassium phosphate monobasic, pH 7.0). Proteins bound to the column are eluted by a gradient of high phosphate buffer (0.3 M potassium chloride, 340 mM potassium phosphate dibasic, 160 mM potassium phosphate monobasic, pH 7.0). With increasing amounts of PO_4^{-2} ions, these negatively charged ions compete to bind Ca^{+2} ions on the column as well as they bind to positively charge amino acid residues on the protein thus allowing the separation of proteins from the column. Proteins are eluted on the basis of the charge, higher the charge carried by protein later is the protein eluted from the column. Fraction with proteins were identified by ultraviolet absorbance of the fractions (Figure 20) and later checked for MyBPC by denaturing or sodium dodecyl sulfate polyacrylamide gel electrophoresis (SDS-PAGE).

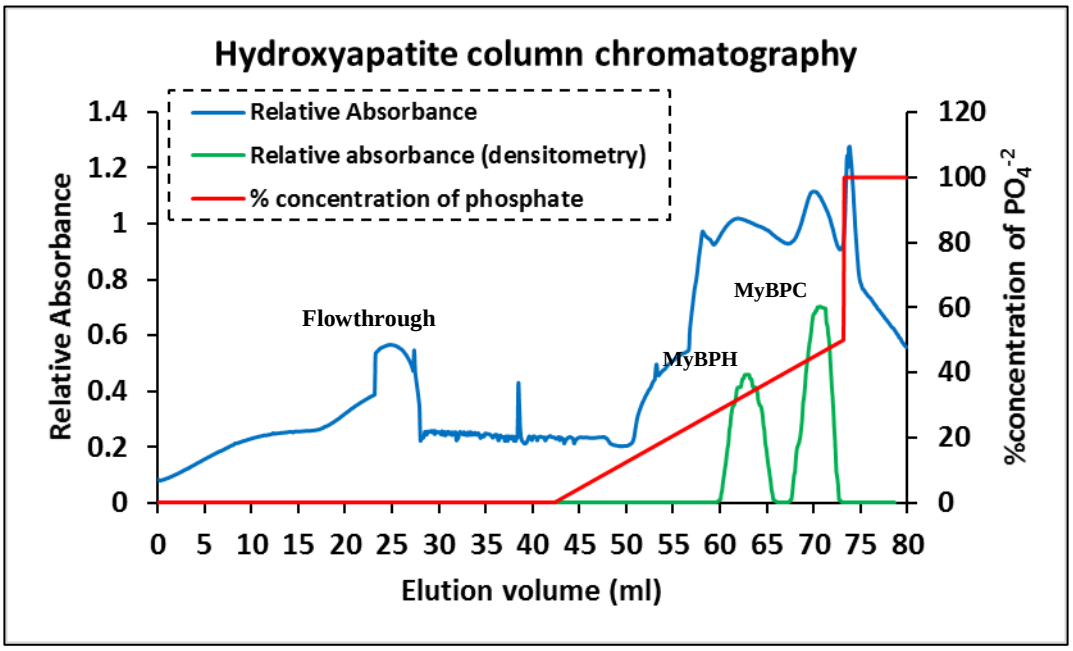

Figure 20. Hydroxyapatite column chromatography of crude MyBPC extract. UV absorbance at 254 nm was read from a flow cell (blue line). SDS-PAGE of the fractions was analyzed by densitometry at mobilities corresponding to MyBPH and MyBPC (green line). The 100% phosphate concentration was at a total of 500 mM phosphate.

To further purify MyBPC, a size exclusion chromatography was performed with Toyopearl HW-55 column low phosphate buffer as used earlier. Proteins are separated on the basis of size in size exclusion chromatography. If the pore size of the resin of the column is less than that of the protein those proteins are eluted out first followed by proteins whose size are smaller than the pore size. These smaller-sized proteins would enter these resin molecules one after another and elute out much later than the larger sized proteins. Toyopearl HW-55 has size exclusion limit of 700,000 Da, and MyBPC has the size of approximately 140,000 Da, thus performing this chromatography would get rid smaller molecular weight proteins. The buffer used for size exclusion chromatography was at 10 mM of phosphate buffer at pH 7.0. Fractions collected (Figure 21) were subjected to denaturing polyacrylamide gel electrophoresis to check the presence of MyBPC at 140,000 - 150,000 Da.

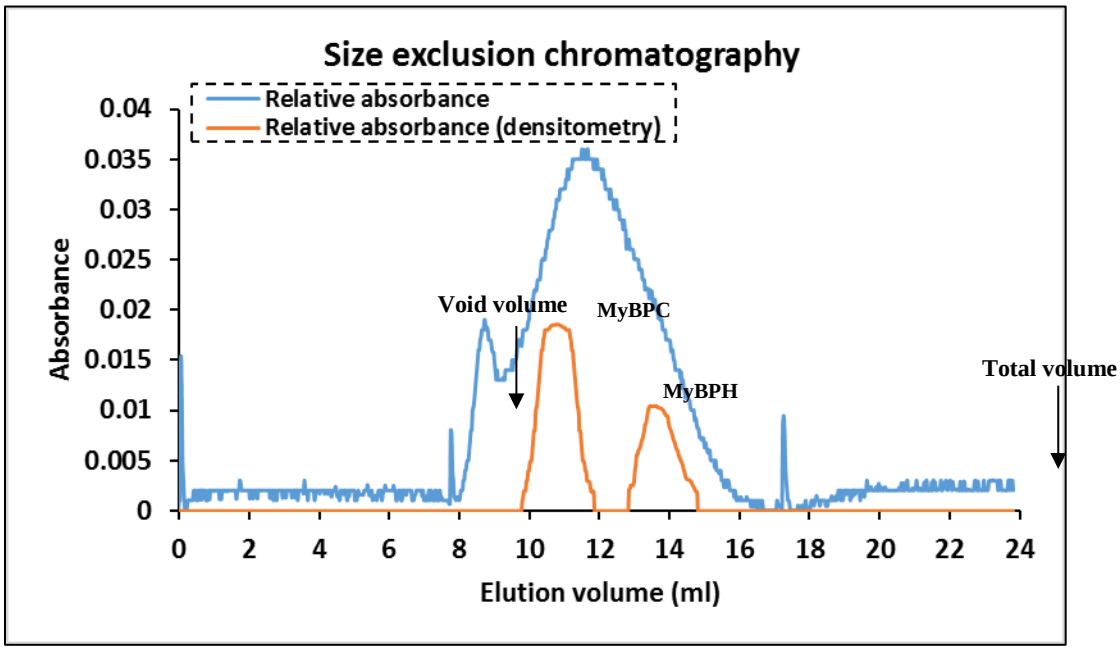

Figure 21. Size exclusion chromatogram of MyBPC fractions. UV absorbance at 254 nm was read from a flow cell (blue line). SDS-PAGE of the fractions was analyzed by densitometry at mobilities corresponding to MyBPH and MyBPC (brown line).

Anion exchange chromatography was performed with the above size exclusion chromatography fractions containing MyBPC to purify it much further. Diethylaminoethanol linked sepharose column are positively charged and allow protein to bind the column through ionic bonds with low salt buffer (20 mM Tris hydrochloric acid, pH 7.5). Proteins are eluted by running a gradient of high salt buffer, where negatively charged chloride ions Cl^- compete with the proteins to bind the positively charged resin thus allowing proteins to be eluted on the basis of charge carried by protein. The fractions containing the purified MyBPC was collected based on the chromatogram (Figure 22A). Denatured polyacrylamide gel electrophoresis confirmed the purification of MyBPC. The gel picture of the fraction containing MyBPC is imaged in Figure 22B. Several isoforms of MyBPC was observed in the gel labelled A, B, C and D.

The gene database indicates three isoforms of myosin binding protein C gene namely, skeletal myosin binding protein C slow type (NC_013672, theoretical molecular weight = 132.53 kDa and theoretical pI at pH 5.7), skeletal myosin binding protein C fast type (NW_003161100, theoretical molecular weight = 127.2 and theoretical pI at pH 6.2) and myosin binding protein C cardiac type (NC_013669, theoretical molecular weight = 140.36 kDa and theoretical pI at pH 6.3). The theoretical molecular weight and pI was calculated by ExPASy online tool. The molecular weight of MyBPC isoform A was at 150 kDa with 75% purity followed by MyBPC isoform B at molecular weight 134 kDa with 8.9% purity, MyBPC isoform C at molecular weight 122 kDa with 11.5% purity and MyBPC isoform D at molecular weight 114 kDa with 4.6% purity. The MyBPC was extracted from rabbit skeletal back muscles and majority of MyBPC purified belonged to isoform A, which could represent either slow type or cardiac type MyBPC while the isoforms B, C and D could represent the different isoforms of low molecular weight fast skeletal type MyBPC.

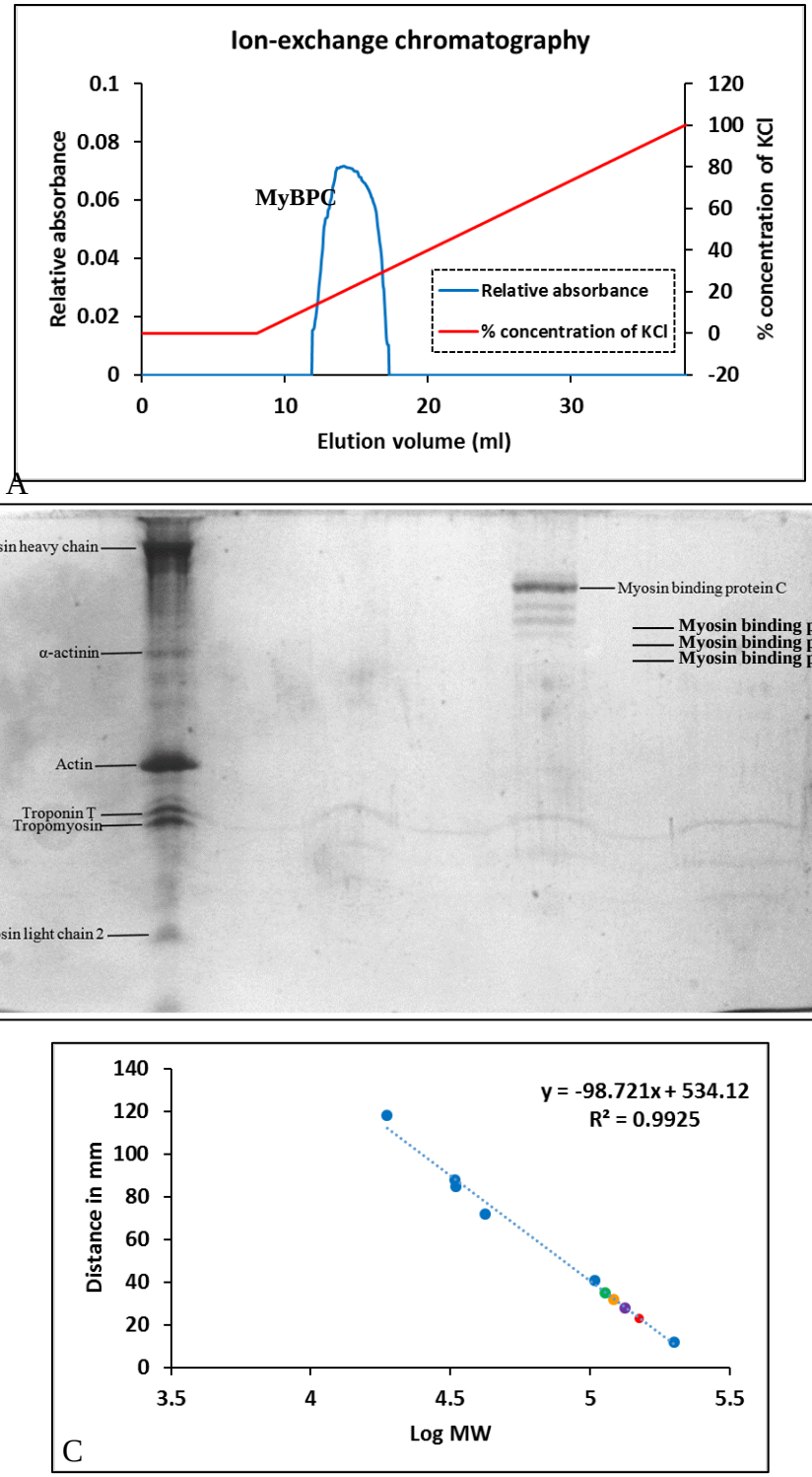

Figure 22. Ion exchange chromatography purification and determination of molecular weight of MyBPC. (A) Chromatogram of purified MyBPC. (B) SDS-PAGE gel of purified myosin binding protein C after ion exchange chromatography (C) Standard curve of distance travelled by standard protein bands versus the log of molecular weight of the proteins with MyBPC isoform A (red plot), MyBPC isoform B (purple plot), MyBPC isoform C (orange plot) and MyBPC isoform D (green plot) plotted.

The verification of MyBPC isoforms from ion exchange fraction was done by performing chromato-focusing and elution of the protein on the basis of its isoelectric point (pI). Chromato-focusing utilizes the isoelectric point of the protein to isolate the protein. Proteins exhibit a positive charge at a pH lower than its pI and a negative charge at a pH above its pI. The pH gradient is setup in the chromoto-focusing column with increasing pH down the column. When a protein is loaded onto the column, it will migrate down the column till its pI is reached, since protein is positively charged. After the level of its pI is reached and pH increases, the protein becomes negatively charged and will bind to the positively charged column.

If the buffer passing through the column has a pH lower than protein's pI, the protein will become positively charged and will not bind to the column but remain in the buffer. The protein will migrate down the column to where the pH is above its pI hence the protein will gain a negative charge and again bind to the column. This process continues until the protein is eluted out of the column. Protein eluted out will be in its pI. Hence, checking the pH as well as running a denaturing polyacrylamide gel electrophoresis will confirm the purification of the MyBPC.

The column used for chromato-focusing was Polybuffer Exchanger 94, and 25 mM imidazole at pH 6.5 was used to load the protein fractions from the previously performed anion ion exchange chromatography. Ten times diluted Polybuffer 74 with a pH 4.2 was used to create a pH gradient from 4.0 to 7.0. The calculated pI of unphosphorylated rabbit slow type skeletal MyBPC (NC_013672) is at pH 5.7 (ExPASy) and pH 5.6 (ANTHEPROT). The protein eluted was at pH around 5.6 (Figure 23) confirming that protein fractions obtained after anion exchange chromatography were indeed unphosphorylated slow type skeletal MyBPC, since phosphorylated MyBPC would have a lower pI (Saber *et al*., 2008). Furthermore, the MyBPC was purified from frozen rabbit skeletal myofibrils and with no additional calcium or kinase treatment to induce

phosphorylation of serine residues (McClellan *et al*., 2001). Purified MyBPC was further flash freezed in liquid nitrogen and stored at -70 ^{0}C in small aliquots for further use.

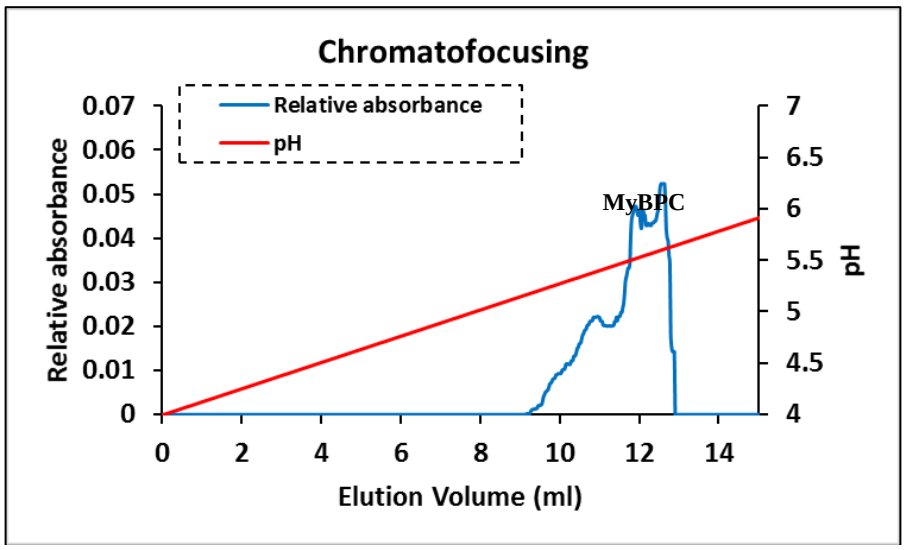

Figure 23. Chromatogram for verification of MyBPC by chromatofocusing. UV absorbance at 254 nm was read from a flow cell (blue line).

All the above column chromatography procedures were performed on a fast protein liquid chromatography system from Pharmacia Biotech in the Root lab. All the columns used were also obtained from Pharmacia Biotech.

Polyacrylamide gel electrophoresis performed to analyze the chromatography fractions were of discontinuous and denaturing type. The 2% stacking gel and 10% resolving gel were prepared by polymerizing acrylamide with linker bisacrylamide with ammonium persulfate, tetramethylethylenediamine and sodium dodecyl sulfate. Stacking gel was prepared in 0.5 M Tris hydrochloric acid buffer with pH 6.8 and resolving gel was prepared in 1.5 M Tris hydrochloric acid buffer with pH 8.8. Running buffer for electrophoresis was made of 25 mM Tris hydrochloric acid, 0.1% sodium dodecyl sulfate, 0.2 M glycine with the pH 8.3. Protein fractions were denatured by boiling the fractions with loading buffer (glycerol, 2-mercaptoethanol, 10% sodium dodecyl sulfate and 0.1% bromophenol blue in 0.5 M Tris hydrochloric acid buffer with pH 6.8). Staining

of the gels was done in solution containing 0.25% Coomassie brilliant blue G250 with 1:5:6 acetic acid: methanol: water and destained with solution containing 1:1:14 methanol: acetic acid: water.

3.2 Gravitational Force Spectroscopy

GFS was performed with purified MyBPC and the whole rabbit skeletal myosin molecule. Controls were performed by tethering whole myosin molecule to the edge of the cover slip and silica beads coated with polyclonal anti-S2 antibody. The effect of MyBPC over myosin S2 was confirmed with the same setup except the whole skeletal myosin was incubated with purified MyBPC in a 1:1 equimolar ratio. Measurements were made in both rotational and free-fall mode of GFS.

3.2.1 Force versus Distance

The flexibility and stability of myosin S2 measured with free fall mode GFS gave the necessary evidence for the stabilizing effect of MyBPC over myosin S2. Myosin S2 flexibility was tested by pulling the myosin molecule perpendicular to the myosin thick filament axis by GFS. The perpendicular uncoiling of myosin S2 coiled coil to test the stability of myosin coiled coil was utilized because when myosin molecule pulled parallel to its filament axis by tethering the myosin molecule close to its myosin S1-S2 hinge by MF30 antibody and LMM by MF20 had no correlation with the lengths observed based on the force imparted. The force-distance curve for the parallel pull of myosin coiled coil was readily fit by a wormlike chain (WLC) model (Root *et al*., 2006) (Figure 24A).

$$f(x) = \left(\frac{k_B T}{p}\right)\left[\frac{1}{4(1 - x/L)^2} - \frac{1}{4} + \frac{x}{L}\right]$$

in which $f(x)$ is the force at extension x, k_B is Boltzmann's constant, T is the absolute temperature, p is the persistence length, and L is the contour length.

The WLC fit gave a contour length of 131 ± 16 nm at forces less than 25 pN and 249 ± 6 nm at forces higher than 45.5 pN resulting in 1.9 fold extension of myosin molecule at higher forces which is consistent with an α-helix to parallel β-strand transition (Root *et al*., 2006). Similarily, the force-distance curve of DNA when pulled parallel to its long axis is also fit well by the WLC model with a B to Z DNA transition at nearly 60 pN (Cluzel *et al*., 1996; Smith *et al*., 1996). DNA was stretched parallel to its long axis by GFS. DTPA tagged dCTP amplified DNA was tethered to aminosilanated immobile glass coverslip edge and glass bead by carbodiimide and N-hydroxysuccinamide coupled cross-linking mechanism as utilized to couple actin in GFS method section. DNA measurements for GFS, were made at room temperature, in buffer containing 10 mM Tris hydrochloride, 50 mM potassium chloride, and 2 mM magnesium chloride at pH 8.3. The force-distance curve for parallel stretching of DNA by GFS also fitted the WLC model (Figure 24B) and yielded a contour length 1.8 times higher for DNA molecule at high force load leading to Z DNA conformation compared to one at low force resulting from the B DNA conformation. The altered DNA extension trace at lower forces may be due to the partial single stranded form of DNA at lower ionic strength conditions as observed by Smith *et al*., 1996.

While the force-extension curve of DNA stretched parallel to its long axis is well fit by WLC, when DNA is unzipped perpendicular to its long axis, the resulting force-distance curve is best fit by a model other than the WLC fit (Cocco *et al*., 2002; Krautbauer *et al*., 2003). Similarly, when the myosin coiled coil is unzipped perpendicular to its long axis, a different model better fits the data. The apparent logarithmic fit of these data from unzipping myosin suggest that the force is entropically driven.

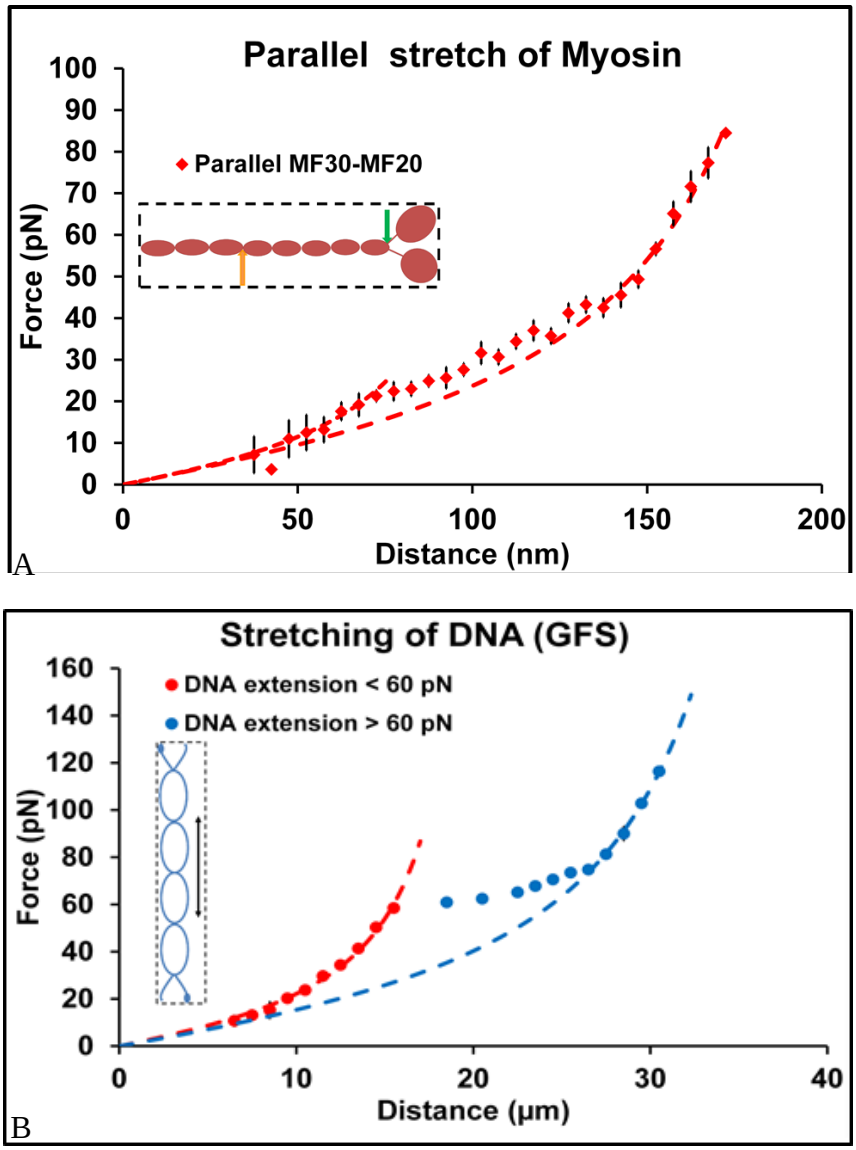

Figure 24. Parallel stretching of myosin and DNA molecule by GFS. (A) Stretching of myosin molecule (red) parallel to its filament axis by tethering the molecule with MF30 (green arrow) at myosin S2 and MF20 (orange arrow) at LMM. The force-distance curve (red circles) for the parallel stretch of myosin molecule (n = 5) with WLC fit (red dashed lines). (B) Stretching of DNA molecule parallel to its long axis. A composite trace of force-distance curve, with a DNA molecule (red circles) stretched at forces less than 60 pN fitted (red dashed line) to WLC model and another DNA molecule (blue circles) stretched at forces higher than 60 pN with WLC fit (blue dashed lines). Inset figure (dashed box) of DNA molecule (blue) with DTPA tagged dCTP (blue circle) stretched in the direction of the black bidirectional arrow.

The following equation was used to fit the force-distance trace for GFS measurements (Singh, R.R., Dunn, J.W *et al*., 2017) which gave the correlation between the length observed to the

amount of force applied when the myosin molecule was pulled perpendicular to thick filament axis as explained;

$$\int F \cdot dx = \int dG = \int dH - \int T\, dS,$$

in which F is force, G is free energy, H is enthalpy, T is temperature, S is entropy, and x is the extension.

$$F \int -dx = \int dH - k\, T \ln \Omega = \int dH - k\, T \Sigma\, p_i \ln p_i \approx \int dH - v\, k\, T\, x \ln x$$

in which Ω is the number of microstates from the third law of thermodynamics, k is Boltzman's constant, p_i is the probability that a microstate will be occupied, and v is an approximate proportionality constant between the extension x and p_i. The sign of $\int -dx$ is negative because the force vector of the molecule resisting stretch is in an opposite direction to the externally applied force and extension (Figure 25).

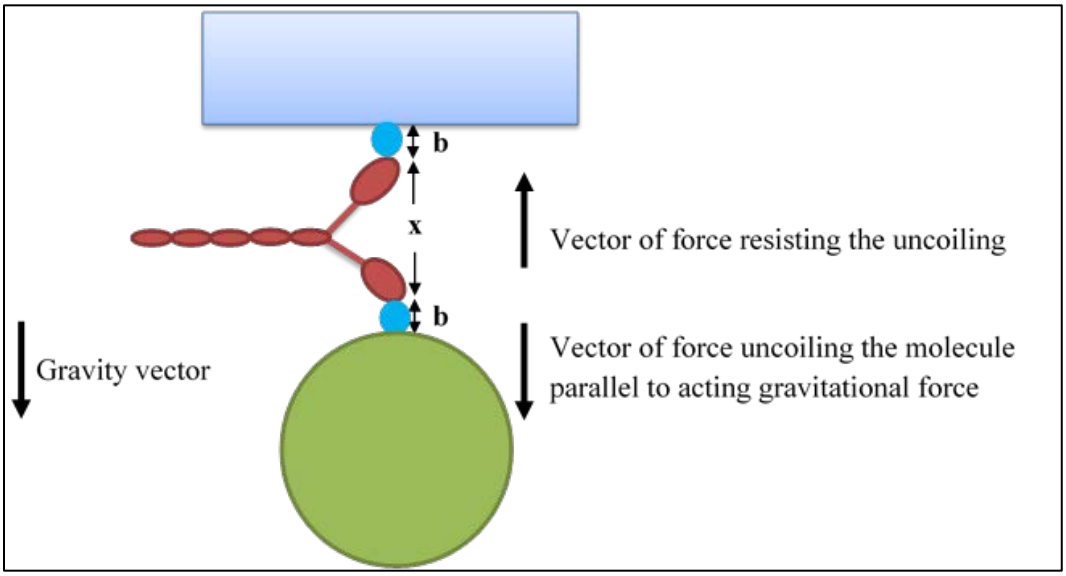

Figure 25. Force vectors acting on a molecule in GFS. A myosin molecule (red) tethered between edge of coverslip (blue square) and silica bead (green sphere) by its S1 heads with actin (cyan). Two opposing forces acting on myosin molecule, one resisting the uncoiling of myosin (upward pointing arrow) and the other uncoiling the molecule (downward pointing arrow) in the direction of gravity vector, where x is the extension and b is the length of linker.

$$F = v\, k\, T \ln x - \int dH / \int dx = a \ln (x + b) + c,$$

where a; is a proportionality constant, b; is the length of the linker, and c; is the change in enthalpy with extension that is assumed to be relatively constant.

For a single observation, the following data was observed. In the absence of MyBPC, the myosin S2 was able to uncoil to a length of 115 nm with a force of 6.59 pN (Figure 26A). While in presence of MyBPC the uncoiling length was 125 nm at a force of 21.35 pN (Figure 26B). The hysteresis observed on the force trace was not statistically significant ($p_{control}$ = 0.52 and p_{test} = 0.47) indicating that the process of uncoiling and recoiling of myosin coiled coil was rather a simple folding and unfolding process with no significant build up of intermediate states observed. Several measurements were averaged for statistical analysis with the force required to uncoil myosin S2 to a total length of 100 nm of 6.1 pN ± 0.1 in the absence of MyBPC (n = 7) and 20.5 pN ± 0.5 in presence of MyBPC (n = 10) (Figure 27, Table 1).

The formula for the fit derived for the perpendicular pull of myosin molecule, gave the correlation coefficient (R) as 0.98 both in the absence of MyBPC and in the presence of MyBPC (Table 1). Comparisons of force versus distance traces of myosin in absence and presence of MyBPC yielded clear evidence for the stabilization of myosin S2 region in presence of MyBPC (Figure 28).

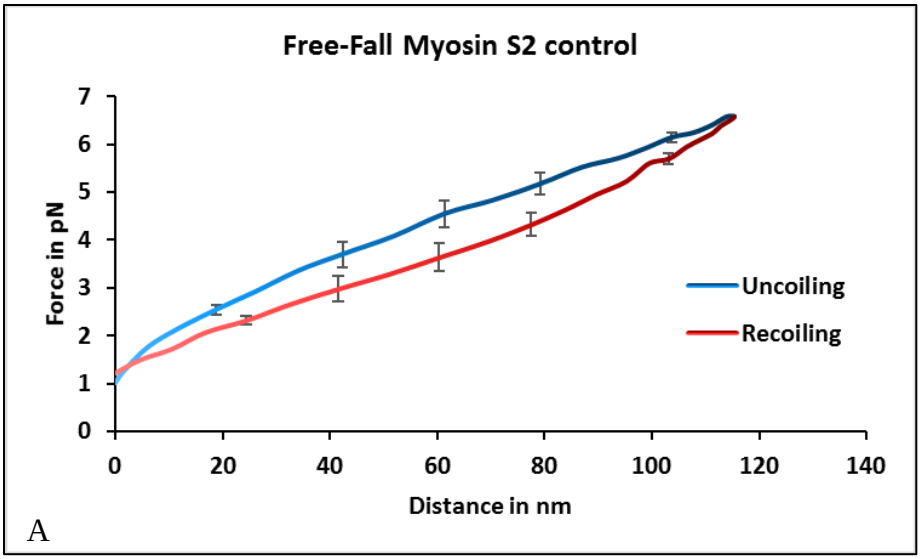

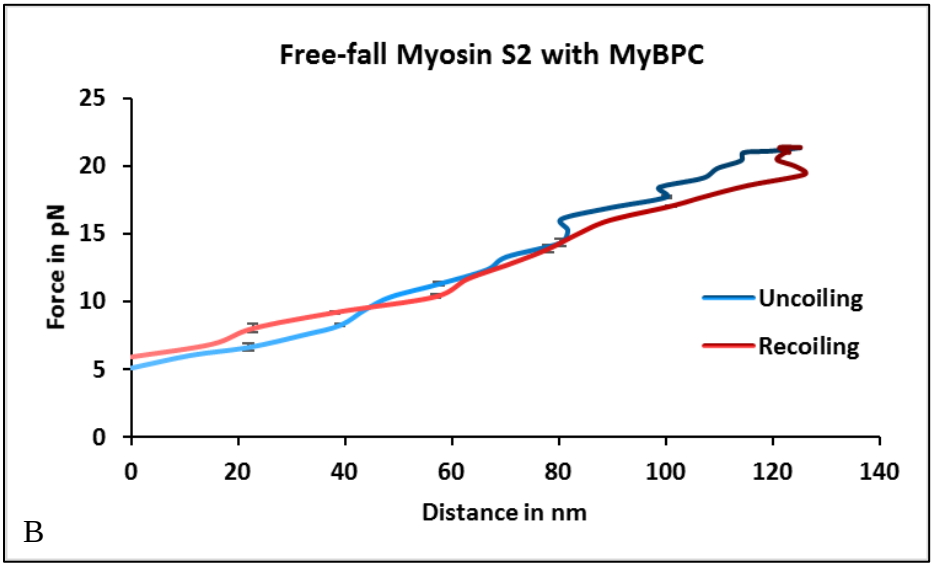

Figure 26. Free-fall mode data of Myosin S2 without and with MyBPC. (A) Uncoiling and recoiling of myosin S2 in absence of MyBPC. (B) Uncoiling and recoiling of myosin S2 in presence of MyBPC. There is no statistical significant difference for the hysteresis between uncoiling and recoiling plots with p values greater than 0.05 at 0.52 for control and 0.47 for test with MyBPC.

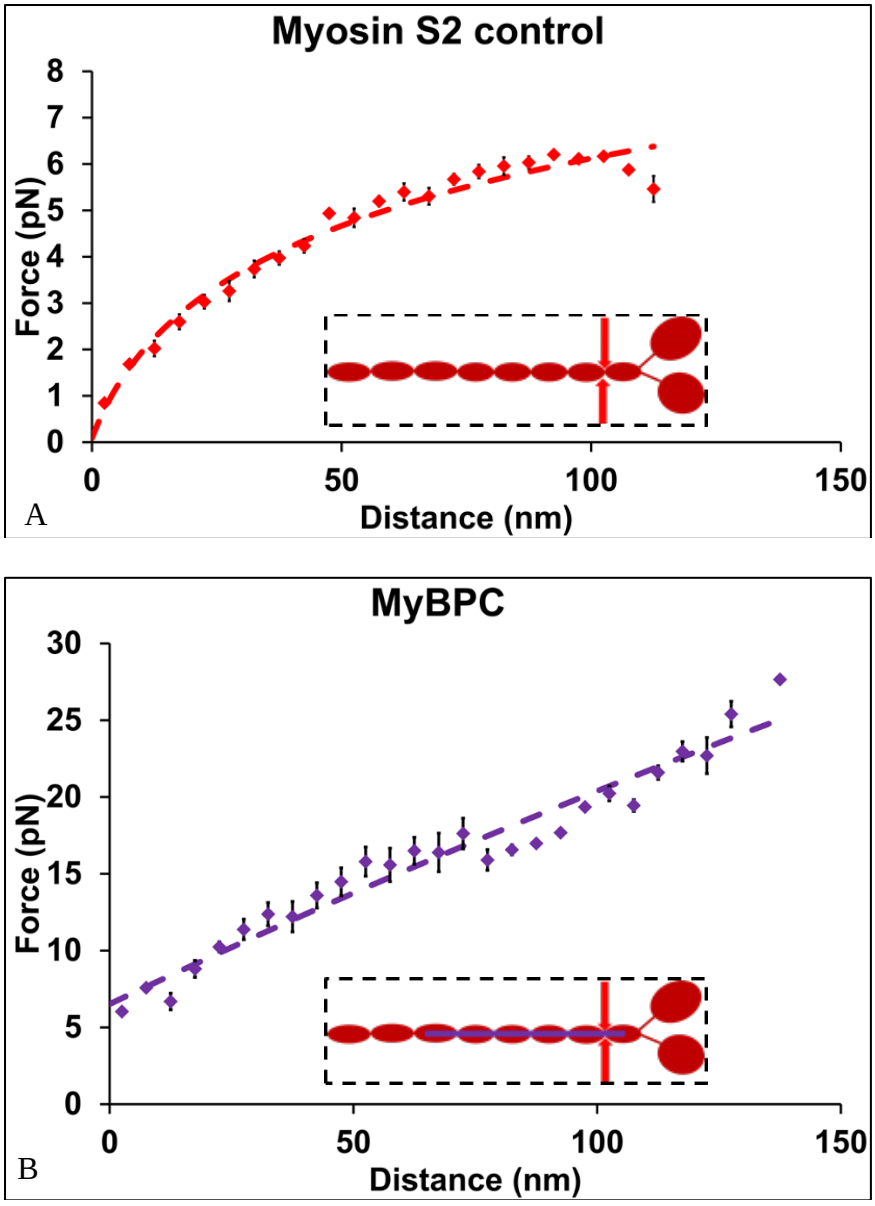

Figure 27. Data fit for average of force versus distance of myosin S2 in absenc e and presence of MyBPC. (A) Force versus distance trace for myosin in absence of MyBPC (n=7). (B) Force versus distance trace for myosin S2 in presence of MyBPC (n=10). In dashed box; cartoon of a myosin molecule (red) with MyBPC (purple) tethered at myosin S2 region with polyclonal anti-S2 antibody (red arrow) for GFS.

	No. of molecules (n)	Length (nm)	Force (pN)	Correlation coefficient (R)
Myosin S2 (Control)	7	100	6.1 ± 0.1	0.98
Myosin S2 with MyBPC (Test)	10	100	20.5 ± 0.5	0.98

Table 1. Length of uncoiled myosin S2 molecule in absence and presence of MyBPC measured with GFS.

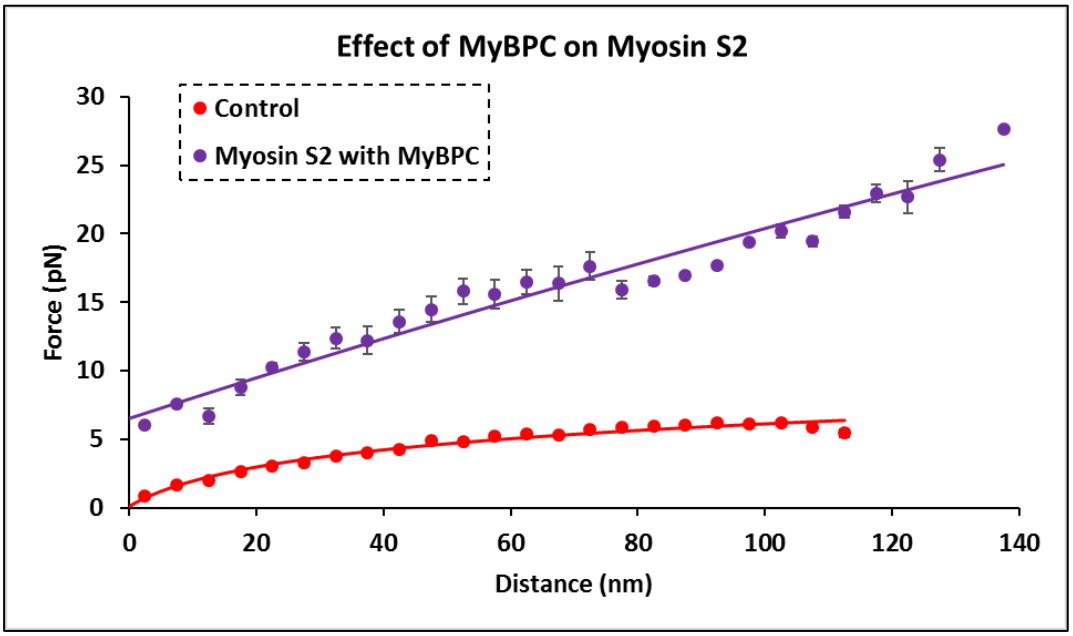

Figure 28. Effect of MyBPC on Myosin S2 flexibility. Myosin S2 in absence of MyBPC (red) is flexible with forces maxing out at 6.1 pN to uncoil a distance of 100 nm, while in presence of MyBPC (blue) the myosin S2 becomes more stabilized with 20.5 pN of force required to uncoil the same distance of 100 nm. (The error bars for the control plot are smaller than the data points)

GFS measurements made to uncoil myosin molecules in presence of MyBPC required more force to uncoil the myosin molecule. The effect is at the myosin S2 region, since polyclonal anti-S2 antibody attachment to myosin S2 region was utilized to uncoil the myosin molecule, and MyBPC being unphosphorylated binds to myosin S2 with its N-terminal region, thus confirming the stabilization of an already flexible myosin S2 coiled coil.

3.3 *In vitro* Motility Assay

With the result observed from GFS assay of MyBPC on myosin S2, the next step is to check whether the stabilization of myosin S2 by MyBPC has an effect over the motility produced through acto-myosin interaction. *In vitro* motility of fluorescently labelled actin filaments over myosin thick filament or myosin HMM would be able to corroborate the effect of stabilized myosin S2 by MyBPC over the force produced. The expected result is that the stabilized myosin S2 by the binding of MyBPC would decrease the motility of actin filaments.

The *in vitro* motility assay setup includes the immobilization of whole myosin thick filaments on the coverslip instead of classically used myosin HMM. The idea behind the use of whole myosin thick filament was to favor the binding of MyBPC. Since MyBPC requires the LMM along with the myosin S2 to bind to myosin thick filament, use of myosin HMM alone won't be sufficient enough to bind MyBPC. For the assay, the motility of actin filaments in absence of MyBPC and later adding equimolar concentration of MyBPC to the same slide preparation gave the comparison of motility of actin filaments in absence and presence of MyBPC.

The histogram for the motility of actin in absence and presence of MyBPC is plotted (Figure 29A). The histogram clearly indicates the shift of actin motility towards reduced motility in presence of MyBPC. Sliding velocity of actin filament in absence of MyBPC was on an average 6.7 um/sec ± 0.2 (n = 33). On the other hand, the average sliding velocity of actin filaments in presence of MyBPC was 5.0 um/sec ± 0.1 (n = 44) (Figure 29B). Student's t-test for two samples with equal variances gave a p value of 0.01×10^{-5} stating the reduction in sliding velocity of actin filament in presence of MyBPC is statistically significant.

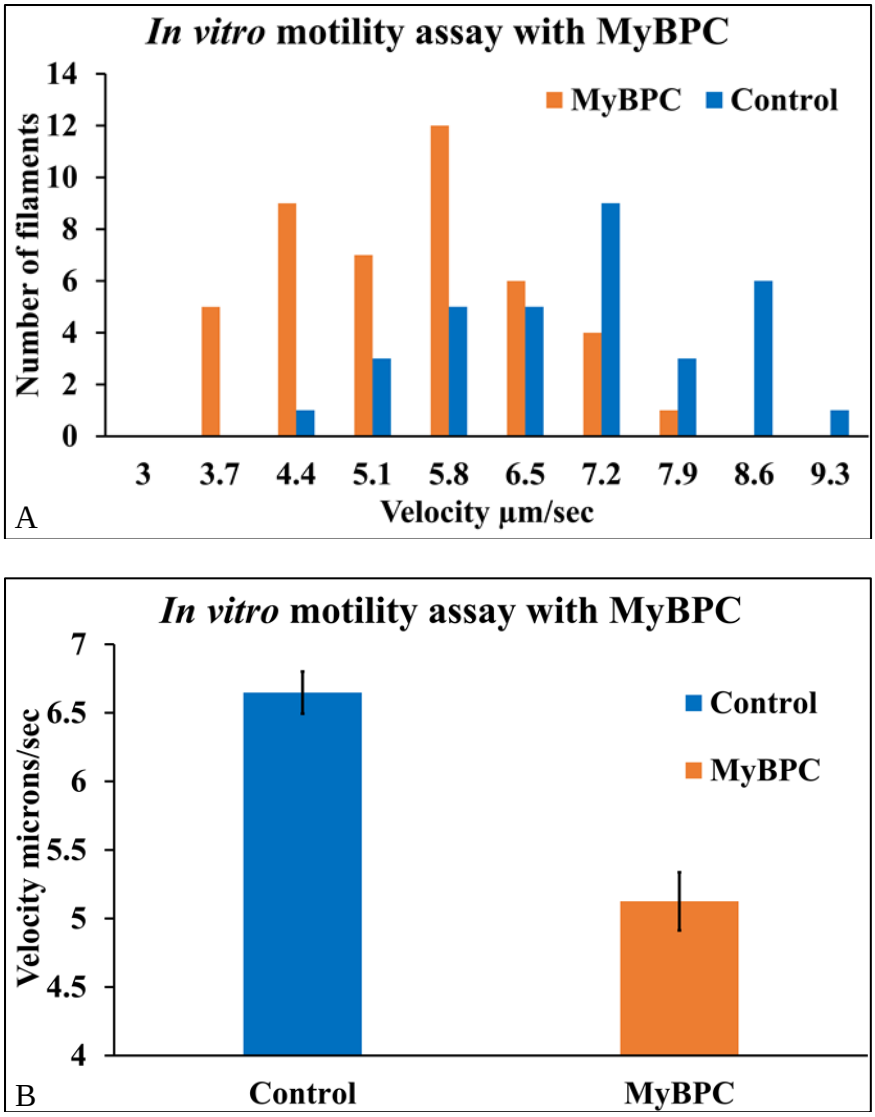

Figure 29. Histogram of *in vitro* motility assay with MyBPC. (A) Histogram plot showing distribution of in-vitro actin filament motility over myosin thick filaments in the absence (blue) (n=33) and presence (orange) of full-length skeletal MyBPC (n=44). (B) Histogram showing average velocity of actin filaments in absence (blue) and presence (orange) of full-length skeletal MyBPC.

3.4 Conclusion

GFS experiments performed with whole skeletal myosin and purified skeletal MyBPC established that binding of MyBPC to the myosin molecule stabilized the myosin S2 region. The force required to pull the myosin molecule at its S2 region in presence of MyBPC was 3.35 times

more than the force required to pull the myosin molecule in absence of MyBPC (Figure 28, Table 1). The effect of MyBPC is at the myosin S2 region since the point of attachment used to tether the myosin molecule for GFS assay was at the myosin S2 region by the virtue of polyclonal anti-S2 antibody.

The *in vitro* motility assay was performed with immobilized whole myosin thick filaments in presence of MyBPC. The motility of fluorescently-labelled actin filaments was slowed down by the presence of MyBPC. The sliding velocity of actin filaments in absence of MyBPC was 6.7 μm/sec ± 0.2 and in the presence of MyBPC the sliding velocity was reduced to 5.0 μm/sec ± 0.1 (Figure 29). This is for the first time where the binding of whole length MyBPC to myosin thick filament had a diminishing effect over sliding velocity of actin filaments (Singh, R.R., Dunn, J.W *et al*., 2017). The results from GFS and *in vitro* experiments confirms that binding of MyBPC to the myosin molecule stabilized the myosin S2 region and this stabilized myosin S2 region was able to reduce the motility of actin over the myosin filaments bound with MyBPC.

Performing competitive ELISA with MyBPC would be redundant, since it has already been proven that MyBPC binds to myosin molecule at its S2 region (Starr, R., and Offer, G. 1978; Weisberg, A., and Winegrad. S. 1996). The myofibrillar contractility assay was not performed since myofibrils already have their own native MyBPC so adding additional MyBPC won't be readily able to incorporate into myofibrils due to its size and the fact that myofibrils are likely already saturated with its own MyBPC.

The experiments were performed by binding of MyBPC to myosin molecule or thick filament with the known fact that MyBPC binds to the myosin S2 region of myosin molecule, thus any effect seen in *in vitro* motility experiments, were due to binding of MyBPC to myosin thick filament in myosin S2 region. The GFS experiment also relayed the message that the binding of

MyBPC to the myosin molecule stabilized the myosin S2 region. These results thus give a direct correlation between the stability of myosin S2 and availability of myosin S1 heads (N_t) to bind actin thin filaments.

CHAPTER 4

STABILIZER PEPTIDE AND MYOSIN SUBFRAGMENT-2

4.1 Introduction and Idea behind the Design and Use of Stabilizer Peptide

The design of stabilizer peptide to stabilize the myosin S2 coiled coil was based on an idea from an earlier study, where an antibody raised against the whole myosin S2 coiled coil reduced the isometric force produced by the myosin molecule with no hindrance to myosin S1 activity to bind actin thin filaments and its ATPase activity (Sugi *et al*., 1992; Tsuchiya *et al*., 1998). Hence a molecule which can wrap around the myosin S2 coiled coil like an antibody against the whole myosin S2 should be able to replicate the effects of the antibody and reduce the isometric force produced. Along with this observation, there were FHC mutation hotspots identified in the glutamate rich region in the proximal myosin S2 region (924-942) which result in the hypertrophy of heart due to hypercontraction.

To alleviate the hypercontraction of heart muscles with a similar effect as that of antibody raised against whole myosin S2, the idea to use positively charge lysine residues which can bind to the glutamate rich myosin S2 region was developed. Several computer simulations of different lengths of polylysine residues along with varying the lysine residue with other amino acids were performed by members of the Root laboratory to find the optimal structure which will wrap around the same glutamate rich region (924-942) of human β-cardiac myosin S2 with higher binding affinity. The stabilizer peptide obtained was used for further investigations below.

The stabilizer peptide thus designed through computer simulations to bind and wrap around the myosin S2 coiled coil in the glutamate rich region was expected to stabilize the myosin S2 coiled coil and decrease the amount of force produced through acto-myosin contraction. To check whether the stabilizer peptide binds to the same glutamate rich region of myosin S2 region it was designed against, cELISA was performed to check the specificity and binding affinity of the

stabilizer peptide to the myosin S2 region. GFS experiments were performed to evaluate the proposed stabilizing effect of the stabilizer peptide over the myosin S2 region. Myofibrillar contractility assays were performed to verify that the binding of the stabilizer peptide to myosin S2 decreases the amount of shortening in myofibrils with the stabilizer peptide. *In vitro* motility assays were performed to confirm that binding of stabilizer peptide to myosin S2 would reduce the amount of motility produced through acto-myosin interaction observed through reduced sliding of actin filaments over HMM.

4.2 Competitive ELISA of Stabilizer Peptide to Myosin S2

4.2.1 Minimum Dilution of Primary Polyclonal Anti-S2 Antibody to Bind Rabbit Skeletal Myosin

To perform successful cELISA of stabilizer peptide for myosin S2 against primary polyclonal anti-S2 antibody, two values were evaluated to setup the experiment. First was the minimum dilution of antibody with assay buffer that would give a positive optical density. Second was the amount of cardiac myosin S2 peptide would compete with rabbit skeletal myosin S2 to bind polyclonal anti-S2 antibody.

The wells of the microtiter plate were coated with approximately, 200 nanograms of rabbit skeletal myosin diluted with cELISA assay buffer overnight. Several dilutions of primary polyclonal anti-S2 antibody were prepared in assay buffer. The primary antibody dilutions created with assay buffer were in the increasing exponential order of 2 for example; 1:2, 4, 8...,512. This series of diluted primary polyclonal anti-S2 antibody were added in replicates to the wells of microtiter plates. After incubation for an hour, the unbound primary polyclonal anti-S2 antibody was washed with PBS and blocking buffer. Enzyme linked secondary antibody diluted 30,000 times in blocking buffer was added to all the wells and incubated at room temperature for an hour.

After incubation, the plates were washed with detergent buffer, and later BCIP substrate was added. The microtiter plate was placed on a light box next to an optical density calibration scale under a video camera to record the color development in plates. The video was analyzed by Image J to acquire the optical density in the wells. The dissociation constant (K_d) of primary polyclonal anti-S2 antibody to rabbit skeletal myosin S2 was at dilution titer of 127 ± 4 of diluted primary polyclonal anti-S2 antibody (Figure 30). For optimal OD development, 1:64 dilution of primary polyclonal anti-S2 antibody was used in the following cELISA assays.

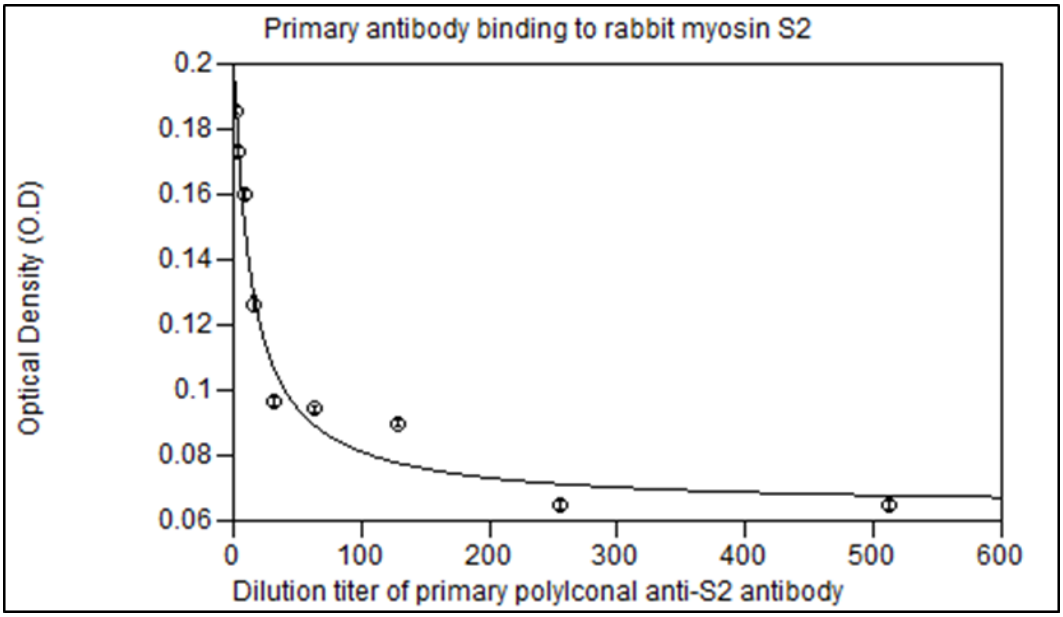

Figure 30. Optical density versus dilutions of primary anti-S2 antibody. Mapped on x-axis is the dilution titers for primary polyclonal anti-S2 antibody.

4.2.2 Concentration of Human Cardiac Myosin S2 Peptide Required to Bind Primary Polyclonal Anti-S2 Antibody

To evaluate the amount of cardiac myosin S2 peptide that would compete with rabbit skeletal myosin S2 to bind primary polyclonal anti-S2 antibody, the microtiter plate was coated with rabbit skeletal myosin first and to that was added two fold dilutions of stock of human cardiac myosin S2 peptide from 1:2 to 1:1024. To the myosin S2 peptide, 1:64 diluted primary polyclonal

antibody was added. After the washing step, secondary antibody is added followed by BCIP and development of color or OD was recorded and the video was analyzed by Image J. The OD will increase as the concentration of human cardiac myosin S2 decreases. With decreasing amounts of human cardiac myosin S2, the primary polyclonal anti-S2 antibody would bind to the available rabbit skeletal myosin allowing the enzyme conjugated secondary antibody to bind thus there will be increasing color development upon addition of BCIP substrate.

The minimum amount of human cardiac myosin S2 peptide that would bind primary polyclonal anti-S2 antibody was at a dilution of 1:32 with dissociation constant (K_d) corresponding to a dilution of 32 ± 1 from the stock (Figure 31). Such a high binding affinity was expected, since primary polyclonal anti-S2 antibody was raised against the same human cardiac myosin S2 peptide.

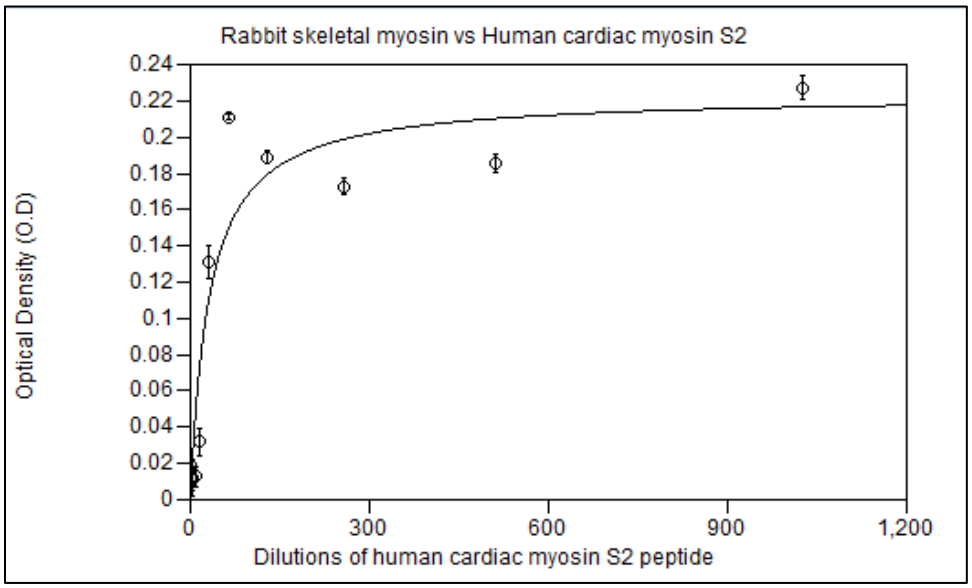

Figure 31. cELISA for competitive binding of polyclonal anti-S2 antibody to human β-cardiac myosin S2 and rabbit skeletal myosin S2.

4.2.3 Stabilizer Peptide versus Polyclonal Anti-S2 Antibody

The cELISA performed to determine the specificity of stabilizer peptide to myosin S2 begins with the 96 well microtiter plate coated with rabbit skeletal myosin and adding to it the previously determined 1:64 diluted primary polyclonal antibody along with the 1:32 diluted human cardiac myosin S2 to all the wells. To the myosin S2, two fold dilutions of stabilizer peptide from 0 to 250 nm are added in replicates to the wells. Unbound protein complexes are washed off by PBS and blocking buffer. Enzyme conjugated secondary antibody is added to the wells and allowed to conjugate for an hour. After washing with detergent buffer, color developing substrate BCIP is added and development of color in the wells is recorded. The video is analyzed by Image J to get the OD in the wells.

The trend in the OD observed was from low to high and back to low OD with increasing concentrations of stabilizer peptide (Figure 32A). In the wells in which there were no stabilizer peptide added, the primary polyclonal antibody would bind to human cardiac myosin S2 peptide and get washed away, hence the secondary antibody would not have enough primary antibody left to bind thus resulting in a low OD.

As the amount of stabilizer peptide is increased in the succesive wells, the OD kept on increasing. With the increasing amounts of stabilizer peptide, the stabilizer peptide would bind to the available human cardiac myosin S2 peptide, thus primary polyclonal anti-S2 antibody won't have enough human cardiac myosin S2 peptide to bind to. Hence, the primary antibody would bind to the next available myosin S2 site, which is on the rabbit skeletal myosin molecule coated on to the wells. Therefore, the primary antibody would remain stuck on to the wells after the washing step, thus allowing the development of color and OD upon addition of the secondary antibody and BCIP substrate.

A

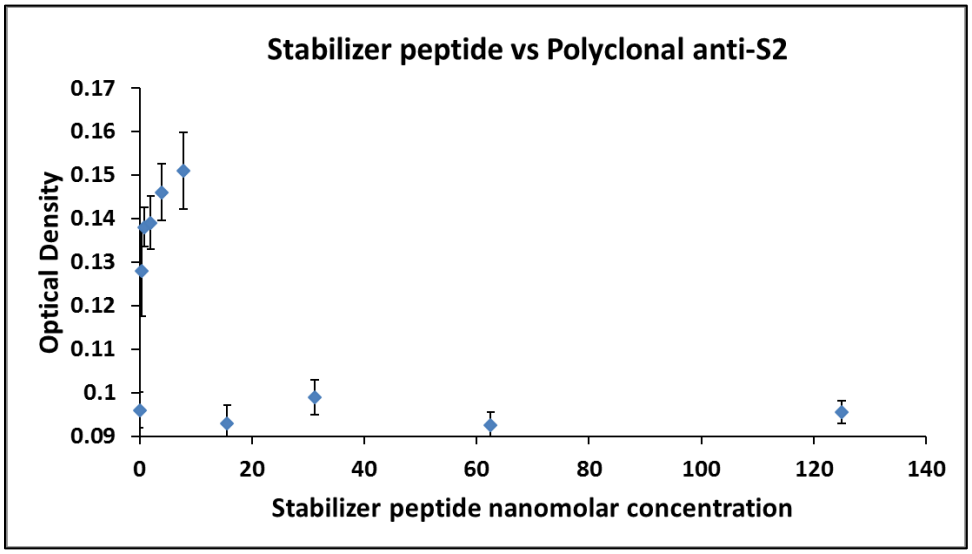

B

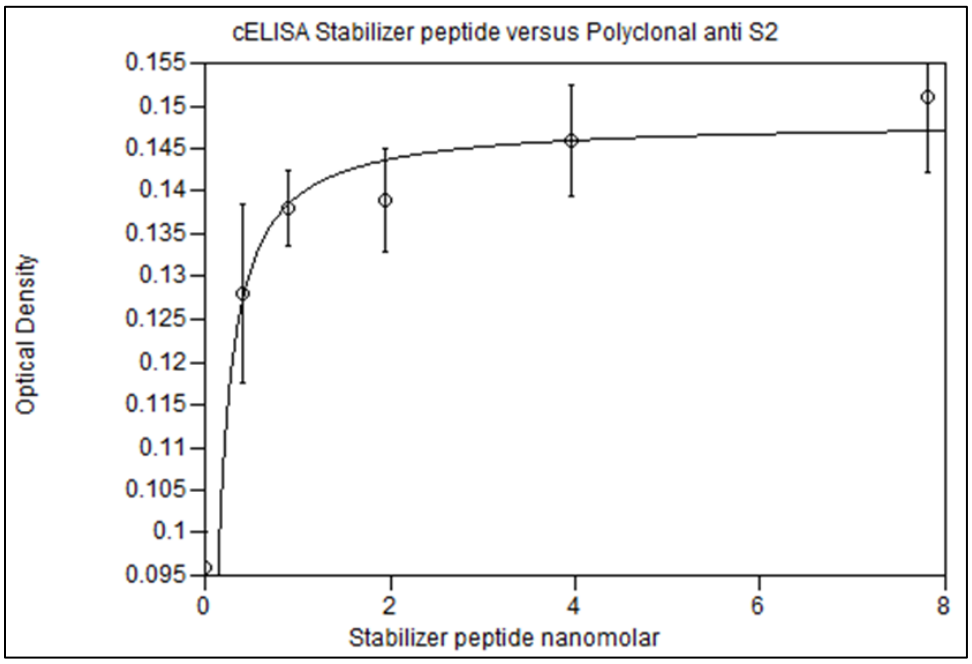

Figure 32. cELISA of stabilizer peptide versus polyclonal anti-S2 antibody. (A) OD versus increasing amounts of stabilizer peptide concentration. The low-high-low OD trend observed states the specific binding of stabilizer peptide to human cardiac myosin S2 peptide. (B) Curve fit to the initial data points from panel (A) to determine the binding affinity of stabilizer peptide to human cardiac myosin S2 peptide.

With the increasing amounts of stabilizer peptide comes a stage where the stabilizer peptide would saturate all the available human cardiac myosin S2 peptide and later would go and bind to the myosin S2 region available on the rabbit skeletal myosin coated on to the wells. As a result,

the primary polyclonal anti-S2 antibody won't have enough sites available to bind either the human cardiac myosin S2 peptide or the rabbit skeletal myosin molecule. Since the enzyme conjugated secondary antibody won't have enough primary antibody left to bind, there follows a sharp decline in the OD.

The minimum dissociation constant (K_d) for stabilizer peptide was calculated by the following derived formula (Creighton, T.E. 1993);

$M = K_A*B_A /A = K_P*B_P /P$, where; M = Myosin concentration, A = primary antibody concentration, P = stabilizer or destabilizer peptide concentration, $K_A = K_d$ for primary antibody binding, $K_P = K_d$ for the binding of stabilizer or destabilizer peptide, B_A = antibody bound, and B_P = stabilizer or destabilizer peptide bound.

Therefore, $B_A / B_P = (K_P*A)/(K_A*P)$

When P=IC50, then $B_A = B_P$, so

$K_P = IC50*K_A /A$

The curve fit gave the dissociation constant of stabilizer peptide binding to human cardiac myosin S2 peptide at 1.37 nM ± 0.02 (Figure 32B). The minimum dissociation constant (K_d) for the monomer of stabilizer peptide binding to rabbit skeletal myosin was calculated at 6 nM ± 2. This K_d value could be greater if the concentration of primary antibody is not much greater than the myosin S2 concentration. The cELISA results established that the stabilizer peptide designed has a high binding affinity to human cardiac myosin S2 peptide. The stabilizer peptide is also prefers to bind to human cardiac myosin S2 over rabbit skeletal myosin S2.

4.3 Gravitational Force Spectroscopy with the Stabilizer Peptide

The stabilizer peptide was designed with the aim to bind and stabilize the myosin S2 coiled

coil and reduce the amount of contraction and overall force produced through acto-myosin interaction. The cELISA experiment confirmed the specificity of the stabilizer peptide to the myosin S2 region, since the stabilizer peptide competed with the site-specific polyclonal antibody. Next was to verify the stabilization of myosin S2 coiled coil by the stabilizer peptide. This verification was done by performing the GFS assay with rabbit skeletal myosin in the presence of stabilizer peptide.

When the GFS assay was performed with polyclonal anti-S2 antibody as the point of attachment to tether the myosin molecule treated with stabilizer peptide, few beads were tethered to edge of the coverslip compared to control. The observed beads in the assay with myosin treated with stabilizer peptide gave similar force traces as that for myosin without the stabilizer peptide, thus stating that there was competition between antibody and stabilizer peptide to bind myosin at the S2 region. Hence, the point of attachment to tether the myosin molecule between the immobile edge of the coverslip and mobile beads, was at the acto-myosin S1 binding region and not by the polyclonal anti-S2 antibody binding.

The edge of the coverslips and silica beads are coated with G-actin molecules. The slide thus prepared would have myosin molecule suspended by its myosin S1 heads binding to the actin molecule on edge of the coverslip and silica beads. The control for this assay was setup by tethering rabbit skeletal myosin sans stabilizer peptide between the actin-coated immobile edge and mobile beads. To assay the effect of stabilizer peptide binding to the myosin S2 region, GFS was performed with myosin molecules incubated with stabilizer peptide and tethering these treated myosin molecules at its myosin S1 heads with immobile edge and mobile beads coated with G-actin molecule. From the force-distance curve fits, the force required to uncoil the myosin molecule for a length of 50 nm in absence and presence of stabilizer peptide was 3.6 ± 0.4 pN and 5.5 ± 0.1

pN respectively (Figure 33 and Table 2). The R value for control and test force-distance curve fits were 0.99 and 0.92 respectively (Table 2).

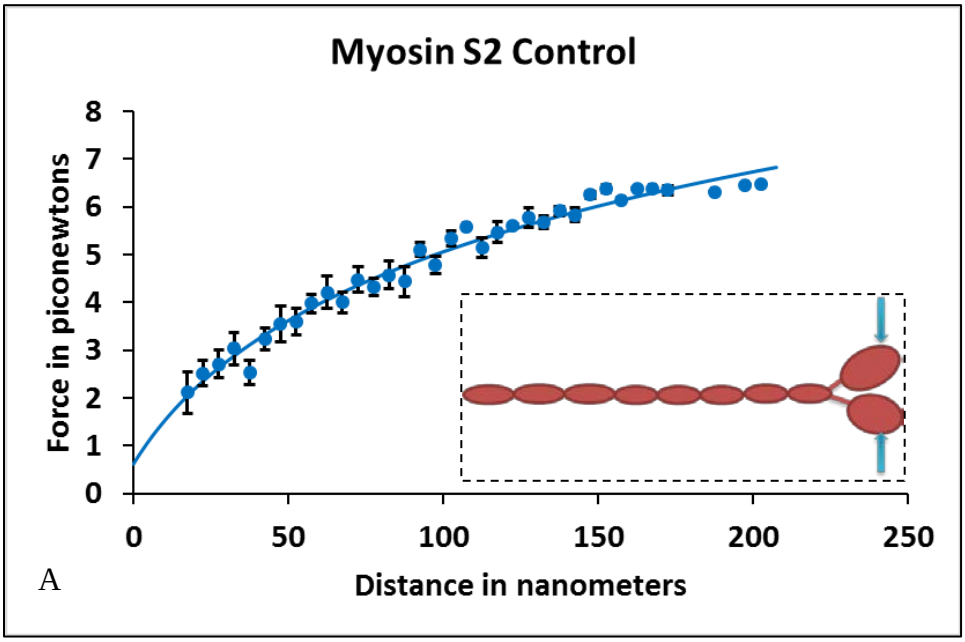

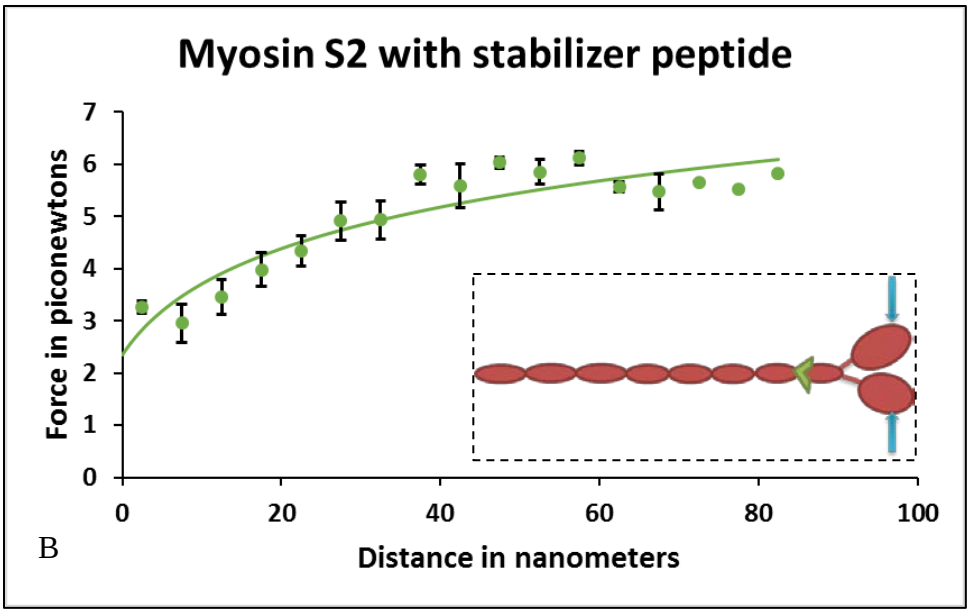

Figure 33. GFS curve fit for average forces to distance for the effect of stabilizer peptide on the myosin S2 coiled coil. (A) Force-distance curve for myosin molecule in the absence of stabilizer peptide (n =7). (B) Force-distance curve for myosin molecule in the presence of stabilizer peptide (n = 6). In dashed box; cartoon of a myosin molecule (red) with stabilizer peptide (green) tethered at myosin S1 actin with actin (cyan arrow) for GFS.

	No. of molecules (n)	Length (nm)	Force (pN)	Correlation coefficient (R)
Myosin S2 (Control)	7	50	3.6 ± 0.4	0.99
Myosin S2 with stabilizer peptide (Test)	6	50	5.5 ± 0.1	0.92

Table 2. Length of uncoiled myosin S2 molecule in absence and presence of stabilizer peptide measured with GFS.

The force-distance curve fits of myosin molecule uncoiled in the absence and presence of stabilizer peptide showed the stabilizing effect of stabilizer peptide on S2 of myosin molecule with 1.5 times the force required to uncoil myosin in presence of stabilizer peptide (Figure 34 and Table 2). The myosin molecule when uncoiled from its myosin S1 heads has a similar shape force-distance trace but longer extensions than that when uncoiled from myosin S2 region (Singh, R.R., Dunn, J.W *et al*., 2017). Since the stabilizer peptide is specific to myosin S2, the stabilizing effect observed was due to binding of the stabilizer peptide to myosin S2.

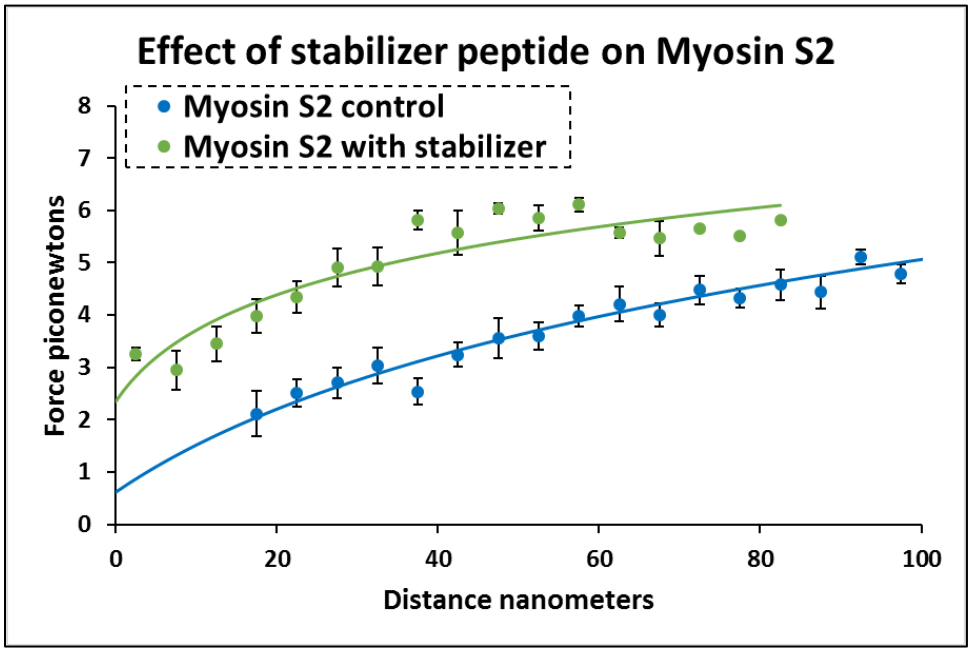

Figure 34. Comparison of force-distance curves of myosin molecule without stabilizer peptide (blue) and myosin molecule with stabilizer peptide added (red).

4.4 Myofibrillar Contractility Assay with Stabilizer Peptide

The cELISA and GFS experiments with stabilizer peptide confirmed that the stabilizer peptide is specific to myosin S2 as well as having a stabilizing effect on the myosin molecule at its S2 region. The next test was to verify whether the stabilization of this myosin S2 region has an effect on the contractility of myofibrils.

The myofibrillar contractility assay with stabilizer peptide is able to verify the stabilization effect of myosin S2 by stabilizer peptide on myofibrillar contraction. For the assay, rabbit skeletal myofibrils were washed several times with assay buffer. Small amounts of myofibrils were placed on a glass slide and imaged through the microscope. To the same myofibrils, ATP was added to a final concentration of 1 mM, and the myofibrils were imaged after 30 minutes to allow the myofibrils to take up ATP and allow the sarcomeres to shorten. These myofibrils are again imaged through microscope.

To test the effect of stabilizer peptide on the myofibrils, the washed rabbit skeletal myofibrils were incubated at room temperature with different concentrations of stabilizer peptide ranging 1-100,000 nM in the multiples of 10. The myofibrils incubated with stabilizer peptide were placed on to a coverslip and imaged through the microscope. To the same myofibrils, 100 µl of assay buffer with 1 mM ATP are added and the myofibrils were imaged after 30 minutes to allow the myofibrils to take up ATP resulting in sarcomere shortening.

Length of the sarcomere measured before and after addition gave the percentage contraction observed in the myofibrils without and with stabilizer peptide. For the control, the percentage contraction in the myofibril was at 22.3% ± 0.2 (Figure 35A). The percentage contraction observed in the myofibrils incubated with increasing concentrations of stabilizer peptide was reduced and saturated to 18.6% ± 0.5 at 1000 nM of stabilizer peptide (Figure 34A).

The dissociation constant of stabilizer peptide binding to myofibrils was calculated to be 6 nM ± 1 stating the high binding affinity of stabilizer peptide to myosin S2 present in myofibrils (Figure 35B).

A

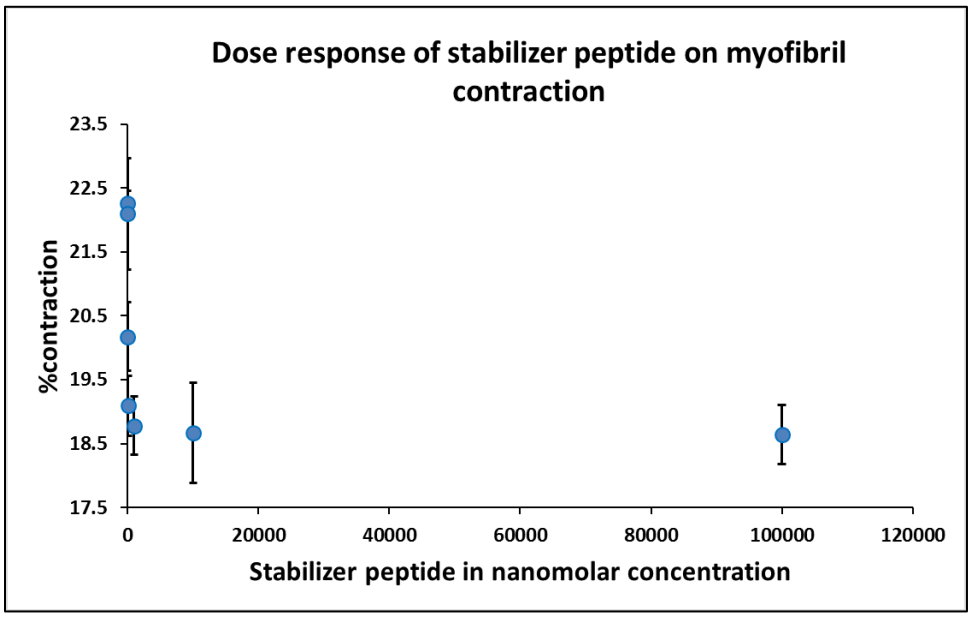

B

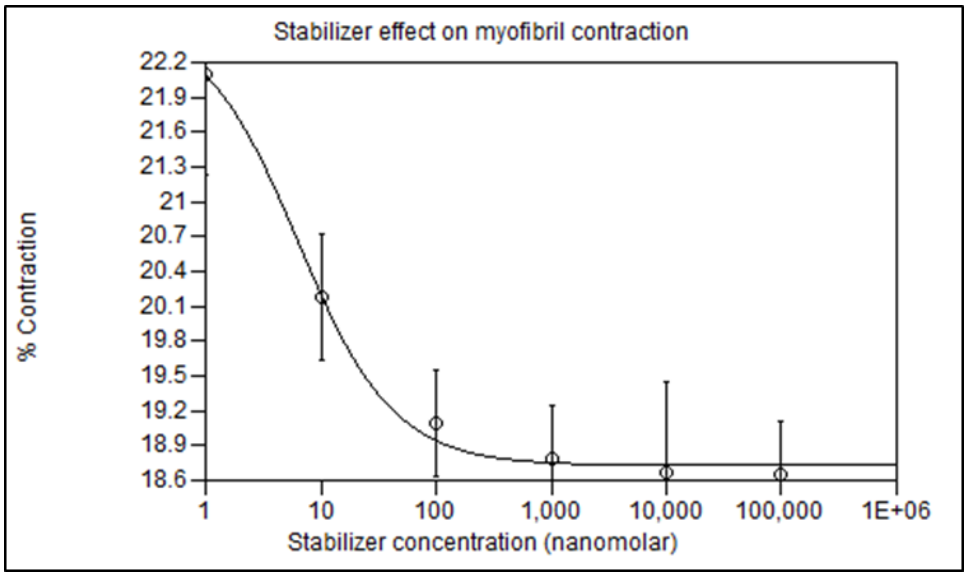

Figure 35. Dose response of stabilizer peptide on myofibril contraction. (A) Percentage of contraction versus stabilizer in nanomolar concentration. (B) Curve fit for percentage of contraction versus stabilizer in nanomolar concentration in the logarithmic power of 10.

4.5 *In vitro* Motility Assay of Actin Filaments over Myosin HMM Incubated with Stabilizer Peptide

The results from the myofibrillar contractility assay confirmed that the presence of stabilizer peptide slowed down contraction in myofibrils. Previously, cELISA and GFS experiments conveyed that stabilizer peptide binds to the myosin S2 region and stabilizes that region. Thus it can be said that stabilization of myosin S2 region upon stabilizer peptide binding has an inhibiting effect on contraction of myofibrils. The *in vitro* motility assay would be an ideal test to confirm the inhibiting effect of stabilizer peptide to force produced through acto-myosin interaction.

The setup of *in vitro* assay began with the extraction of myosin HMM from rabbit skeletal myosin by the virtue of digestion with α-chymotrypsin. The extracted myosin HMM was purified to yield myosin HMM with active myosin S1 heads by mixing and centrifuging the extracted myosin HMM with actin filaments along with ATP and magnesium chloride. Myosin HMM was used instead of whole myosin thick filaments, since stabilizer peptide binds to myosin S2 region; which is a part of myosin HMM, hence purified myosin HMM with stabilizer peptide would be ideal to test the effect stabilizer peptide over sliding velocity of actin filaments.

The purified myosin HMM with active myosin S1 heads are immobilized on dichloromethylsilane treated coverslips. An additional step to reduce the amount of dead myosin S1heads is performed by washing the myosin HMM coated coverslip with unlabeled actin filaments with addition of ATP in assay buffer through perfusion chamber. The next step was the addition of fluorescently labelled actin filaments followed by addition of ATP in AB-BSA-GOC buffer. These fluorescently labelled actin filaments were imaged by ICCD. To the same *in vitro* slide, stabilizer peptide diluted in AB-BSA-GOC buffer with ATP is added to test the motility of the same fluorescently labelled actin filaments in the presence of stabilizer peptide. Thus enabling

a comparison of the effect of stabilizer peptide on the motility of actin filaments upon binding to the myosin S2 region of myosin HMM.

The *in vitro* motility assay was performed with two different concentrations of stabilizer peptide, 20 nM and 100 nM. The histogram for the velocity of actin filaments in the absence and presence of stabilizer peptide is plotted (Figure 36A). The distribution for the velocity of actin filaments in the absence of stabilizer peptide was observed mostly for velocities more than 7.0 microns/second and in the presence of stabilizer peptide the velocities were observed at less than 7.0 microns/second. The histogram of the average velocity of actin filaments is plotted (Figure 36B). The average velocity of actin filaments in the absence of stabilizer peptide was 7.2 μm/second ± 0.3 (n = 26), while in the presence of 20 nM stabilizer it was reduced to 6.2 μm/second ± 0.3 (n = 23) and 6.2 μm/second ± 0.1 (n = 24) in the presence of 100 nM (Figure 36B). Student's t test confirmed the velocities observed of actin filaments in control and in presence of either 20 nM or 100 nM was statistically significant with p values less than 0.05 (Table 3) . While the velocities observed in presence of 20 nM and 100 nM were not statistically significant from each other with a p value greater than 0.05 (Table 3) indicating that the effect of 20 nM stabilizer peptide was statistically same as that of 100 nM stabilizer on the motility of actin filaments.

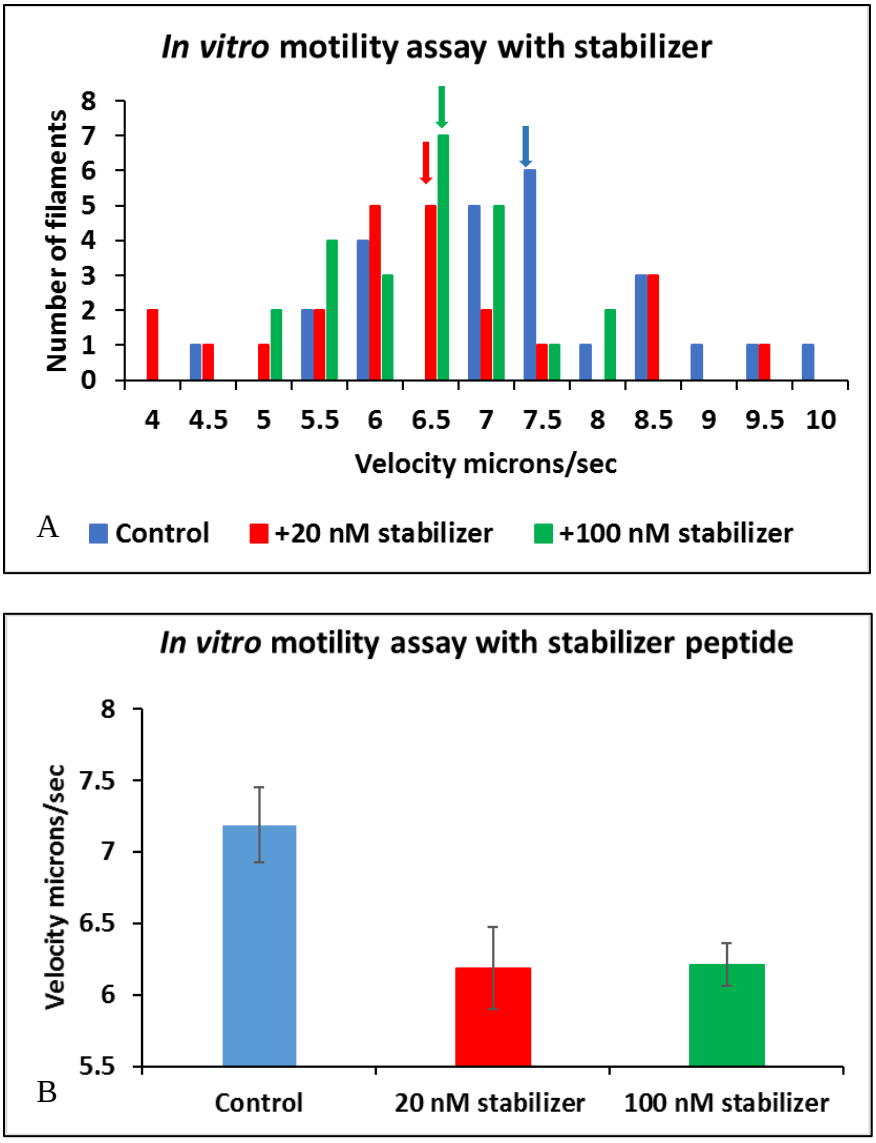

Figure 36. Histogram for the velocity of actin filaments in the presence of stabilizer peptide. (A) Histogram for the number of actin filaments with their respective velocity, control (blue); velocity of actin in absence of stabilizer peptide, test (red); velocity of actin filaments in the presence of 20 nM stabilizer peptide and test (green); velocity of actin filaments in the presence of 100 nM stabilizer peptide. (B) Histogram for the average velocities of actin filaments in control (blue) (n = 26), test with 20 nM stabilizer peptide (red) (n = 23) and test with 100 nM stabilizer peptide (green) (n = 24).

Sample: Velocity of actin filaments	p (T ≤ t) one - tail	p (T ≤ t) two - tail
Control and 20 nM stabilizer peptide	0.74×10^{-2}	0.48×10^{-2}
Control and 100 nM stabilizer peptide	0.17×10^{-2}	0.33×10^{-2}
20 nM stabilizer peptide and 100 nM stabilizer peptide	0.47	0.94

Table 3. Table for student's t-test to signify the effect of stabilizer peptide over the velocity of actin filaments.

4.6 Conclusion

The stabilizer peptide was designed to bind to myosin S2 and stabilize the coiled coil in that region with the implication that this stabilization of myosin S2 coiled coil would have an inhibiting effect on the contraction in myofibrils and over all force produced through acto-myosin interaction.

The cELISA experiment demonstrated that stabilizer peptide and polyclonal anti-S2 antibody competed to bind human cardiac myosin S2 peptide and rabbit skeletal myosin S2. The experiment performed established that the stabilizer peptide was specific to myosin S2 and especially to the proximal myosin S2 region (924-942). The stabilizer peptide had a high binding affinity to human cardiac myosin S2 peptide with a dissociation constant of 1.37 nM ± 0.02 compared to that of rabbit skeletal myosin S2 with minimum dissociation constant (K_d) at 6 nM ± 2 (Figure 32).

In the course of the experiment it was also found that stabilizer peptide was also cross specific where it could bind to myosin S2 of human cardiac myosin and rabbit skeletal myosin with relatively high specificity to human cardiac myosin S2 over rabbit skeletal myosin.

The GFS experiment performed with stabilizer peptide on rabbit skeletal myosin was able to show that binding of the stabilizer peptide stabilized the myosin S2 region. In the absence of stabilizer peptide, the myosin molecule was able to uncoil at lower forces with the force required to uncoil the myosin molecule to a length of 50 nm equalling 3.6 pN ± 0.4. In the presence of stabilizer peptide, to uncoil the myosin molecule to the same length of 50 nm equalled 5.5 pN ± 0.1, which was 1.5 times higher than in absence of stabilizer peptide (Figure 34, Table 2). The binding of stabilizer peptide to myosin molecule thus stabilized the myosin coiled coil since force required to pull the myosin molecule in presence of stabilizer peptide was higher than in the absence of the stabilizer peptide. The cELISA experiment already showed that stabilizer peptide binds to myosin S2, hence the stabilization of myosin molecule by stabilizer peptide should be at the myosin S2 region.

Myofibrillar contractility assay performed showed that stabilization of the myosin S2 region upon binding of stabilizer peptide reduced the percentage of contraction in myofibrils treated with stabilizer peptide. The percent contraction of myofibrils in the control was approximately at 22.3% ± 0.2 which dropped down to approximately 18.6% ± 0.5 in increasing amounts of stabilizer peptide. The IC50 of stabilizer peptide decreasing the percentage of contraction in myofibrils was at 6 nM ± 1 (Figure 35).

The *in vitro* motility of fluorescently labelled actin filaments over myosin HMM treated with stabilizer peptide was decreased compared to the motility of actin filaments over myosin HMM with no treatment of stabilizer peptide. The velocity of actin filaments in the control assay was 7.2 µm/second ± 0.3, and in the test assay with 20 nM stabilizer peptide was reduced to 6.2 µm/second ± 0.3, while the test assay with 100 nM stabilizer peptide was at 6.2 µm/second ± 0.1 (Figure 36). The *in vitro* motility assay thus performed, showed that sliding of actin filaments over

myosin HMM treated with stabilizer peptide was reduced compared to control. Reduction in the velocity of actin may be explained by a reduction in acto-myosin interaction and thus overall decrease in the amount of force produced.

The experiments performed were able to substantiate that a stabilized myosin S2 region has an inhibiting effect over myofibril contraction, acto-myosin interaction and overall force produced. The aforesaid experiments were performed with wild type rabbit skeletal myosin with no changes introduced to myosin S1 heads or the myosin S1-S2 hinge. The only modulation was the binding of stabilizer peptide to myosin molecule. And cELISA has already, shown that binding was specific to myosin S2, hence the decreased contraction and motility observed was due to binding of stabilizer peptide to myosin S2. The GFS experiment showed that this binding stabilized the myosin molecule at the S2 region due to specific binding of stabilizer peptide. Thus stabilization of myosin S2 coiled coil by stabilizer peptide had a role in controlling the amount of myosin S1 heads (N_t) available to bind actin filaments, evidenced by reduction in contraction of myofibrils and motility of actin over myosin HMM treated with stabilizer peptide.

CHAPTER 5

DESTABILIZER PEPTIDE AND MYOSIN SUBFRAGMENT-2

5.1 Introduction and Idea behind the Design and Use of Destabilizer Peptide

The idea for destabilizer peptide was to destabilize the myosin S2 coiled coil and increase the amount of myosin S1 heads available to bind actin filaments, thus resulting in increase in myofibril contraction and overall force produced through acto-myosin interaction. This property of destabilizer would be useful in cardiomyopathy mutations which results in dilated cardiomyopathy and heart failure due to hypocontraction in heart muscles, thus increasing the amount of contraction in heart muscles with hypocontraction could alleviate the defects caused by hypocontraction. The methodology behind the destabilization came from observations of the effects of the binding of polyclonal anti-S2 antibody to myosin S2. The polyclonal anti-S2 was raised against a single α-helix of the myosin S2 coiled coil, thus polyclonal anti-S2 antibodies will have two sites to bind in a myosin S2 coiled coil at each individual α-helix. Thus both the α-helices when occupied by polyclonal anti-S2 antibody would interfere with the natural coiled coil formation between α-helices of myosin S2 resulting in a destabilized coiled coil.

Thus, the GFS and myofibrillar contractility assays were performed with rabbit skeletal myosin and polyclonal anti-S2 antibody to check for the effect of the destabilized myosin S2 coiled coil. GFS performed with polyclonal anti-S2 antibody-treated rabbit skeletal myosin gave uncoiling of myosin molecule compared at lower forces than those of the control. Myosin uncoiled to a length of 178 nm with the force of 2.75 pN in presence of polyclonal anti-S2 antibody, while the uncoiled length of myosin in control was 136 nm with the force of 6.39 pN (Figure 37). Thus, the GFS assay confirmed that the polyclonal anti-S2 had a destabilizing effect on myosin molecule at myosin S2, since antibody was against the myosin S2 itself. Myofibrillar contractility assay performed with myofibrils incubated with polyclonal anti-S2 antibody gave a much higher

percentage of contraction than control myofibrils. Percent contraction in control myofibrils was 21% ± 2 and it rose to 34% ± 2 in the case of myofibrils treated with polyclonal anti-S2 antibody (Figure 38).

This effect of polyclonal anti-S2 on the myosin S2 coiled coil and myofibril contraction lead to the idea to develop a small peptide which could simulate the same effects as that of the site-specific polyclonal anti-S2 antibody. Hence, the destabilizer peptide designed was the modified form of single α-helix of human β-cardiac myosin S2 (924-942), which have a higher binding affinity to natural single α-helix of human β-cardiac myosin S2 thus interrupting the natural coiled coil formation of myosin S2 coiled coil.

Destabilizer peptide thus designed will be able to destabilize the myosin S2 coiled coil, and the effect of this destabilized coiled coil over myofibril contraction and force produced through acto-myosin interaction could be studied. Destabilizer peptide specificity to myosin S2 region was tested by performing the competitive ELISA. The destabilization of the myosin coiled coil was tested by performing the GFS experiments with rabbit skeletal myosin treated with destabilizer peptide. The myofibrillar contractility assay was performed to study the effect of destabilizer peptide on the contraction of myofibrils treated with the destabilizer peptide. The *in vitro* motility assay was performed to assay the effect of destabilizer peptide bound myosin HMM over the actin filaments thus establishing the effect of destabilizer peptide over the force produced through acto-myosin contraction.

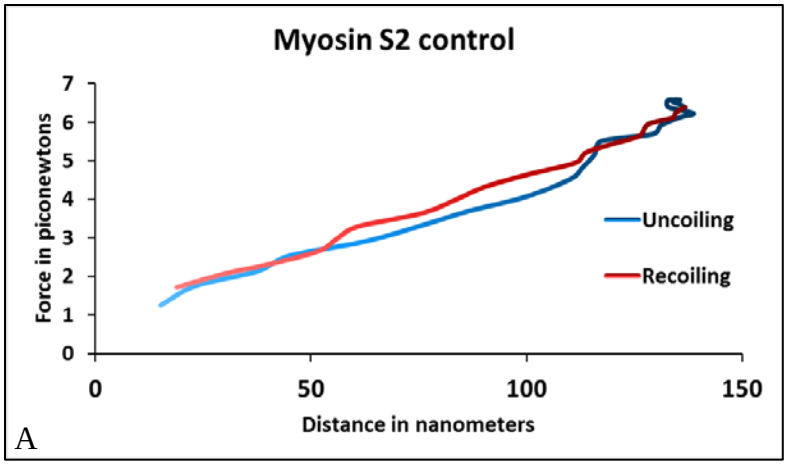

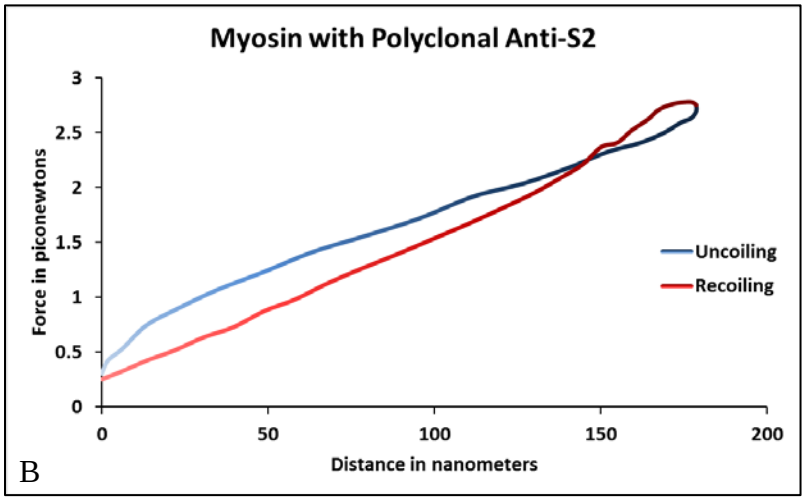

Figure 37. Force-distance trace for myosin treated with polyclonal anti-S2 antibody. (A) Force-distance curve for myosin molecule without polyclonal anti-S2 antibody. (B) Force-distance curve for myosin molecule with polyclonal anti-S2 antibody.

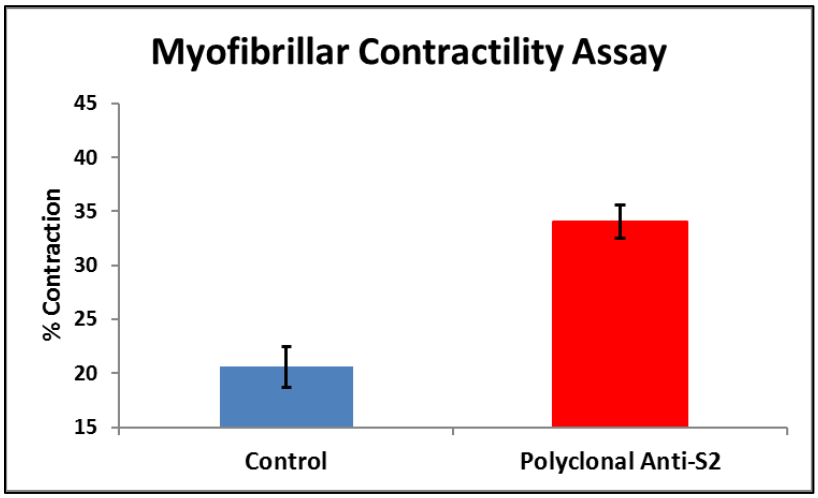

Figure 38. Percentage contraction in myofibrils without (blue) and with polyclonal anti-S2 antibody (red).

5.2 Competitive ELISA of Destabilizer Peptide to Myosin S2

The first experiment performed was to test whether the destabilizer peptide designed was specific to myosin S2 and does not bind anywhere else along the length of myosin molecule. The cELISA was performed to compete destabilizer peptide with site-specific polyclonal anti-S2 antibody to bind human cardiac myosin S2 peptide and rabbit skeletal myosin S2.

The assay began with coating a 96 well microtiter plate with rabbit skeletal myosin molecule overnight. To each of the wells 1:64 diluted primary polyclonal anti-S2 antibody was added followed by a 1:32 diluted solution of human cardiac myosin S2. Different concentrations of destabilizer peptide in nanomolar units were added to the wells in replicates. After incubation at room temperature for an hour, the unbound protein complexes were washed with PBS and blocking buffer. Enzyme conjugated secondary antibody were added on to the wells and allowed conjugate for an hour at room temperature. After washing the wells with detergent buffer, color developing BCIP substrate were added on to the wells. Images of the color developed in the wells were captured and analyzed in Image J.

The trend in the optical density with different concentrations of destabilizer peptide observed was from low OD to high OD and back again to low OD (Figure 39). This trend in OD was expected, since the wells with no destabilizer peptide had their primary polyclonal anti-S2 bound to human cardiac myosin S2 peptide and this complex gets washed off, thus there are low amounts of primary antibody left for the enzyme conjugated secondary antibody to bind resulting in lower OD.

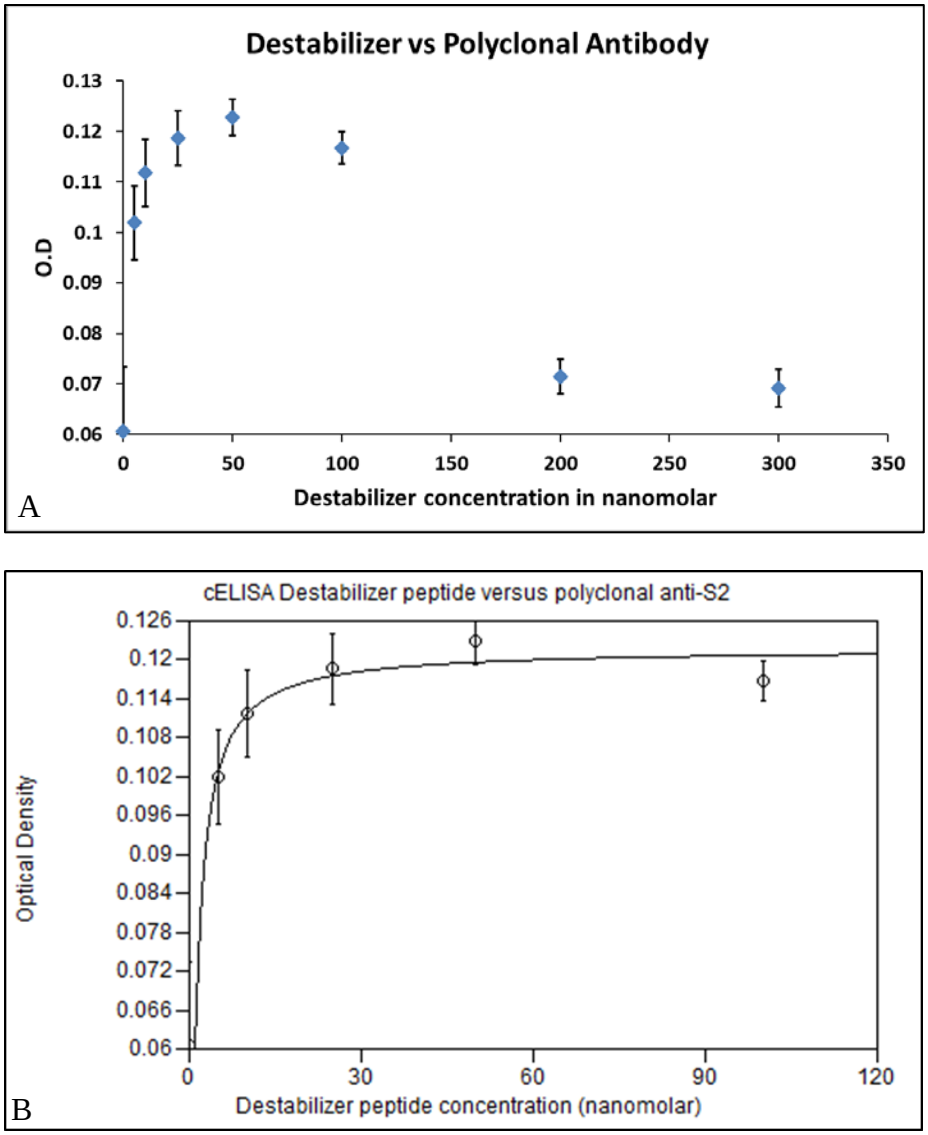

Figure 39. The cELISA of destabilizer peptide versus polyclonal anti-S2 antibody. (A) OD with increasing concentration of stabilizer peptide gave the trend of low-high-low OD. (B) Curve fit of OD with increasing destabilizer concentration to calculate the dissociation constant (K_d).

As the concentration of the destabilizer peptide kept on increasing, the destabilizer peptide would bind to human cardiac myosin S2 peptide, resulting in primary polyclonal anti-S2 antibody to go and bind to next available myosin S2 site on rabbit skeletal myosin bound to well walls. Thus the enzyme conjugated secondary antibody would have primary antibody to bind to resulting in higher OD with increasing concentration of destabilizer peptide.

The drop in OD is observed, because at high concentration of destabilize peptide where the destabilizer peptide would saturate all the available human cardiac myosin S2, the leftover destabilizer peptide would go and bind to the myosin S2 region in rabbit skeletal myosin bound to the wells of the microtiter plate. Primary polyclonal anti-S2 would have less myosin S2 sites available to bind, leading to lower OD upon addition of enzyme conjugated secondary antibody.

This trend in OD thus confirms that the destabilizer peptide designed was specific to myosin S2, especially at the proximal myosin S2 (924-942), since the destabilizer peptide competed with the binding of polyclonal anti-S2 antibody. The binding affinity of destabilizer peptide was high with a dissociation constant of 6 nM ± 3, and the binding affinity for monomer of destabilizer peptide to rabbit skeletal myosin S2 was calculated to have a minimum dissociation constant (K_d) at 75 nM ± 36.

The cELISA experiment with destabilizer peptide showed that the destabilizer peptide was specific to myosin S2, and it was able to bind to both human cardiac myosin S2 and rabbit skeletal myosin S2. The destabilizer peptide had more potent and higher binding affinity to human cardiac myosin S2 compared to rabbit skeletal myosin S2.

5.3 Gravitational Force Spectroscopy with Destabilizer Peptide

The destabilizer peptide was specific to the myosin S2 region and also cross specific in that it can bind to both human cardiac myosin S2 and rabbit skeletal myosin S2, as shown by cELISA experiment. The next assay performed was to check whether the designed destabilizer peptide can destabilize the myosin S2 coiled coil. GFS with rabbit skeletal myosin treated with destabilizer peptide was performed to confirm the destabilizing effect of destabilizer peptide at myosin S2 coiled coil.

For the GFS assay, the rabbit skeletal myosin molecule was tethered between immobile edge and mobile bead with the help of actin and myosin rigor binding. The edge of the glass coverslips and silica beads were coated with actin molecules. The slide for the GFS was prepared, with the successful tethering of rabbit skeletal myosin molecule between the actin-coated immobile edge and mobile beads. To test the effect of the destabilizer peptide, the rabbit skeletal myosin molecules incubated with destabilizer peptide were tethered similarly as described earlier. GFS measurements were performed to get force-distance curves for the uncoiling of the myosin molecule without and with destabilizer peptide when pulled from its myosin S1 heads in both the directions perpendicular to its thick filament axis.

From the force-distance curve fit of myosin molecule in absence of destabilizer peptide, to uncoil the myosin molecule to a length of 100 nm the force required was 4.9 ± 0.1 pN (n = 7) (Figure 40A, Table 4). In presence of destabilizer peptide, to uncoil the myosin molecule to a length of 100 nm, the force required was 3.09 ± 0.05 pN (n = 7) (Figure 40B, Table 4). The correlation coefficient (R) for the control was 0.98 and for the test sample it was 0.99. The force-distance traces, when compared in the absence and presence of destabilizer peptide showed the enhancement of the flexibility of myosin S2 coiled coil with 1.6 times less force required to uncoil the myosin molecule in presence of destabilizer peptide (Figure 41, Table 4).

The GFS of the rabbit skeletal myosin molecule with destabilizer peptide confirmed the destabilizing effect of destabilizer peptide to myosin molecule, since the force required to uncoil the myosin molecule in the presence of destabilizer peptide was less when compared to that of the control. The cELISA demonstrated specific binding of the destabilizer peptide to myosin S2, thus destabilization of myosin coiled coil by destabilizer peptide has to be at the myosin S2 region.

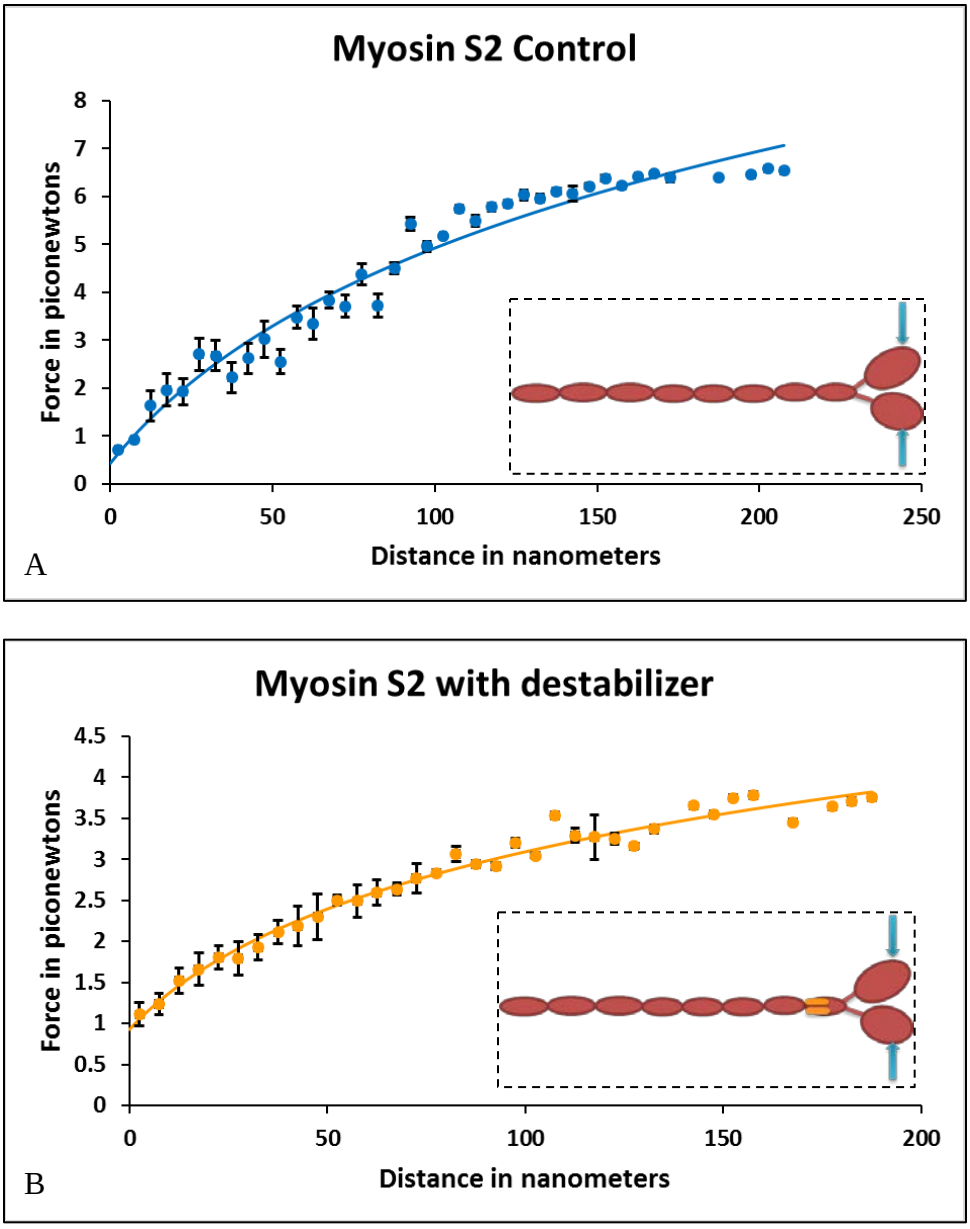

Figure 40. The force-distance curve for the GFS experiment with rabbit skeletal myosin treated with destabilizer peptide. (A) Force-distance curve for uncoiling of myosin molecule with no destabilizer peptide added (n = 7). (B) Force-distance curve for uncoiling of myosin molecule with destabilizer peptide added (n = 7). In dashed box; cartoon of a myosin molecule (red) with destabilizer peptide (orange) tethered at myosin S1 region with actin (cyan arrow) for GFS.

	No. of molecules (n)	Length (nm)	Force (pN)	Correlation coefficient (R)
Myosin S2 (Control)	7	100	4.9 ± 0.1	0.98
Myosin S2 with destabilizer peptide (Test)	7	100	3.09 ± 0.05	0.99

Table 4. Length of uncoiled myosin S2 molecule in absence and presence of MyBPC measured with GFS.

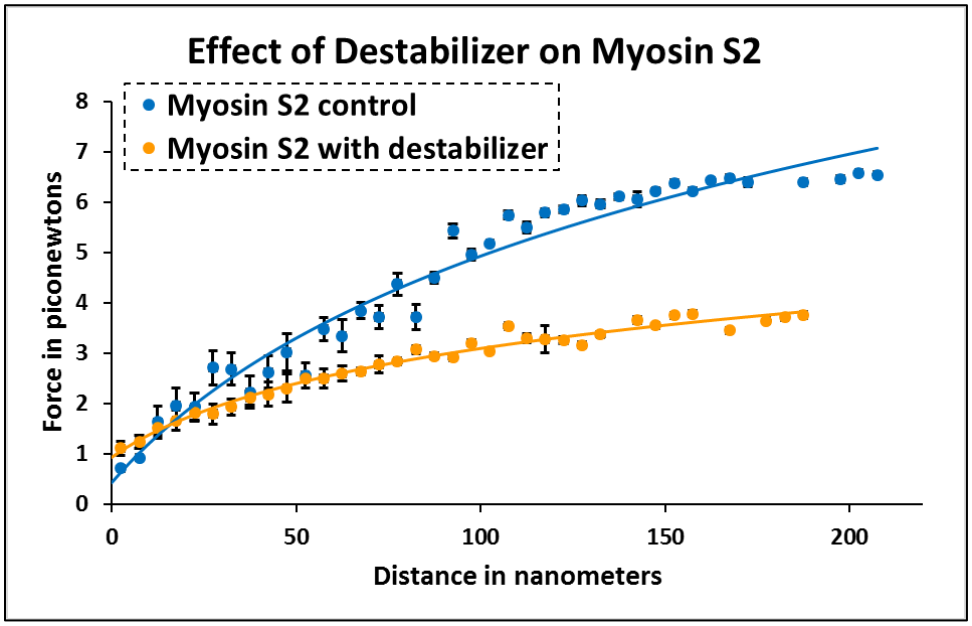

Figure 41. Comparison of force-distance curve for control (blue) and test (red) assay for myosin molecule treated with destabilizer peptide.

5.4 Myofibrillar Contractility Assay with Destabilizer Peptide.

The GFS and cELISA experiments proved the specificity of the destabilizer peptide to the myosin S2 region and destabilization of the same upon binding. To study the effect of the destabilization of myosin S2 coiled coil on the contraction in myofibrils, the myofibrillar contractility assay was performed in rabbit skeletal myofibrils treated with different concentrations of destabilizer peptide.

For the control assay, the rabbit myofibrils were washed thoroughly with assay buffer and a small amount of myofibrils was placed on a glass coverslip and imaged through microscope. To the same myofibrils, ATP was added to a final concentration of 1 mM to allow the shortening of sarcomeres in the myofibrils. The difference in the length of the sarcomere before and after addition of ATP gave the percentage of contraction in sarcomeres of myofibril in the absence of destabilizer peptide.

For the test assay, washed rabbit myofibrils were incubated at room temperature for two hours with different nanomolar concentrations of destabilizer peptide ranging from none to 1000 nM. These destabilizer treated myofibrils were imaged for sarcomeres before and after addition of ATP to calculate percentage contraction in these myofibrils.

With increasing concentrations of destabilizer peptide, the percentage contraction in sarcomeres kept on increasing and saturated at concentrations above 40 nM. The percentage contraction rose from the control value of 18.6% ± 1.2 to a final value of 38.3% ± 0.5 at 1000 nM of the destabilizer peptide. The EC50 of destabilizer peptide binding to myofibrils was calculated to be at 7.2 nM ± 2.7 (Figure 42).

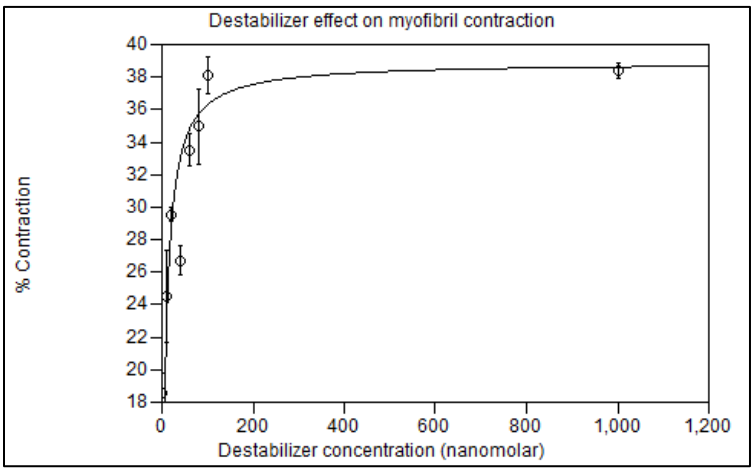

Figure 42. Percentage contraction in sarcomeres versus destabilizer peptide concentration. With increase in destabilizer peptide the percentage contraction in sarcomeres also increased. Curve fit to yield the EC50 for destabilizer peptide binding to myofibrils.

The myofibrillar contractility assay with destabilizer peptide confirmed that destabilization of myosin S2 coiled coil by destabilizer peptide resulted in increased contraction in myofibrils treated with destabilizer peptide. In the assay, the only factor added to myofibrils was increased dosage of destabilizer peptide, thus stating the direct relation between destabilization of myosin S2 coiled coil and increase in contraction of myofibrils treated with destabilizer peptide.

5.5 The *In vitro* Motility Assay of Actin Filaments over Myosin HMM Incubated with Destabilizer Peptide

The cELISA, GFS and myofibrillar contractility assays with destabilizer peptide were able to substantiate that destabilization of the myosin S2 coiled coil leads to increased contraction in myofibrils. The *in vitro* motility assay was performed to correlate whether, destabilization of myosin S2 coiled coil also leads to increase in motility produced through acto-myosin interaction. The increase in the motility of actin filaments over myosin molecules treated with destabilizer peptide confirmed that the destabilized myosin S2 coiled coil lead to an increase in overall force produced through acto-myosin interaction.

The *in vitro* assay began with immobilizing purified myosin HMM on dichloromethylsilane coated glass coverslip. Unlabeled actin filaments were added, followed by addition of ATP diluted in AB-BSA buffer, to the slide to allow the blocking of dead myosin S1 heads. Fluorescently labeled actin filaments were added and allowed to conjugate for a few minutes over the active myosin S1 heads on the coverslip. ATP diluted in AB-BSA-GOC buffer was added and imaged through the ICCD added to the microscope, to capture the movement of actin filaments. To the same slide, the destabilizer peptide and ATP diluted in AB-BSA-GOC buffer was added to image the sliding of actin filaments over myosin HMM with destabilizer peptide. The *in vitro* motility assay was performed with 20 nM and 100 nM destabilizer peptide.

The observed motility of actin filaments was faster compared to control irrespective of the concentration of destabilizer peptide. The histogram for motility of actin filaments in control and test assays with 20 nM and 100 nM destabilizer peptide showed a differential distribution. For the control, the motility of actin filaments were in range of 6.5 microns/second, while test assay with 20 nM and 100 nM had motility in the range of 8.0 microns/second (Figure 43A). The average velocity of actin filaments in the control assay was 6.8 µm/second ± 0.2 (n = 20), for test assay with 20 nM destabilizer peptide was 8.2 µm/second ± 0.2 (n =22) and test assay with 100 nM destabilizer peptide was 8.4 µm/second ± 0.4 (n = 19) (Figure 43B). The difference in velocities of the actin filaments in control and test assays with 20 nM destabilizer peptide or control and test assay with 100 nM destabilizer peptide were statistically significant with p values less than 0.05; however, the difference of velocities in both the test assays were not statistically significant with a p value greater than 0.05.

A

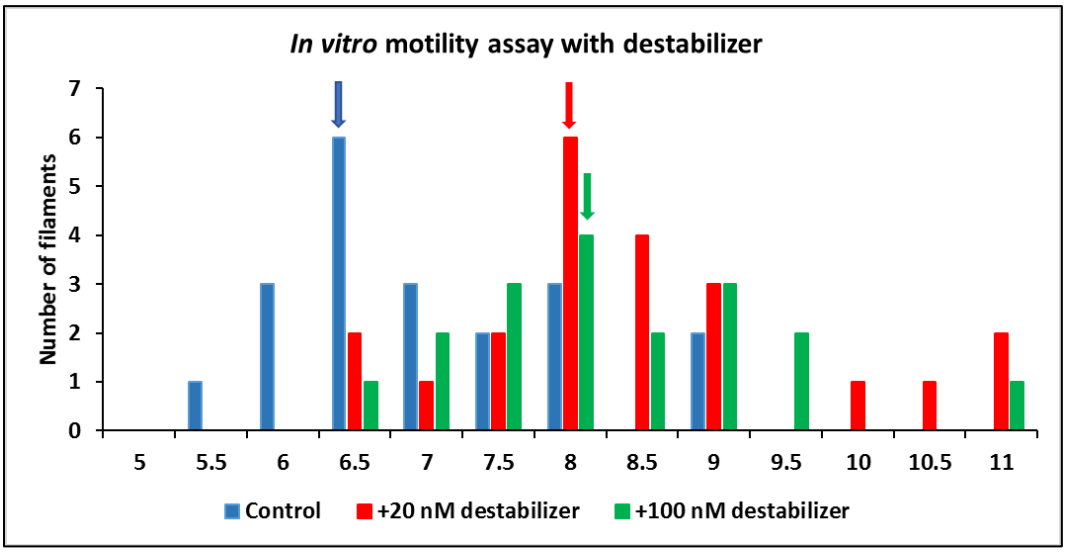

B

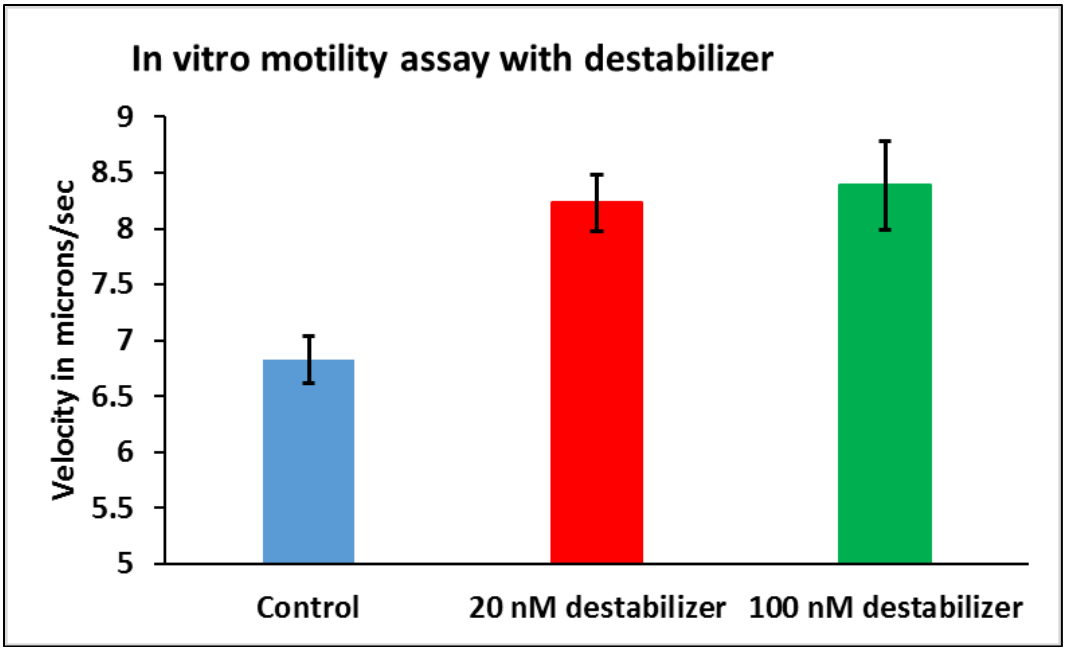

Figure 43. Histogram for the velocity of actin filaments in presence of destabilizer peptide. (A) Histogram for the number of actin filaments with their respective velocity, control (blue); velocity of actin in absence of destabilizer peptide, test (red); velocity of actin filaments in presence of 20 nM destabilizer peptide and test (green); velocity of actin filaments in presence of 100 nM destabilizer peptide. (B) Histogram for the average velocities of actin filaments in control (blue) (n = 20), test with 20 nM destabilizer peptide (red) (n = 22) and test with 100 nM destabilizer peptide (green) (n = 19).

Sample: Velocity of actin filaments	**p (T ≤ t) one - tail**	**p (T ≤ t) two - tail**
Control and 20 nM destabilizer peptide	0.01×10^{-2}	0.02×10^{-2}
Control and 100 nM destabilizer peptide	0.08×10^{-2}	0.15×10^{-2}
20 nM destabilizer peptide and 100 nM destabilizer peptide	0.37	0.73

Table 5. Table for student's t-test to signify the effect of destabilizer peptide over the velocity of actin filaments.

The increased motility of actin filaments over myosin HMM treated with the destabilizer peptide confirmed that destabilization of the myosin S2 coiled coil directly influenced the increase

in motility of the actin filaments, thus increasing the overall force produced through acto-myosin interaction. The assay also showed that the destabilizer peptide at lower concentration was potent in increasing the motility of actin filaments, since five times the lower concentration of destabilizer peptide utilized had no statistically significant difference in their respective velocities.

5.6 Conclusion

The cELISA experiment with destabilizer peptide confirmed the specificity of the destabilizer peptide to the proximal myosin S2 region. The destabilizer peptide was able to compete with the polyclonal anti-S2 antibody to bind to human cardiac myosin S2 peptide and myosin S2 on rabbit skeletal myosin. The cELISA also showed the high binding affinity of destabilizer peptide to human cardiac myosin S2 peptide with a dissociation constant (K_d) at 6 nM ± 3 compared to rabbit skeletal myosin S2 with a dissociation constant (K_d) at 75 nM ± 36 (Figure 39).

The GFS performed with rabbit skeletal myosin treated with destabilizer peptide confirmed the destabilization of myosin coiled coil. The force required to uncoil the myosin molecule with destabilizer peptide was 1.6 times less than the force required to uncoil the myosin molecule with no destabilizer peptide added (Figure 41).

The myofibrillar contractility assay showed that myofibrils treated with destabilizer peptide had increased contraction when compared to the control. The increase in contraction of myofibrils was also observed with increased concentration of destabilizer peptide. The EC50 of destabilizer peptide was less than 10 nM. The percentage contraction in control was approximately at 18.6% ± 1.2, which rose to a maximum of 38.3% ± 0.5 in presence of destabilizer peptide (Figure

42). Thus the destabilized myosin S2 leads to an increase in contraction of sarcomeres in the myofibril.

The *in vitro* motility assay also confirmed the effect of the destabilized myosin S2 on the force produced through acto-myosin interaction. The velocity of actin filaments over myosin molecules treated with destabilizer peptide was higher compared to control. Average velocity of actin filaments in the control assay was 6.8 μm/second ± 0.2, while for the test assay with 20 nM destabilizer peptide it was 8.2 μm/second ± 0.2 and for the test assay with 100 nM destabilizer peptide it was 8.4 μm/second ± 0.4 (Figure 43). Thus the *in vitro* motility assay confirmed that an increase in motility produced through acto-myosin interaction was due to destabilized myosin S2 coiled coil by destabilizer peptide.

All the experiments performed confirm that a destabilized myosin S2 coiled coil leads to an increase in contraction of sarcomeres and overall force produced through acto-myosin interaction. The destabilization of the myosin S2 coiled coil was achieved through binding of the destabilizer peptide designed to bind myosin S2 in the proximal region (924-942). The increase in contraction and force produced due to a destabilized myosin S2 coiled coil should be due to an increase in the number of active myosin S1 heads (N_t) available to bind actin filaments, since the experiments were performed with myosin, myofibril and myosin HMM treated with destabilizer peptide, the only region which would have been affected by destabilizer peptide would be the myosin S2 region, and the effect observed was the destabilization of myosin coiled coil at S2 region. Thus confirming the correlation between destabilized myosin S2 coiled coil and increased contraction of sarcomeres along with the increased force production due to increase in number myosin S1 heads (N_t) available.

CHAPTER 6

DISCUSSION

6.1 Binding to Myosin S2

Before testing the effect of stability of the myosin S2 coiled coil on contraction in myofibrils and force produced, the stability of myosin S2 coiled coil was tested by binding with its natural binding partner myosin binding protein C and two peptides designed to bind myosin S2 them being the stabilizer and destabilizer peptide. Confocal microscopy results of myofibrils treated with fluorescently labelled stabilizer and destabilizer peptide highlighted the A bands of the sarcomere in particular with no fluorescence detected in the Z line, which corroborated that the designed peptides were specific to muscle myosin and did not bind nonmuscle myosin or actin filaments (Singh, R.R., Qadan, M.M *et al*., 2017). Stabilizer and destabilizer peptides were tested by cELISA to verify their binding specificity and affinity to myosin S2 of muscle myosin. Both the peptides were competed against polyclonal anti-S2 antibody to bind human cardiac myosin S2 and rabbit skeletal myosin S2. The cELISA experiment with both the peptides gave a similar trend with the OD observed. The trend was from low OD – high OD – low OD with increasing concentrations of the peptides (Figure 32 and Figure 39).

When there were no peptides added to the wells, the human cardiac myosin S2 peptide would bind most of the primary polyclonal anti-S2 antibody in the wells and get washed away leading to low OD. With increasing amounts of peptides added to the wells, they competed with primary polyclonal anti-S2 antibody to bind to human cardiac myosin S2 peptide, allowing primary polyclonal anti-S2 antibody to bind the myosin S2 on rabbit skeletal myosin adsorbed on the wells resulting in higher OD. After saturation of all the available human cardiac myosin S2 peptide with the designed peptides, the remainder of designed peptides was bound to myosin S2 on rabbit skeletal myosin S2 adsorbed on the wells, causing the OD to decline. This observed trend

in OD thus confirmed the specificity of designed peptides to myosin S2. The binding affinity of stabilizer and destabilizer peptide to human cardiac myosin S2 was higher with K_d values at 1.37 nM ± 0.02 and 6 nM ± 2 respectively, compared to rabbit skeletal myosin S2 with K_d values at 6 nM ± 3 and 75 nM ± 36, respectively. This result showed the high binding affinity of both stabilizer and destabilizer peptides to myosin S2. The cELISA also revealed the cross specificity of both the designed peptides to human β-cardiac myosin S2 and rabbit skeletal myosin S2 with greater affinity for the human β-cardiac myosin S2.

6.2 Stability of the Myosin S2 Coiled Coil

Gravitational force spectroscopy was performed to test the stability of the myosin S2 coiled coil in the presence of MyBPC, stabilizer and destabilizer peptide. The spectroscopy studies have shown that myosin S2 is more flexible than LMM which behaved like a rigid cylinder (Highsmith *et al*., 1977). Also electron microscopy studies revealed more bending in the S2 than LMM (Walker *et al*., 1985). Recently it has been demonstrated that myosin S2 coiled coil is flexible compared to myosin LMM by gravitational force spectroscopy (Singh, R.R., Dunn, J.W *et al*., 2017). Thus the effect of the myosin S2 binding proteins over the stability of myosin S2 coiled coil was measured by gravitational force spectroscopy. Uncoiling of myosin S2 was performed in the absence and presence of myosin S2 binding proteins to reveal their effect on the stability of myosin S2 coiled coil.

Whole length skeletal MyBPC bound to skeletal rabbit myosin molecule increased the stability of the myosin S2 coiled coil. The force required to uncoil myosin in the presence of MyBPC was 3.35 times more than in its absence (Figure 28). The myosin molecule was uncoiled at myosin S2 with the help of polyclonal anti-S2 antibody required to tether the myosin molecule

for GFS. Thus the binding of MyBPC to the myosin molecule had a stabilizing effect over the myosin S2 coiled coil. MyBPC binds with high affinity to LMM (K_d less than 500 nM), but with weaker affinities for actin (K_d less than 4300 nM), and S2 (K_d = 5000 nM) (Gruen, M., and Gautel M. 1999; Moos *et al*., 1975; Rybakova *et al*., 2011). Thus, LMM likely acts as a docking site for MyBPC while its N-terminal region interacts with other sites due to increased effective concentration. It is unlikely that such an increase in stability can be conferred by binding of MyBPC to LMM alone, so MyBPC is interacting with S2 at concentrations well below its K_d to S2 due to its higher effective concentration. Also the MyBPC used in these experiments were in dephosphorylated form as indicated by its pI around 5.6 (Saber *et al*., 2008, McClellan *et al*., 2001) and MyBPC in its phosphorylated form has its interaction abolished to myosin S2 (Rybakova *et al*., 2011; Kensler *et al*., 2017).

Stabilizer peptide added to skeletal myosin molecule also had a stabilizing effect over the myosin coiled coil at myosin S2. The force required to uncoil the myosin coiled coil in the presence of stabilizer peptide was 1.5 times more than in its absence (Figure 34). Since the binding of the stabilizer peptide is specific to myosin S2, the binding property of myosin S1 to actin was used to uncoil the myosin molecule in GFS. The force required to uncoil myosin molecule at its myosin S1 end or at myosin S2 region specific to polyclonal anti-S2 are similar (Singh, R.R., Dunn, J.W *et al*., 2017). Thus, the binding of the stabilizer peptide to the myosin molecule stabilizes the coiled coil at myosin S2 region.

In contrast, the other designed peptide, the destabilizer, enhanced the flexibility of myosin coiled coil at myosin S2. The force required to uncoil the myosin coiled coil in presence of destabilizer peptide was 1.6 times less than in its absence (Figure 41). Destabilizer peptide being

specific to myosin S2 the enhanced flexibility of myosin coiled coil observed was localized at myosin S2 region.

The GFS performed on whole length skeletal myosin in presence of MyBPC, stabilizer and destabilizer peptide, showed that coiled coil at myosin S2 was stabilized by MyBPC and stabilizer peptide and destabilized or enhanced flexibility by destabilizer peptide. The specific binding of MyBPC, stabilizer and destabilizer peptide to myosin S2 altered the stability of the myosin S2 coiled coil.

6.3 Sarcomere Shortening of Myofibril

The altered stability of the myosin S2 coiled coil upon binding of myosin S2 binding proteins and its effect over sarcomere shortening was assayed with the myofibrillar contractility assay. Sarcomere shortening was measured before and after addition of ATP to skeletal myofibrils treated with myosin S2 binding proteins. The stabilitization of myosin S2 by MyBPC in sarcomeres and its effect on sarcomere shortening were not performed, since the myofibrils already contain MyBPC.

The stabilizer peptide treated myofibrils underwent reduced shortening of sarcomeres upon addition of ATP. The sarcomere shortening dropped from 22.3% ± 0.2 contractility to 18.6% ± 0.5 in the presence of the stabilizer peptide. The binding affinity of stabilizer peptide to the myofibrils was at 6 nM ± 1 (Figure 35). This assay thus revealed that the stability of the myosin S2 by the stabilizer peptide reduced the shortening of sarcomeres compared to control. This reduction in shortening of sarcomeres by a stable myosin S2 coiled coil further supports the idea that a stable myosin S2 would reduce or regulate the amount of myosin S1 heads available to bind actin filaments.

The destabilizer peptide treated myofibrils showed an increase in shortening of sarcomeres. The percentage contraction in myofibrils rose from 18.6% ± 1.2 to a maximum of 38.3% ± 0.5 in presence of destabilizer peptide upon addition of ATP. The binding affinity of destabilizer peptide to myofibrils was at 7.2 nM ± 2.7 (Figure 42). The destabilizer peptide enhances the flexibility of the myosin S2 coiled coil. This enhanced flexibility of the myosin S2 resulted in increased contraction in myofibrils thus corroborating the idea that an unstable myosin S2 coiled coil would allow more myosin S1 heads to be available to bind actin filaments.

6.4 The *In vitro* Motility of Actin Filaments

The *in vitro* motility of actin filaments over myosin molecule or myosin thick filaments treated with myosin S2 binding proteins was performed to test the effect of altered stability of myosin S2 coiled coil over the motility of actin filaments. The motility of actin filaments over skeletal myosin thick filaments treated with whole length skeletal MyBPC was reduced compared to the control. The motility of actin filaments was reduced by 22% in the presence of MyBPC (Figure 29). This reduction in the motility of actin filaments by MyBPC would be either by binding of MyBPC to actin or the myosin S2 depending on the phosphorylation of MyBPC. MyBPC in its unphosphorylated state in a mouse model had impaired contractile function, thus suggesting that phosphorylation is required for maximal crossbridge attachment (Colson *et al*., 2008; Mamidi *et al*., 2016). The MyBPC used was in its unphosphorylated state according to the measured higher pI of MyBPC around 5.6. Also, the MyBPC phosphorylation does not affect the K_d of MyBPC for actin, however phosphorylation has been reported to reduce the B_{max} (Weith *et al*., 2012; Rybakova *et al*., 2011; Shafer *et al*., 2009). Thus indicating that reduced motility of actin is due to binding of unphosphorylated MyBPC to myosin thick filaments.

The motility of actin filaments over myosin molecules treated with stabilizer peptide was reduced by 14% (Figure 36). The stabilizer peptide enhances the stability of myosin S2 which in turn reduced the motility of actin filaments thus providing the evidence that a stabilized myosin S2 coiled coil regulates the myosin S1 heads available to bind actin. In contrast, the motility of actin filaments rose by 18% when myosin molecules were treated with destabilizer peptide (Figure 43). The destabilizer peptide enhances the flexibility of the myosin S2 coiled coil, this increased flexibility resulted in increased motility of actin filaments, thus confirming that a destabilized myosin S2 coiled coil increased the number of myosin S1 heads to bind actin, hence the observed increased motility in actin filaments.

6.5 Conclusions

In conclusion, the stability of myosin S2 coiled coil could be altered. This altered stability had an effect over the sarcomere shortening in myofibrils and the force required to propel the actin filaments over myosin.

The gravitational force spectroscopy experiments showed that the stability of myosin S2 coiled coil could be altered by MyBPC and stabilizer peptide enhancing the stability of myosin S2 coiled coil, and, on the other hand, the destabilizer peptide decreasing the stability and inreasing the flexibility of myosin S2 coiled coil. The more the force required to uncoil the myosin coiled coil, the more stable the myosin coiled coil and vice versa, in the presence of myosin S2 binding proteins. The GFS allowed the uncoiling of myosin S2 region on myosin coiled coil depending on the point of attachment for myosin molecule to be tethered. The measured force-distance curves showed the changes in entropy with extension as the enthalpy component appears to have a relatively constant change with extension or the graphs would not fit a logarithmic curve.

Variations in stability (enthalpy) along the coiled coil should show up as deviations from the logarithmic fit to the force-distance curve. MyBPC binding greatly impacts the logarithmic fit which is likely due to the enthalpic contribution of MyBPC binding to myosin S2 (Figure 28).This deviation from the logarithmic fit after adding MyBPC suggest a substantial change in the number of noncovalent bonds to increase the enthalpy component. This implies that MyBPC may bind at many places along S2 to stabilize it by affecting the enthalpy. The stabilizing peptide had less of an impact on the logarithmic fit and the magnitude of force increase than MyBPC stating the binding of stabilizer peptide to myosin S2 had fewer noncovalent bond formations suggesting its binding was restricted to a selected area unlike MyBPC (Figure 34). In addition, the smaller destabilizing peptide added to entropy of the myosin S2 by breaking the crucial myosin S2 coiled coil interaction, which seemed to be clear after 50 nm of molecular length which is the site for destabilizer to bind myosin S2. After 50 nm the myosin molecule unravels much faster with less force required indicating a crucial spot for myosin S2 coiled coil formation (Figure 41).

Furthermore, the myofibrillar contractility assay with stabilizer and destabilizer peptide myofibrils showed that sarcomere shortening or percentage contractility decreased and increased respectively. Thus connecting the stability of myosin S2 coiled coil to sarcomere shortening. Since the GFS experiments with stabilizer peptide conveyed the enhanced stability to myosin S2 coiled coil, thus the stable myosin S2 coiled coil would be thought to reduce the sarcomere shortening of myofibrils treated with stabilizer peptide. Also the stabilizer peptide being highly specific to muscle myosin S2, thus reduced shortening observed due to the enhanced stability of myosin S2 coiled coil by stabilizer peptide. In contrast, the destabilizer peptide enhanced the flexibility of myosin S2 as observed in GFS experiments, with an increased amount of sarcomere shortening in myofibrils treated with destabilizer peptide. The destabilizer peptide being specific to myosin S2,

confirmed that a destabilized myosin S2 coiled coil increased the amount of contraction or sarcomere shortening in myofibrils.

The *in vitro* motility of actin filaments over myosin treated with MyBPC, stabilizer and destabilizer peptide gave another line of evidence for the effect of stable or unstable myosin S2 coiled coil over the amount of force produced through acto-myosin interaction to slide the actin filaments. The MyBPC and stabilizer peptide are shown to stabilize the myosin S2 coiled coil and reduced the sliding velocity of actin filaments, while the enhanced flexibility of myosin S2 coiled coil induced by the destabilizer peptide increased the motility of actin filaments. Thus experiments performed in this study establish that the stability of the myosin S2 coiled coil affects the contraction in myofibrils and the amount of force produced through acto-myosin interaction. The MyBPC and stabilizer peptide enhanced the stability of myosin S2 coiled coil resulting in a declined contractility in myofibrils and velocity of actin filaments. The destabilizer peptide decreased the stability of the myosin S2 coiled coil resulting in enhanced contractility in myofibrils and velocity of actin filaments. Another conclusion which could be drawn is that the stability of myosin S2 coiled coil could easily be altered by these small synthetic peptides.

The myosin S2 coiled coil is known to be more flexible than LMM, based on the proteolysis of myosin S2 giving long and short S2 fragments while LMM had constant sized fragments (Sutoh *et al*., 1978). The spectroscopic measurements made showed that LMM was more like a rigid cylinder and myosin S2 was more flexible (Highsmith *et al*., 1977). Electron microscopy showed more bending at the myosin S2 compared to LMM (Walker *et al*., 1985). Force spectroscopy data also showed that the myosin S2 region was more flexible than LMM, and that the flexibility of myosin S2 region in a myosin molecule was independent of its association in the myosin thick filament (Singh, R.R., Dunn, J.W *et al*., 2017).

Also, the data suggested that myosin S2 is more flexible at its N-terminal position, which is in line with the data observed in scallop myosin S2 that had an unstable N-terminal region (Li *et al*., 2003). Along these lines, the flexibility of the N-terminal coiled coil is thought to increase the step size of some nonmuscle myosins (Rock *et al*., 2005). The variable myosin head positions observed by electron microscopy in vertebrate striated muscle may be due to this unstable N-terminal coiled coil. Thus the effect of stable or unstable myosin S2 coiled coil observed over myofibrillar contraction and force generated through acto-myosin interaction could be explained by the number of myosin S1 heads (N_t) being available to bind actin. A stable myosin S2 would reduce the myosin S1 heads available to bind actin and vice versa with an unstable myosin coiled coil.

Cryo-electron micrographs have shown that invertebrate skeletal myosin have their myosin S1 heads folding back on to its myosin S2 backbone (Woodhead *et al*., 2005; Alamo *et al*., 2008; Pinto *et al*., 2012). Molecular constructs of myosin S1 and S2 and MyBPC have shown that the N-terminal region of myosin S2 is required to bind myosin S1 heads along with MyBPC (Nag *et al*., 2017). Thus the myosin S2 coiled coil structure would be assumed to regulate the availability of myosin S1 heads by its altered stability. Stable myosin S2 coiled coil could provide the conformation for myosin S1 heads to fold back and rest on to the myosin S2 coiled coil, while a much more flexible myosin S2 coiled coil won't have the conformation for myosin heads to bind and would allow these myosin S1 heads to participate in contraction (Figure 44).

The *in vitro* motility assay with the destabilizer peptides showed that 20 nM of the peptides was sufficient to achieve the maximum effects on the motility of actin filaments, since there was no statistically significant difference between the motility of actin in presence of 20 nM or 100 nM of the peptides. Similarly in myofibrillar contractility assays, the maximal effective concentrations

of the destabilizer peptide was also less than 10 nM. In contrast, the cELISA showed the K_d of the destabilizer peptide binding to rabbit skeletal myosin molecule was 75 nM which is substantially greater than 20 nM. This difference between the binding affinity and the effect of the destabilizer peptide over motility and myofibril contractility suggest that there is cooperativity in the effect of these peptides on myosin and its function.

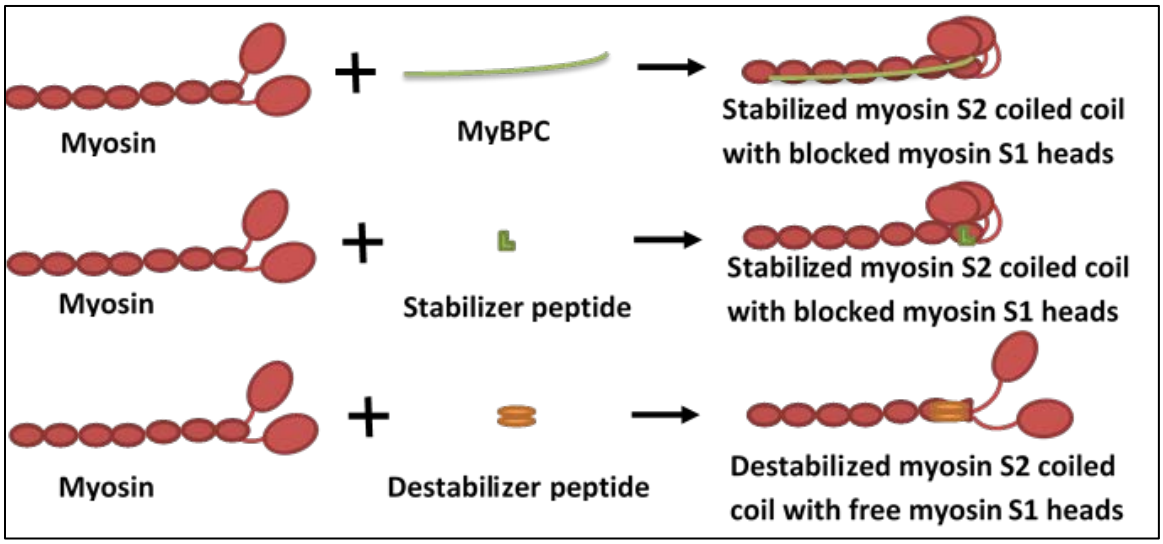

Figure 44. Effect of myosin S2 binding proteins on myosin S2 coiled coil. Myosin molecule (red) stabilized by MyBPC (green line) and stabilizer peptide (green L shaped) and destabilized by destabilizer peptide (orange).

The cooperativity could be explained by a model in which one folded myosin molecule would influence the other adjacent myosin molecules to have the same folded state. For example, if stabilizer peptides would act on few myosin molecules and allow the myosin heads of these molecules to fold back and assume a switched off position, these few affected molecules would influence the adjacent myosin molecules to assume the switched off state and vice versa in case of the destabilizer peptide (Figure 45). In the muscle, there are far fewer MyBPC molecules than myosin and they are restricted in the C zone of the sarcomere, so such a cooperative mechanism could enable larger impacts by MyBPC on contractility.

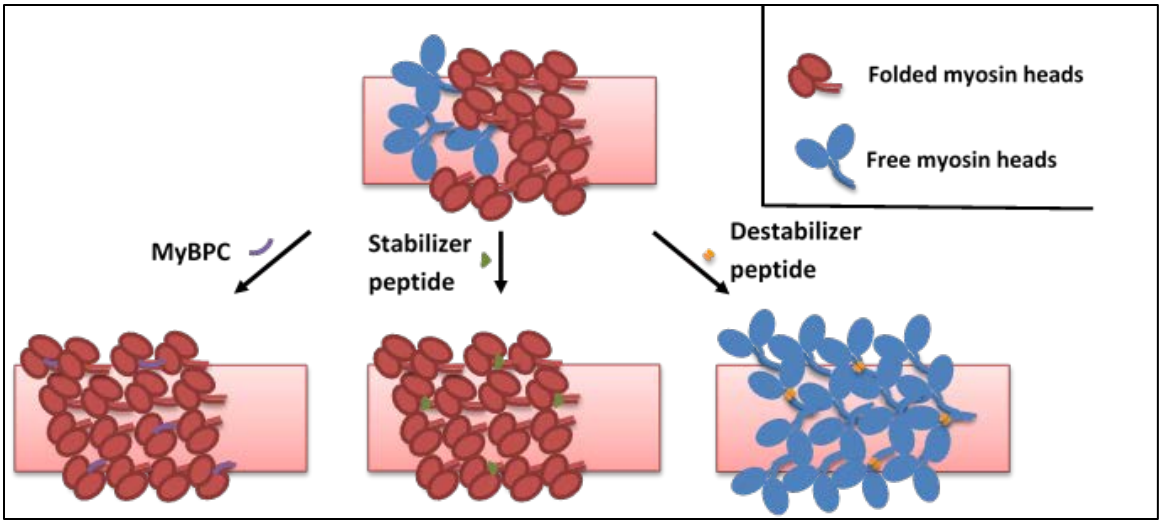

Figure 45. Cooperative effect of MyBPC, stabilizer and destabilizer peptide over the orientation of myosin S1 heads on myosin thick filament.

The effect of stable myosin S2 over force generation has been demonstrated by utilization of antibody against the whole myosin S2, which would likely reduce the flexibility of the same. That antibody inhibited the force generation in skinned muscle fibers (Sugi *et al*., 1992). Similarly MyBPC used in this study, stabilized the myosin S2 coiled coil, and it reduced the motility of actin filaments. The MyBPC molecule along its length binds from LMM to the myosin S2 region of the myosin molecule. However, MyBPC is approximately 40-45 nm long and 2-3 nm wide molecule with single-molecule electron microscopy images displaying the flexibility of the molecule (Flashman *et al*., 2004; Craig *et al*., 2014). The C8-C10 domain binds to myosin LMM while the remaining C0-C7 does not have specificity to LMM. Also the C0-C2 has affinity for actin thin filaments and myosin S2 (Gautel *et al*., 1995, Gruen *et al*., 1999; Luther *et al*., 2011).

Figure 46 left explains how the molecule, MyBPC, would have bound to the myosin molecule in the single molecule gravitational force spectroscopy based on the binding specificity of MyBPC to myosin. MyBPC being 40 nm long and myosin LMM being 95 nm long with myosin S2 being 65 nm long (Lowey *et al*., 1969), with specificity of MyBPC to both LMM and N-terminal region of myosin S2, to allow a 40 nm long MyBPC to bind both the N-terminal myosin

S2 and LMM simultaneously, would require the bending at flexible myosin S2-LMM hinge region (Gautel *et al*., 1995; Gruen *et al*., 1999; Holmes, K.C. and Geeves, M.V. 2000; Huxley, A.F. and Simmons, R.M. 1971; Lu, R.C. and Wong, A. 1985).

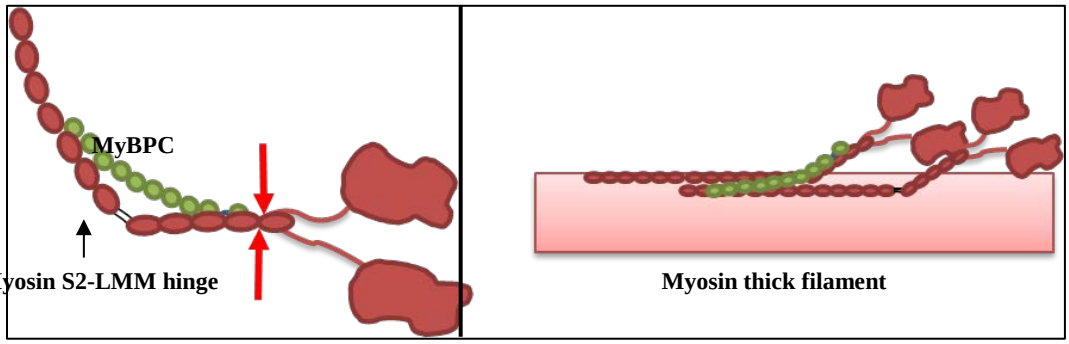

Figure 46. Representation of MyBPC binding to myosin in single molecule and thick filament form. (Left) MyBPC (green) binds to myosin molecule (red) with myosin being pulled at myosin S2 by polyclonal anti-S2 antibody (red arrows) in GFS. (Right) MyBPC (green) controlled the motility of actin filaments in *in vitro* motility assay, by binding to LMM of one myosin molecule with its C-terminal end and to myosin S2 of another myosin molecule with it N-terminal end in a myosin thick filament.

How the MyBPC bound myosin thick filament reduced the motility of actin filaments is represented by the figure (Figure 46 right). The binding of MyBPC in myosin thick filament, based on its size and specificity can be explain by C-terminal region of MyBPC binding to myosin LMM of one myosin molecule and the N-terminal end binding to myosin S2 of an adjacent myosin molecule (Starr, R., and Offer, G. 1978; van Dijk *et al*., 2014).

The MyBPC enhanced the stability of myosin S2 coiled coil and reduced the motility of actin filaments, thus it would be a reasonable statement that a stable myosin S2 reduced the acto-myosin interaction. Also, the MyBPC used was in its unphosphorylated state and known to bind myosin S2 rather than actin, thus reduced acto-myosin interaction observed was due to the binding of MyBPC to myosin and not to actin filaments (Colson *et al*., 2008; Mamidi *et al*., 2016; Saber *et al*., 2008). MyBPC binding does not affect the myosin S1 region, the only region affected is the

myosin S2 coiled coil, and thus a stable myosin S2 reduced the amount of myosin S1 heads available to bind actin filaments in *in vitro* motility assays.

The effect of the stabilizer peptide was similar to that of MyBPC on the stability of myosin S2 coiled coil. Stabilizer peptide was specific and had a higher binding affinity to the myosin S2 region. It enhanced the stability of the myosin S2 coiled coil and also resulted in reduced sarcomere shortening and reduced acto-myosin interaction. Again a stable myosin S2 coiled coil was able to affect and reduce the contraction in myofibrils and motility of actin filaments. The stabilizer peptide used was specific to myosin S2 and would not bind actin as observed through confocal microscopy (Singh, R.R., Qadan, M.M et al., 2017). Also if it had non-specific binding to myosin S1 heads there would have been a drastic change to the contractility of myofibrils, and it would have hindered with the attachment of the myosin molecule to actin coated edge and silica bead in GFS, where the myosin molecules were uncoiled. The results with stabilizer peptide again gave the conclusive interpretation that a stable myosin S2 coiled coil would reduce the amount myosin S1 heads available to bind actin thus decline in sarcomere shortening and acto-myosin interaction.

Unlike MyBPC and stabilizer peptide, the destabilizer peptide enhanced the flexibility of myosin S2 coiled coil. Previously, the melting of myosin S2 coiled coil by a laser temperature jump, accelerated the actin sliding in the *in vitro* motility assay and enhanced the contractility of muscle fibers (Davis, J.S., and Harrington, W.F. 1998; Kato *et al*., 1999). In these studies, with enhanced flexibility of myosin S2 coiled coil, the contraction in myofibrils and acto-myosin interaction were enhanced. Like the stabilizer peptide, the destabilizer peptide was also specific to myosin S2 region. Thus a more flexible myosin S2 coiled coil was able to contribute more myosin S1 heads available to bind actin, hence, the observed increment in contractility of myofibrils and acto-myosin interaction.

This study thus supports a function for myosin S2 coiled coil and its role in contraction of striated muscles. The stability or flexibility of myosin S2 coiled coils have opposite effects on the contraction of skeletal muscle. A stable myosin S2 coiled coil decreases and a flexible myosin S2 coiled coil increases the amount of contraction. These results add to the significance of myosin S2 region and explain why mutations in the same region would cause lethal cardiomyopathies. Also, this study highlights the effect of the MyBPC binding to the myosin S2 coiled coil structure. This could explain the hypercontraction observed in cardiac myofibrils of FHC heart caused by mutation in MyBPC (Adhikari *et al*., 2016). Mutated MyBPC would result in declined stable myosin S2 and increased flexibility of myosin S2 coiled coil thus allowing more myosin S1 heads available leading to hypercontraction.

The folding back of myosin S1 heads on a stable myosin S2 coiled coil, could be tested by creating the crystal structure of a stable myosin S2 with stabilizer peptide and observe the orientation of myosin S1 heads on myosin S2. Electron microscopy images of myosin thick filaments treated with stabilizer peptide could also reveal the orientation of myosin S1 heads upon stabilized myosin S2 coiled coil. Another reason this structure could affect contractility would be the restriction of rotation of lever arm of myosin by a stable myosin S2 coiled coil and free rotation of lever arm of myosin by a flexible myosin S2.

The effect of stability of myosin S2 coiled coil over muscle contraction in skeletal form is tested; however, these tests should be performed with cardiac and smooth muscle type to better understand the effect of myosin S2 coiled coil on all muscle types. Stabilizer and destabilizer peptides were designed to be used as potential drugs to reverse the effects caused by increased or decreased contraction in cardiac myocytes of FHC or DCM heart respectively. These peptides needs to be tested with animal models of cardiomyopathy mutants and whether they are effective

with expected result for stabilizer peptide to control the increased contraction and destabilizer peptide to increase the decreased contraction in mutant cardiac myocytes. These peptides could have a potential application to regulate cardiac arrhythmias and an alternative to traditionally used beta blockers.

Another probable application of this study would be to develop drugs to target the stability of the myosin S2 coiled coil to regulate the contraction of muscles. Drugs designed to affect the stability of the myosin S2 coiled coil, would not affect the ATPase activity nor the actin binding of myosin S1 directly, but would modulate the number of myosin S1 heads binding actin, even in pathological conditions due to mutations in myosin S1 heads. The R403Q mutation in myosin S1 heads at the actin binding region, resulted in disarrayed acto- myosin interaction also had faster rates of cross-bridge relaxation (Volkmann *et al*., 1997; Witjas-Paalberends *et al*., 2014; Nag *et al*., 2015).

In contrast, another FHC mutation, R453C, increases the ensemble force by increased binding to actin which could be the reason for hypercontractility in FHC hearts (Sommese *et al*., 2013). Altering the stability of the myosin S2 coiled coil of R403Q or R453C mutant cardiac myosin can increase or decrease the availability of myosin S1 heads. Since the R403Q mutation decreases the acto-myosin interaction by increasing number of myosin S1 heads, the destabilizer peptide would be helpful to counteract it, and the increased myosin S1 heads binding to actin caused by the R453C mutation could similarly be regulated by decreasing the myosin S1 heads. Thus, myosin S2 region can be altered to change the cross bridge kinetics and could be used as a therapeutic target for muscles with defects in cross bridge formation.

REFERENCES

Adhikari, A.S., Kooiker, K.B., Sarkar, S.S., Liu, C., Bernstein, D., Spudich, J.A., and Ruppel, K.M. (2016) Early-Onset Hypertrophic Cardiomyopathy Mutations Significantly Increase the Velocity, Force, and Actin-Activated ATPase Activity of Human β-Cardiac Myosin. *Cell Rep. 17*, 2857-2864.

Alamo, L., Wriggers, W., Pinto, A., Bártoli, F., Salazar, L., Zhao, F.Q., Craig, R., and Padrón, R. (2008) Three-dimensional reconstruction of tarantula myosin filaments suggests how phosphorylation may regulate myosin activity. *J Mol Biol. 384*, 780-797.

Al-Khayat, HA. (2013) Three-dimensional structure of the human myosin thick filament: clinical implications. *Glob. Cardiol. Sci. Pract. 3*, 280-302.

Beckett, E.B. (1963) Histochemistry of cardiac muscle. *Biochem Clin. 2*, 51-60.

Challice, C.E. and Viragh, S. (1973) Ultrastructure of the Mammalian Heart. p2-p36. Academic Press, INC., New York.

Cho, K.W., Lee, J., and Kim, Y. (2016) Genetic variations leading to familial dilated cardiomyopathy. *Mol Cells. 39*, 722-727.

Cluzel, P., Lebrun, A., Heller, C., Lavery, R., Viovy, J.L. Chatenay, D., and Caron, F. (1996) DNA: an extensible molecule. *Science. 271*, 792-794.

Cocco, S., Marko, J.F., and Monasson, R. (2002) Theoretical models for single-molecule DNA and RNA experiments: from elasticity to unzipping. *C. R. Physique 3*, 569–584.

Colson, B.A., Bekyarova, T., Locher, M.R., Fitzsimons, D.P., Irving, T.C., and Moss, R.L. (2008) Protein kinase A-mediated phosphorylation of cMyBP-C increases proximity of myosin heads to actin in resting myocardium. *Circ Res. 103*, 244–251.

Cooke, P. (1976) A filamentous cytoskeleton in vertebrate smooth muscle fibers, *J. Cell Biol. 68*, 539–556.

Craig, R., Lee, K.H., Mun, J.Y., Torre, I., and Luther, P.K. (2014) Structure, sarcomeric organization, and thin filament binding of cardiac myosin-binding protein-C. *Pflugers Arch. 466*, 425-431.

Creighton, T.E. (1993) Proteins: Structures and Molecular Properties, p338-p339, W.H. Freeman, U.S.A.

Davis, J.S., and Harrington, W.F. (1998) Force generation by muscle fibers in rigor: a laser temperature-jump study. *Proc Natl Acad Sci U S A. 84*, 975-979.

de Tombe, P.P., Mateja, R.D., Tachampa, K., Ait Mou, Y., Farman, G.P., and Irving, T.C. (2010). Myofilament length dependent activation. *J. Mol. Cell. Cardiol. 48*, 851–858.

Dunn, J.W., Root, D.D. (2011) Demonstrating the uses of the novel gravitational force spectrometer to stretch and measure fibrous proteins. *J. Visualized Exp. 49*, 2624.

Ebashi, S., Endo, M. and Ohtsuki, I. (1969) Control of Muscle Contraction. *Q. Rev. Biophys. 2*, 351-384.

Elliott, A., and Offer, G. (1978) Shape and flexibility of the myosin molecule. *J. Mol. Biol. 123*, 505-519.

Erdmann, J., Daehmlow, S., Wischke, S., Senyuva, M., Werner, U., Raible, J., Tanis, N., Dyachenko, S., Hummel, M., Hetzer, R., Regitz-Zagrosek, V. (2003) Mutation spectrum in a large cohort of unrelated consecutive patients with hypertrophic cardiomyopathy. *Clin. Genet. 64*, 339-349.

Flashman, E., Redwood, C., Moolman-Smook, J., and Watkins, H. (2004) Cardiac myosin binding protein C: its role in physiology and disease. *Circ Res. 94*, 1279–1289.

Frederiksen, D.W., and Cunningham, L.W. (1982) The Contractile Apparatus and the Cytoskeleton. *Methods in Enzymology 85* Part B, Academic Press, New York.

Fürst, D.O., Vinkemeier, U., Weber, K. (1992) Mammalian skeletal muscle C-protein: purification from bovine muscle, binding to titin and the characterization of a full-length human cDNA. *J. Cell Sci. 102*, 769-778.

Fusi, L., Brunello, E., Yan, Z., and Irving, M. (2016) Thick filament mechano-sensing is a calcium-independent regulatory mechanism in skeletal muscle. *Nat. Commun. 7*, 13281.

Gautel, M., Zuffardi, O., Freiburg, A., and Labeit, S. (1995) Phosphorylation switches specific for the cardiac isoform of myosin binding protein-C: a modulator of cardiac contraction? *EMBO J. 14*, 1952–1960.

Godfrey, J.E., and Harrington, W.F. (1970) Self-association in the myosin system at high ionic strength. I. Sensitivity of the interaction to pH and ionic environment. *Biochemistry 9*, 886–895.

Goldman, Y.E. (1987) Kinetics of the Actomyosin ATPase in Muscle Fibers. *Annu. Rev. Physiol. 49*, 637-654.

Goodson, H.V. and Spudich, J.A. (1993) Molecular Evolution of the Myosin Family: Relationships Derived from Comparisons of Amino Acid Sequences. *Proc. Natl. Acad. Sci. U.S.A. 90*, 659- 663.

Gordon, A.M., Homsher, E., and Regnier, M. (2000). Regulation of contraction in striated muscle. Physiol. Rev. 80, 853–924

Greaser, M.L. and Gergely, J. (1971) Reconstitution of Troponin Activity from Three Protein Components. *J. Biol. Chem. 246*, 4226-4233.

Gruen, M., and Gautel M. (1999) Mutations in beta-myosin S2 that cause familial hypertrophic cardiomyopathy (FHC) abolish the interaction with the regulatory domain of myosin-binding protein-C. *J Mol Biol. 286*, 933-949.

Gruen, M., Prinz, H., and Gautel, M. (1999) cAPK-phosphorylation controls the interaction of the regulatory domain of cardiac myosin binding protein C with myosin-S2 in an on-off fashion. *FEBS Lett. 453*, 254-259.

Gundapaneni, D., Xu, J., and Root, D.D. (2005) High flexibility of the actomyosin crossbridge resides in skeletal muscle myosin subfragment-2 as demonstrated by a new single molecule assay. *J Struct Biol. 149*, 117-126.

Highsmith, S. (1977) The effects of temperature and salts on myosin subfragment-1 and F-actin association. Arch. Biochem. *Biophys. 180*, 404–408.

Holmes, K.C. and Geeves, M.V. (2000) The structural basis of muscle contraction. *Phil. Trans. R. Soc. Lond. B 355*, 419–431.

Holmes, K.C., Popp, D., Gebhard, W. and Kabsch, W. (1990) Atomic Model of the Actin Filament. *Nature 347*, 44-49.

Huxley, A.F. (1964) Muscle. *Annu. Rev. Physiol. 26*, 131-152.

Huxley, A.F. and Niedergerke, R. (1954) Structural Changes in Muscle During Contraction; Interference Microscopy of Living Muscle Fibres. *Nature 173*, 971-973.

Huxley, A.F. and Simmons, R.M. (1971) Proposed mechanism of force generation in striated muscle. Nature 233, 533–538.

Jean, M. (2003) How to Subdue a Swelling Heart. *Science*. *300*, 1492-1496.

Jeffries, C.M., Lu, Y., Hynson, R.M., Taylor, J.E., Ballesteros, M., Kwan, A.H., Trewhella, J. (2011) Human cardiac myosin binding protein C: structural flexibility within an extended modular architecture. *J. Mol. Biol. 414*, 735-748.

Kato, H., Nishizaka, T., Iga, T., Kinosita, K. Jr., and Ishiwata, S. (1999) Imaging of thermal activation of actomyosin motors. *Proc Natl Acad Sci U S A. 96*, 9602-9606.

Kensler, R.W., Craig, R., and Moss, R.L. (2017) Phosphorylation of cardiac myosin binding protein C releases myosin heads from the surface of cardiac thick filaments. *Proc. Natl. Acad. Sci. U.S.A. 114*, 1355-1364.

Kinosita, K.Jr.,Ishiwata, S., Yoshimura,H., Asai,H., and Ikegami, A. (1984) Submicrosecond and Microsecond Rotational Motions of Myosin Head in Solution and in Myosin Synthetic Filaments As Revealed by Time-Resolved Optical Anisotropy Decay Measurements. *Biochemistry 23*, 5963-5975.

Kooij, V., Holewinski, R.J., Murphy, A.M., Van Eyk, J.E. (2013) Characterization of the cardiac myosin binding protein-C phosphoproteome in healthy and failing human hearts. *J. Mol. Cell. Cardiol. 60*, 116-120.

Krautbauer, R., Rief, M., and Gaub, H.E. (2003) Unzipping DNA Oligomers. *Nano Letters 3*, 493-496.

Kron, S.J., Toyoshima, Y.Y., Uyeda, T.Q.P., and Spudich, J.A. (1991) Assays for actin sliding movement over myosin-coated surfaces. *Methods Enzymol. 196*, 399-446.

Levine, R., Weisberg, A., Kulikovskaya, I., McClellan, G., and Winegrad, S. (2001) Multiple structures of thick filaments in resting cardiac muscle and their influence on cross-bridge interactions. *Biophys J. 81*, 1070–1082.

Li, Y., Brown, J.H., Reshetnikova, L., Blazsek, A., Farkas, L., Nyitray, L., and Cohen, C. (2003) Visualization of an unstable coiled coil from the scallop myosin rod. *Nature 424*, 341-345.

Lim, M.S., and Walsh, M.P. (1986) Phosphorylation of skeletal and cardiac muscle C-proteins by the catalytic subunit of cAMP-dependent protein kinase. *Biochem. Cell Biol. 64*, 622–630.

Lowey, S., Slayter, H.S., Weeds, A.G., and Baker, H. (1969) Substructure of the myosin molecule. I. Subfragments of myosin by enzymic degradation. *J Mol Biol. 42*, 1–29.

Lu, R.C. and Wong, A. (1985) The amino acid sequence and stability predictions of the hinge region in myosin subfragment 2. *J. Biol. Chem 260*, 3456–3461.

Luther, P.K., Winkler, H., Taylor, K., Zoghbi, M.E., Craig, R., Padron, R., Squire, J.M., and Liu, J. (2011) Direct visualization of myosin-binding protein C bridging myosin and actin filaments in intact muscle. Proc Natl Acad Sci U S A. 108, 11423–11428.

Lymn, R.W. and Taylor, E.W. (1971) Mechanism of adenosine triphosphate hydrolysis by actomyosin. *Biochemistry 10*, 4617–4624.

Mamidi, R., Gresham, K.S., Verma, S., and Stelzer, J.E. (2016) Cardiac Myosin Binding Protein-C Phosphorylation Modulates Myofilament Length-Dependent Activation. *Front Physiol. 7*, 38.

McClellan, G., Kulikovskaya, I., and Winegrad, S. (2001) Changes in cardiac contractility related to calcium-mediated changes in phosphorylation of myosin-binding protein C. *Biophys J. 81*, 1083-1092.

McNally, E.M., Barefield, D.Y., and Puckelwartz, M.J. (2015) The genetic landscape of cardiomyopathy and its role in heart failure. *Cell Metab. 21*, 174-82.

Mohamed, A.S., Dignam, J.D., and Schlender, K.K. (1998) Cardiac myosin-binding protein C (MyBP-C): identification of protein kinase A and protein kinase C phosphorylation sites. *Arch. Biochem. Biophys. 358*, 313–319.

Moos, C., Offer, G., Starr, R., and Bennett, P. (1975) Interaction of C-protein with myosin, myosin rod and light meromyosin. *J. Mol. Biol. 97*, 1-9.

Muir, A.R. (1965) Further observations on the cellular structure of cardiac muscle. *J Anat. 99*, 27-46.

Mun, J.Y., Gulick, J., Robbins, J., Woodhead, J., Lehman, W., and Craig, R. (2011) Electron microscopy and 3D reconstruction of F-actin decorated with cardiac myosin-binding protein C (cMyBP-C). *J. Mol. Biol. 410*, 214-25.

Mun, J.Y., Previs, M.J., Yu, H.Y., Gulick, J., Tobacman, L.S., Beck Previs, S., Robbins, J., Warshaw, D.M., and Craig, R. (2014) Myosin-binding protein C displaces tropomyosin to activate cardiac thin filaments and governs their speed by an independent mechanism. *Proc. Natl. Acad. Sci. U.S.A. 111*, 2170-2175.

Nag, S., Sommese, R.F., Ujfalusi, Z., Combs, A., Langer, S., Sutton, S., Leinwand, L.A., Geeves, M.A., Ruppel, K.M., and Spudich, J.A. (2015) Contractility parameters of human β-cardiac myosin with the hypertrophic cardiomyopathy mutation R403Q show loss of motor function. *Sci Adv. 1*.

Nag, S., Trivedi, D.V., Sarkar, S.S., Adhikari, A.S., Sunitha, M.S., Sutton, S., Ruppel, K.M., and Spudich, J.A. (2017) The myosin mesa and the basis of hypercontractility caused by hypertrophic cardiomyopathy mutations. *Nat Struct Mol Biol. 24*, 525-533.

Ochsnaer, M. (1997) Ca2+ transient, cell volume, and microviscosity of the plasma membrane in smooth muscle. *Biochem. Pharmacol. 53*, 1765-1777.

Offer, G., Moos, C., and Starr, R. (1973) A new protein of the thick filaments of vertebrate skeletal myofibrils: extraction, purification and characterisation. *J Mol Biol. 74*, 653–676.

Pinto, A., Sánchez, F., Alamo, L., and Padrón, R. (2012) The myosin interacting-heads motif is present in the relaxed thick filament of the striated muscle of scorpion. *J Struct Biol. 180*, 469-478.

Previs, M.J., Mun, J.Y., Michalek, A.J., Previs, S.B., Gulick, J., Robbins, J., Warshaw, D.M., and Craig, R.(2016) Phosphorylation and calcium antagonistically tune myosin-binding protein C's structure and function. *Proc. Natl. Acad. Sci. U.S.A. 113*, 3239–3244.

Previs, M.J., Previs, S.B., Gulick, J., Robbins, J., and Warshaw, D.M. (2012) Molecular Mechanics of Cardiac Myosin Binding Protein-C in Native Thick Filaments. *Science 337*, 1215–1218.

Price, H.M. (1963) The skeletal muscle fiber in the light of electron microscope studies. A review. *Am J Med. 35*, 589-605.

Ratti, J., Rostkova, E., Gautel, M., and Pfuhl, M. (2011) Structure and interactions of myosin-binding protein C domain C0: cardiac-specific regulation of myosin at its neck? *J Biol Chem. 286*, 12650-12658.

Rayment, I., and Holden, H.M. (1994) The three-dimensional structure of a molecular motor. *Trends Biochem Sci. 19*, 129-34.

Rayment, I., Smith, C., and Yount, R. G. (1996) The active site of myosin. *Annu. Rev. Physiol. 58*, 671–702.

Rees, M.K., and Young, M. (1967) Studies on the isolation and molecular properties of homogeneous globular actin. Evidence for a single polypeptide chain structure. *J. Biol. Chem. 242*, 4449-4458.

Reisler, E., Cheung, P., and Borochov, N. (1986) Macromolecular assemblies of myosin. *Biophys. J. 49*, 335-342.

Richard, P., Charron, P., Carrier, L., Ledeuil, C., Cheav, T., Pichereau, C., Benaiche, A., Isnard, R., Dubourg, O., Burban, M., Gueffet, J.P., Millaire, A., Desnos, M., Schwartz, K., Hainque, B., and Komajda, M. (2003) Hypertrophic cardiomyopathy: distribution of disease genes, spectrum of mutations, and implications for a molecular diagnosis strategy. *Circulation 107*, 2227-2232.

Rock, R.S., Ramamurthy, B., Dunn, A.R., Beccafico, S., Rami, B.R., Morris, C., Spink, B.J., Franzini-Armstrong, C., Spudich, J.A., and Sweeney, H.L. (2005) A flexible domain is essential for the large step size and processivity of myosin VI. *Mol Cell. 17*, 603-609.

Root, D.D., and Reisler, E. (1992) Cooperativity of thiol-modified myosin filaments. ATPase and motility assays of myosin function. *Biophys. J. 63*, 730-740.

Root, D.D., Yadavalli, V.K., Forbes, J.G., and Wang, K. (2006) Coiled-coil nanomechanics and uncoiling and unfolding of the superhelix and alpha-helices of myosin. *Biophys J. 90,* 2852-2866.

Ruppel, K.M., and Spudich, J.A. (1996) Structure-function analysis of the motor domain of myosin. *Annu Rev Cell Dev Biol. 12*, 543-73.

Rybakova, I.N., Greaser, M.L., and Moss, R.L. (2011) Myosin binding protein C interaction with actin: characterization and mapping of the binding site. *J Biol Chem. 286*, 2008-2016.

Saber, W., Begin, K.J., Warshaw, D.M., and VanBuren, P. (2008) Cardiac myosin binding protein-C modulates actomyosin binding and kinetics in the *in vitro* motility assay. *J Mol Cell Cardiol. 44*, 1053-1061.

Sata, M., Stafford, W., Mabuchi, K., and Ikebe, M. (1997) The motor domain and the regulatory domain of myosin solely dictate enzymatic activity and phosphorylation-dependent regulation, respectively. *Proc. Natl. Acad. Sci. U.S.A. 94*, 91-96.

Schlender, K.K., and Bean, L.J. (1991) Phosphorylation of chicken cardiac C-protein by calcium/calmodulin-dependent protein kinase II. *J. Biol. Chem. 266*, 2811–2817.

Semsarian, C., Ingles, J., Maron, M.S., Maron, B.J. (2015) New perspectives on the prevalence of hypertrophic cardiomyopathy. *J. Am. Coll. Cardiol. 65*, 1249-1254.

Semsarian, C., Ingles, J., Wilde, A.A. (2015) Sudden cardiac death in the young: the molecular autopsy and a practical approach to surviving relatives. *Eur. Heart J. 36*, 1290-1296.

Shaffer, J.F., Kensler, R.W., and Harris, S.P. (2009) The myosin-binding protein C motif binds to F-actin in a phosphorylation-sensitive manner. *J Biol Chem. 284*, 12318-12327.

Siemankowski, R. F., Wiseman, M. O. and White, H. D. (1985) ADP Dissociation from Actomyosin Subfragment 1 is Sufficiently Slow to Limit the Unloaded Shortening Velocity in Vertebrate Muscle. *Proc. Natl. Acad. Sci. U.S.A. 82*, 658–662.

Singh, R.R, Qadan, M.M., Aboonasrshiraz, N., Quedan, D.M., Wang, D., and Root D.D. (2017) Peptides designed to destabilize the myosin coiled coil enhance myofibril shortening while peptides that stabilize the coiled coil inhibit myofibril shortening. *Biophysical Journal. 112*, 557a.

Singh, R.R., Dunn, J.W., Qadan, M.M., Hall, N., Wang, K.K., and Root, D.D. (2017) Whole length myosin binding protein C stabilizes myosin S2 flexibility as measured by gravitational force spectroscopy. *Archives of Biochemistry and Biophysics,* Unpublished.

Smith, S.B., Cui, Y., and Bustamante, C. (1996) Overstretching B-DNA: the elastic response of individual double-stranded and single-stranded DNA molecules. *Science. 271,* 795-799.

Sommese, R.F., Sung, J., Nag, S., Sutton, S., Deacon, J.C., Choe, E., Leinwand, L.A., Ruppel, K., and Spudich, J.A. (2013) Molecular consequences of the R453C hypertrophic cardiomyopathy mutation on human β-cardiac myosin motor function. *Proc Natl Acad Sci U S A. 110*, 12607-12612.

Spudich, J.A. (2014) Hypertrophic and Dilated Cardiomyopathy: Four Decades of Basic Research on Muscle Lead to Potential Therapeutic Approaches to These Devastating Genetic Diseases. *Biophys. J. 106*, 1236-1249.

Spudich, J.A. and Watt, S. (1971) The regulation of rabbit skeletal muscle contraction. I. Biochemical studies of the interaction of the tropomyosin-troponin complex with actin and the proteolytic fragments of myosin. *J. Biol. Chem. 246*, 4866–4871.

Starr, R., and Offer, G. (1971) Polypeptide chains of intermediate molecular weight in myosin preparations. *FEBS Lett. 15*, 40-44.

Starr, R., and Offer, G. (1978) The interaction of C-protein with heavy meromyosin and subfragment-2. *Biochem. J. 171*, 813-816.

Sugi, H, Kobayashi, T., Gross, T., Noguchi, K., Karr, T., and Harrington, W.F. (1992) Contraction characteristics and ATPase activity of skeletal muscle fibers in the presence of antibody to myosin subfragment 2. *Proc. Natl. Acad. Sci. U. S. A. 89*, 6134-6137.

Sutoh, K., Sutoh, K., Karr, T. and Harrington, W.F. (1978) Isolation and physico-chemical properties of a high molecular weight subfragment-2 of myosin. *J.Mol.Biol. 126*, 1-22.

Taylor, E.W. (1977) Transient phase of adenosine triphosphate hydrolysis by myosin, heavy meromyosin, and subfragment 1. *Biochemistry 16*, 732-740.

Tesson, F., Richard, P., Charron, P., Mathieu, B., Cruaud, C., Carrier, L., Dubourg, O., Lautié, N., Desnos, M., Millaire, A., Isnard, R., Hagege, A.A., Bouhour, J.B., Bennaceur, M., Hainque, B., Guicheney, P., Schwartz, K., and Komajda, M. (1998) Genotype-phenotype analysis in four families with mutations in beta-myosin heavy chain gene responsible for familial hypertrophic cardiomyopathy. *Hum Mutat. 12*, 385-392.

Trybus, K.M., Huiatt, T.W., and Lowey, S. (1982) A bent monomeric conformation of myosin from smooth muscle. *Proc. Natl. Acad. Sci. U. S. A. 79*, 6151-6155.

Tsuchiya, T., Tanaka, H., Shirakawa, I., Karr, T., and Sugi, H. (1998) Evidence for the essential role of myosin subfragment-2 in the ATP-dependent actin-myosin sliding in muscle contraction. *Jpn. J. Physiol. 48*, 383-387.

van Dijk, S.J., Bezold, K.L., and Harris, S.P. (2014) Earning stripes: myosin binding protein-C interactions with actin. *Pflugers Arch. 466*, 445–450.

Vibert, P., Craig, R., and Lehman, W. (1997). Steric-model for activation of muscle thin filaments. *J. Mol. Biol. 266*, 8–14.

Volkmann, N., Lui, H., Hazelwood, L., Trybus, K.M., Lowey, S., and Hanein, D. (2007) The R403Q myosin mutation implicated in familial hypertrophic cardiomyopathy causes disorder at the actomyosin interface. *PLoS One. 2*, e1123.

Voller, A., Bartlett, A., and Bidwell, D.E. (1978) Enzyme immunoassays with special reference to ELISA techniques. *J Clin Pathol. 31*, 507-520.

Waldmüller, S., Sakthivel, S., Saadi, A.V., Selignow, C., Rakesh, P.G., Golubenko, M., Joseph, P.K., Padmakumar, R., Richard, P., Schwartz, K., Tharakan, J.M., Rajamanickam, C., and Vosberg, H.P. (2003) Novel deletions in MYH7 and MYBPC3 identified in Indian families with familial hypertrophic cardiomyopathy. *J Mol Cell Cardiol. 35*, 623-636.

Walker, J.M. (1996) The Protein Protocols Handbook. p779- p780. Human Press, INC., New Jersey.

Walker, M., Knight, P., and Trinick, J. (1985) Negative staining of myosin molecules. *J Mol Biol. 184*, 535-542.

Walker, S.M., and Schrodt, G.R. (1967) Contraction of skeletal muscle. *Am J Phys Med. 46*, 151-72

Wang, K. (1985) Sarcomere - Associated Cytoskelatal Lattices in Striated Muscle. *Cell Muscle Motil.*, 315-369. Springer US, New York.

Warrick, H.M., and Spudich, J.A. (1987) Myosin structure and function in cell motility. *Annu Rev Cell Biol. 3*, 379-421.

Weisberg, A., and Winegrad. S. (1996) Alteration of myosin cross bridges by phosphorylation of myosin-binding protein C in cardiac muscle. *Proc. Natl. Acad. Sci. U.S.A. 93*, 8999-9003.

Weith, A.E., Previs, M.J., Hoeprich, G.J., Previs, S.B., Gulick, J., Robbins, J., and Warshaw, D.M. (2012) The Extent of Cardiac Myosin Binding Protein-C Phosphorylation Modulates Actomyosin Function in a Graded Manner. *J Muscle Res Cell Motil. 33*, 449–459.

White, H. D. and Taylor, E. W. (1976) Energetics and Mechanism of Actomyosin Adenosine Triphosphatase. *Biochemistry* 15, 5818–5826.

Whitten, A.E., Jeffries, C.M., Harris, S.P., and Trewhella, J. (2008) Cardiac myosin-binding protein C decorates F-actin: implications for cardiac function. *Proc. Natl. Acad. Sci. U.S.A. 105*, 18360-18365.

Witjas-Paalberends, E.R., Ferrara, C., Scellini, B., Piroddi, N., Montag, J., Tesi, C., Stienen, G.J., Michels, M., Ho, C.Y., Kraft, T., Poggesi, C., and van der Velden, J. (2014) Faster cross-bridge detachment and increased tension cost in human hypertrophic cardiomyopathy with the R403Q MYH7 mutation. *J Physiol. 592*, 3257-3272.

Woodhead, J.L., Zhao, F.Q., Craig, R., Egelman, E.H., Alamo, L., and Padrón, R. (2005) Atomic model of a myosin filament in the relaxed state. *Nature 436*, 1195-1199.

Xu, J., and Root, D.D. (2000) Conformational selection during weak binding at the actin and myosin interface. *Biophys J. 79*, 1498-1510.

Yamamoto, K. (1984) Characterization of H-protein, a component of skeletal muscle myofibrils. *J Biol Chem. 259*, 7163-7168.

Yorde, D. E., Sasse, E. A., Wang, T. Y., Hussa, R. O., and Garancis, J. C. (1976) Competitive enzyme linked immunoassay with use of soluble enzyme/antibody immune complexes for labelling. I. Measurement of human choriogonadotropin. *Clin. Chem., 22*, 1372-1377.